Surface Plasmon Resonance-based Investigation of the Human Constitutive Androstane Receptor with regard to Co-activator Binding and Ligand-dependent Activation

Vorgelegt von
Luam Ghebreghiorghis
geboren in Kasala / Sudan

Teile dieser Arbeit wurden zur Veröffentlichung im British Journal of Pharmacology eingereicht (18. März 2011):

Ella Hoffart, Luam Ghebreghiorghis, Andreas K. Nussler, Wolfgang E. Thasler, Thomas S. Weiss, Matthias Schwab and Oliver Burk
The impact of atorvastatin metabolites on induction of drug metabolizing enzymes and membrane transporters by human pregnane X receptor.

Eidesstattliche Erklärung

Hiermit versichere ich, dass ich die vorliegende Arbeit selbstständig und nur unter Verwendung der angegebenen Hilfsmittel und Literatur angefertigt habe.

Stuttgart, den 19.01.2011 _____

(Luam Ghebreghiorghis)

Danksagung

Table of contents

Abbreviations

°C	degree celsius
μ	10^{-6} (micro)
μm	micrometer
μl	microliter
μM	micromolar
A	ampere
A	adenine
AE	Arteether
AF	activation function
ABC	ATP-binding cassette
AM	Artemether
ART	Artemisinin
ATP	adenosine triphosphate
BCIP	5-bromo-4-chloro-3-indolylphosphate
β-ME	β-Mercaptoethanol
Bisa	Bisphenol A
bp	base pair
BSA	bovine serum albumin
C	cytosine
CAR	constitutive androstane receptor (NR1I3)
CCRP	CAR retention protein
cDNA	complementary DNA
CITCO	6-(4-Chlorophenyl)imidazo[2,1- *b*] [1,3]thiazole-5-carbaldehyde *O*-(3,4-dichlorobenzyl)oxime
Clo	Clofibrate
Clot	Clotrimazole
CREB	cAMP-response element binding protein
CYP	cytochrome P450 monooxygenase
Cys	cysteine

dd H$_2$O	double deionized water
DBD	DNA binding domain
DMSO	dimethyl sulfoxide
DNA	desoxy ribonucleic acid
DR	directed repeats
DRIP 205	vitamin D-interacting protein 205
e.g.	exempli gratia
EDTA	ethylenediaminetetraacetic acid
ER	estrogen receptor
ER	everted repeats
EtOH	ethanol
Feno	Fenofibrate
FRET	fluorescence resonance energy transfer
Fc	flow cell
FXR	farnesoid X receptor
G	guanine
g	gram
Glu	glutamic acid
GRIP1	glucocorticoid receptor interacting protein
GST	glutathione S-transferase
h	hour
hCAR	human CAR
HDL	high density lipoprotein
HMG-CoA	3-hydroxy-3-methylglutaryl - coenzyme A
H$_2$O	water
Hsp90	heat shock protein 90
IKP	Dr. Margarete Fischer-Bosch-Institut für Klinische Pharmakologie
IPTG	Isopropyl β-D-1-thiogalactopyranoside
Ile	isoleucine
ml	milliliter
k$_a$	association rate constant
k$_d$	dissociation rate constant
K$_D$	equilibrium dissociation constant

14

kB	kilo base
kDa	kilo Dalton
l	liter
LB	Luria Bertani
LBD	ligand binding domain
LDL	low density lipoprotein
Leu	leucine
m	10^{-3} (milli)
m	meter
mA	milliampere
MD	molecular dynamics
MDR-1	multi-drug resistance protein 1
min	minute
mM	millimolar
µM	micromolar
ml	milliliter
MOPS	3-(N-morpholino) propanesulfonic acid
mCAR	mouse CAR
mRNA	messenger ribonucleic acid
MRP	multidrug resistance-related protein
MW	molecular weight
n	10^{-9} (nano)
NAD(P)H	ß-nicotinamide adenine dinucleotide phosphate
NaOH	sodium hydroxide
NBT	4-nitroblue-tetrazoliumchloride
NCoA1	nuclear receptor co-activator 1
NCoA2	nuclear receptor co-activator 2
NR	nuclear receptor
NR1I3	nuclear receptor subfamily 1, group I, member 3 (see CAR)
OA	okadaic acid
OD	optical density
OH	hydroxy

PAS	Per/ARNT/Sim domain
PB	Phenobarbital
PCR	polymerase chain reaction
PBREM	PB-responsive enhancer module
PBP	proliferator-activated binding protein
PP2A	protein phosphatase 2A
PXR	pregnane X receptor (NR1I2)
RU	response units
RAR	retinoic acid receptor
RID	receptor interaction domains
RNA	ribonucleic acid
rpm	rounds per minute
RXR	retinoid X receptor
s	second
sd	standard deviation
SDS	sodium dodecyl sulfate
Ser	serine
SNP	single nucleotide polymorphism
SRC-1	steroid receptor co-activator 1
SRC-2	steroid receptor co-activator 2
SPR	Surface Plasmon Resonance
t	time
T	thymine
TAE	tris-acetate buffer (pH 8.0) with EDTA
TBS	Tris buffered saline
TEMED	tetramethylethylenediamine
TF	transcription factor
TfbI	transformation buffer I
TfbII	transformation buffer II
TIF-2	transcriptional intermediary factor 2
TPP	Triphenylphosphate
TRAP	thyroid hormone receptor associated protein
TRIS	trishydroxymethylaminomethane
TBST	TBS– Tween 20

UV	ultraviolet
VLDL	very low density lipoprotein
v/v	volume per volume
w/v	weight per volume
wt	wild type
XRS	xenobiotic response element

Zusammenfassung

Xenobiotika, einschließlich Arzneimittel, unterliegen während der Detoxifikation Biotransformationsreaktionen, die eine Ausscheidung außerhalb der Zelle und des Körpers ermöglichen (Goldstein und Faletto, 1993). Die Cytochrom P450-Monooxygenasen (CYPs) stellen die wichtigste Gruppe von Enzymen des Fremdstoffmetabolismus dar. CAR (constitutive androstane receptor) und PXR (pregnane X receptor) scheinen ebenfalls ausschlaggebend für den Metabolismus von Pharmazeutika zu sein. CAR gehört zur Familie von Kernrezeptoren und ist überwiegend für die Regulierung von *CYP2B6* verantwortlich (Baes *et al*., 1994; Honkakoski *et al*., 1998). Die Kernrezeptoren bilden eine Familie von Proteinen, die essenziell für die Regulation von Vorgängen in der Entwicklung, im Metabolismus und in der Homöostase sind. Klassische Kernrezeptoren sind DNA-bindende Transkriptionsfaktoren, die erst durch Bindung eines Liganden die Genexpression induzieren können. Die hervorstechendste Eigenschaft des Kernrezeptors CAR ist seine konstitutive Aktivität, die durch eine liganden-unabhängige Rekrutierung von transktriptionsrelevanten Koaktivatoren erfolgt. Jedoch konnte belegt werden, dass aufgrund von Einwirkung von Phenobarbital (PB) CAR aus dem Cytoplasma in den Kern von Hepatozyten transloziert (Kawamoto *et al*., 1999; Maglich *et al*., 2003). Der Vorgang der Translokation stellt den entscheidenden Regulationsschritt in der Aktivierung von CAR dar (Kawamoto *et al*., 1999). Allerdings aktiviert PB CAR nicht durch direkte Bindung, sondern durch eine Signalkaskade, die abhängig von PP2A (protein phosphatase 2A) zur Dephosphorylierung des Rezeptors führt. Diese Dephosphorylierung kann durch Okadainsäure inhibiert werden (Yoshinari *et al*., 2003; Hosseinpour *et al*., 2006; Kawamoto *et al*., 1999).

Die Koaktivatoren SRC-1 (steroid receptor co-activator 1) und SRC-2 (steroid receptor co-activator 2) gehören zur Familie der p160 Koaktivatoren (Onate *et al*., 1995; Voegel *et al*., 1996). Sie koaktivieren zahlreiche Kernrezeptoren, unter anderem CAR und ER (estrogen receptor) (Forman *et al*., 1998; Muangmoonchai *et al*., 2001; Min *et al*., 2002). Obwohl CAR Liganden-unabhängig Koaktivatoren rekrutiert und aus diesem Grund nicht auf die Bindung eines Agonisten angewiesen ist, um aktiv zu sein, konnte gezeigt werden, dass seine konstitutive Aktivität durch Interaktionen mit einem Liganden zusätzlich erhöht werden kann (Maglich *et al*., 2003; Burk *et al*., 2005).

Im Rahmen dieser Doktorarbeit wurde mithilfe des Biacore 3000 der Kernrezepor CAR untersucht und charakterisiert. Das Biacore 3000 beruht auf dem Prinzip der Oberflächenplasmonresonanz (Surface Plasmon Resonance, SPR) welche die Analyse und Bestimmung der Kinetik, Konzentration, Spezifität, Affinität und Thermodynamik aktiver Moleküle in biomolekularen Interaktionen erlaubt (Turbdar *et al.*, 1959). Zu diesem Zweck müssen die Interaktionspartner nicht mit einem Expressions-Tag versehen werden, um in Echtzeit detektiert werden zu können. Um Bindungen am Biacore messen zu können, wird ein Interaktionspartner auf einer Flusszelle eines Biacore CM5 Chips irreversibel immobilisiert, während der andere in der Laufpufferlösung über die Oberfläche injiziert wird. Das immobilisierte Molekül stellt den „Ligand" dar, während das in Lösung injizierte Molekül als „Analyt" fungiert. Mithilfe von SPR können unter anderem Interaktionen von Proteinen, Lipiden, Nukleinsäuren, ganzen Zellen und sogenannten „small molecules" untersucht werden. „Small molecules" sind niedermolekulare Verbindungen, die vor allem pharmazeutische Arzneimittel ausmachen. Folglich werden die Biacore - Technologien vor allem auf dem Gebiet der pharmazeutischen Forschung, Antikörpercharakterisierung und der „Proteomics" verwendet.

Verschiedene Substanzen wurden aus einem Screening, welches am IKP (Dr. Margarete Fischer-Bosch-Institut für Klinische Pharmakologie) durchgeführt wurde, ausgewählt um den Einfluss auf CAR in Bezug auf die Bindung der Koaktivatoren und die Liganden-abhängige Aktivierung zu untersuchen. Daher bestand das erste Ziel dieser Arbeit in der Expression löslicher CAR, SRC-1 und SRC-2 Proteine in *E. coli*. Des Weiteren sollten die humanen Proteine aus dem Lysat der *E. coli* - Zellen aufgereinigt werden, um sie anschließend für SPR-basierte Bindungsassays zu verwenden. Eines der Hauptziele war herauszufinden in welchem Ausmaß die ausgewählten Substanzen die konstitutive Assoziation von CAR mit SRC-1 oder SRC-2 beeinflussen. Außerdem sollte die Kinetik der Assoziation als auch der Dissoziation des Rezeptor – Koaktivator Komplexes in Anwesenheit und Abwesenheit von Liganden analysiert werden. Aufgrund der beschriebenen SPR (surface plasmon resonance)-basierten Assays könnte ermittelt werden welchen Koaktivator CAR, ohne Berücksichtigung physiologischer Faktoren, bevorzugt, indem unter anderem die Liganden-unabhängige Rezeptor – Koaktivator Bindung untersucht wird. Zusätzlich könnten diese Assays die tatsächliche Wirkung von Agonisten auf die Kinetik der Bildung und des Zerfalls der Komplexe definieren. Die ausgewählten Substanzen umfassten den indirekten Aktivator PB, den inversen Agonisten Clotrimazol und den Agonisten CITCO (Honkakoski *et al.*, 1998; Lempiainen *et al.*, 2005; Maglich *et al.*, 2003). Des Weiteren wurden die

Artemisininsubstanzen, der HMG-CoA (3-Hydroxy-3-Methylglutaryl - Coenzyme A) Reduktaseinhibitor Atorvastatin und seine Metabolite, Fenofibrat, Clofibrat, Triphenylphosphat, Bisphenol A, Androstanol und Androstenol für die Beschreibung des Kernrezeptors CAR ausgewählt (Burk *et al.*, 2005; Kobayashi *et al.*, 2005; Guo *et al.*, 2007; Honkakoski *et al.*, 2004; Jyrkkärinne *et al.*, 2005; Dring *et al.*, 2010; Forman *et al.*, 1998). Abschließend sollte diese Arbeit aufklären, ob Clofibrat, Fenofibrat und die Atorvastatinmetabolite, die CAR aktivieren, als Agonisten oder als indirekte Aktivatoren fungieren (Guo *et al.*, 2007; Kobayashi *et al.*, 2005).

Sowohl der humane Kernrezeptor CAR als auch die humanen Koaktivatoren SRC-1 und SRC-2 konnten löslich in *E. coli*-Zellen exprimiert werden. Dies ermöglichte anschließend die schnelle und einfache Aufreinigung aus dem Lysat. Die Liganden-abhängigen Bindungsassays von CAR und SRC-1 offenbarten eine Hierarchie basierend auf der Rezeptor – Koaktivator Assoziation, die eine Klassifizierung der untersuchten Substanzen in Kategorien von keinen, schwachen oder starken Bindungspartnern ermöglichte. Wie erwartet wurde die Liganden-abhängige Bindung von CAR und SRC-1 im Vergleich zur konstitutiven, Liganden-unabhängigen Bindung durch den bekannten CAR Agonisten CITCO am stärksten erhöht. CITCO führte zu einer 7,3-fach und sowohl Clofibrat als auch Arteether zu einer 5,3-fach höheren Bindung, und bildeten somit die Gruppe der drei effizientesten CAR Agonisten. Anhand der SPR-basierten Bindungsassays konnten Clofibrat und Fenofibrat als CAR Agonisten identifiziert werden wobei ersteres einen deutlich höheren Einfluss hatte. Die Androstanmetabolite hatten keine Auswirkung auf den Rezeptor – Koaktivator Komplex. Die Anwesenheit eines Liganden hatte starken Einfluss auf die CAR – SRC-1 aber nur einen geringen auf die CAR – SRC-2 Assoziation. Eine Liganden-abhängige Erhöhung der konstitutiven Bindung erfolgte in geringerem Maße und eine Klassifizierung der Substanzen nach ihrer Wirkung war schwerer möglich. Die Assoziationshierarchie belegte dass, Arteether, CITCO und Triphenylphosphat die drei effizientesten CAR Agonisten darstellten. Überraschenderweise erhöhte nicht CITCO, sondern Arteether die CAR – SRC- 2 Assoziation am meisten mit einer 2,6-fach höheren Bindung. Dementsprechend erweist sich SRC-1 als leistungsstarkes Hilfsmittel, um putative Agonisten des Kernrezeptors CAR zu identifizieren und zu charakterisieren. CAR – Koaktivator Interaktionen mit und ohne CITCO waren ebenfalls deutlich höher mit DRIP 205 (vitamin D-interacting protein 205) als mit SRC-1, SRC-2 oder SRC-3 (Arnold *et al.*, 2004). Daher sollten weitere Biacoreassays DRIP 205 als alternatives Tool beinhalten, das nicht aus der Familie der p160 Koaktivatoren stammt. Wie

in dieser Arbeit erfolgreich gezeigt werden konnte, ermöglichen SPR-basierte Bindungsassays im Gegensatz zu Zellkultur-basierten Reporterassays eine schellere und leichte Identifizierung von Substanzen als Liganden oder Nicht-Liganden. Darüber hinaus werden Biacore-Assays nicht von zytotoxischen Effekten der zu untersuchenden Substanzen beeinträchtigt.

Im Gegensatz zu den Fibraten, wurden die Atorvastatinmetabolite nicht als CAR Agonisten identifiziert. Da der HMG-CoA Reduktaseinhibitor unter anderem die Expression von *CYP2B6* induziert, ist es wahrscheinlich, dass die CAR Aktivierung über eine PB-änliche Signalkaskade erfolgt (Kobayashi *et al*., 2005; Feidt *et al*., 2010; Kawamoto *et al*., 1999; Yoshinari *et al*., 2003). Dieses Ergebnis schließt allerdings nicht aus, dass andere Vertreter der Statine CAR durch direkte Bindung aktivieren könnten.

Die vorgelegte Arbeit konnte deutlich zeigen, dass die CAR – SRC-1 Bindung durch die ausgewählten Substanzen, insbesondere durch Arteether und Clofibrat, leicht reguliert werden konnte. Im Gegensatz zu CITCO, sind beide Substanzen pharmazeutisch relevant, da Clofibrat zu den lipidsenkenden Mitteln gehört und Arteether gegen schwere *Plasmodium falciparum* - assoziierte Malaria eingesetzt wird (White, 2004). Die Clotrimazol-abhängige Inhibition der Arteether- und Clofibrat-relevanten verstärkten CAR – SRC-1 Assoziation lässt vermuten, dass eine gleichzeitige Einnahme der Liganden mit dem inversen Agonisten zu einer stark verminderten Aktivität des Kernrezeptors *in vivo* führen könnte. Allerdings, übereinstimmend mit der konstitutiven CAR – SRC-2 Bindung, konnte Clotrimazol nur zum Teil als inverser Agonist bestätigt werden, da die liganden-unabhängige Rezeptor – Koaktivator Bindung nicht inhibiert wurde.

Die kinetischen Bindungsassays offenbarten, dass die Liganden-unabhängige Rezeptor – Koaktivator Bindung neun mal schneller mit SRC-1 erfolgte als mit SRC-2. Die Stabilität des Komplexes hingegen war relativ betrachtet schwach und für beide Koaktivatoren ähnlich. Sowohl die Liganden-abhängigen Bindungsassays als auch die Liganden-unabhängigen kinetischen Assays lassen erkennen, dass SRC-1, abgesehen von gewebe-spezifischen Expressionsprofilen, von CAR bevorzugt wird. Vereinbar mit diesem Ergebnis sind mammalian two-hybrid Assays, die mit SRC-1, SRC-2 und SRC-3 (steroid receptor co-activator 3) in Anwesenheit und Abwesenheit des CAR Agonisten CITCO gemacht wurden (Arnold *et al*., 2004). SPR-basierte Kinetikassays mit ERα (estrogen receptor α) und ERβ offenbarten ebenfalls, dass beide Rezeptoren SRC-1 vorzogen (Cheskis *et al*., 2003). Dennoch wurde klar, dass Rezeptoren wie ER ihre wenigen Liganden mit einer viel höheren

Affinität binden als CAR, das wie PXR, mehr Liganden mit einer niedrigeren Affinität bindet. Im Vergleich zur Interaktion von FXR (farnesoid X receptor) und SRC-1, demonstrierte CAR deutlich höhere Bindungsaffinitäten mit jeweils beiden Koaktivatoren (Fujino *et al*., 2003). Daraus folgt, dass die Bindungsstärke der untersuchten Komplexe nicht nur durch den Koaktivator aber auch durch den Rezeptor bestimmt wird.

Da die Liganden-abhängigen Bindungsassays eine charakteristische Verstärkung der Assoziation zeigten, wurden kinetische Assays durchgeführt um den tatsächlichen Einfluss der Liganden auf die Kinetik des CAR – SRC-1 Komplexes zu bestimmen. Überraschenderweise wies der Rezeptor – Koaktivator Komplex geringere Affinitäten auf, und ließ somit vermuten, dass kein Agonist zu einer schnelleren Erkennung von SRC-1 geführt hat. Folglich wurden in Anwesenheit von Agonisten zwar mehr Komplexe von CAR und SRC-1 gebildet, allerdings in einem viel langsameren Tempo im Vergleich zur konstitutiven Bindung. Jedoch zeigten die Liganden-abhängigen Kinetikassays auch, dass offensichtlich zwei Klassen von CAR Liganden existieren. Liganden der ersten Klasse (Artemether, Triphenylphosphat und Fenofibrat) führten zwar zur Bildung von mehr CAR – SRC-1 Komplexen, konnten aber deren Stabilität nicht erhöhen. Die zweite Klassse von CAR Liganden umfasste CITCO, Clofibrat, Arteether und Artemisinin. Diese Gruppe führte zu mehr Komplexbildung und zu einer erhöhten Rezeptor – Koaktivator Stabilität. Die Vertreter dieser Gruppe führten außerdem zu einer deutlich langsameren Assoziation, die möglicherweise durch eine Zweistufenbindung, die eine initiale, schnellere und eine darauffolgende, langsamere Assoziation beinhaltet, erklärt werden könnte. Durch diese Ergebnisse wird die Bedeutung kinetischer Assays als Bestätigung der Bindungsassays offensichtlich, da nur auf diese Weise der Einfluss eines Liganden auf die Assoziation und die Dissoziation des Rezeptor – Koaktivator Komplexes aufgeklärt wird. Diese Erkenntnis ist besonders wichtig für die Identifizierung weiterer CAR Agonisten. Allerdings sollten direkte CAR – Ligandenbindungsassays durchgeführt werden, die darüber hinaus eine weitere Charakterisierung des Rezeptors auf Koaktivator-unabhängige Weise ermöglichen.

Die in dieser Arbeit dargestellten Ergebnisse machen deutlich, dass SPR-basierte Assays den Einfluss von Liganden nicht nur mit einer einfachen Ja / Nein – Antwort darstellen können, sondern eine aussagefähige Charakterisierung der Kinetik ermöglichen. Dies könnte entscheidende Informationen über CAR in seiner dynamischen Funktion als Xenosensor, während der Liganden-abhängigen Aktivierung innerhalb der Detoxifikation *in vivo*, liefern.

Abstract

During detoxification, xenobiotics including pharmaceuticals are subject to biotransformation reactions which enable their excretion outside the cell and the human body. The cytochrome P450 monooxygenases (CYPs) are the most important group of enzymes in xenobiotic metabolism. CAR (constitutive androstane receptor) and PXR (pregnane X receptor) seem to be crucial for pharmaceutical metabolism, too. CAR belongs to the family of nuclear receptors and is mainly responsible for regulation of *CYP2B6* in humans. The most outstanding property of the nuclear receptor CAR is its constitutive activity which results from ligand-independent recruitment of transcriptional co-activators unlike most classical nuclear receptors. Yet, it was also shown that CAR, due to exposure to Phenobarbital (PB), translocates from the cytoplasm into the nucleus of hepatocytes. The co-activators SRC-1 (steroid receptor co-activator 1) and SRC-2 (steroid receptor co-activator 2) belong to the p160 family of co-activators and co-activate many nuclear receptors among others CAR and ER (estrogen receptor). Though CAR recruits ligand-independently co-activators and, therefore, does not need agonist binding to be active, it has been shown that its activity can be further enhanced by interactions with agonists.

In this study Biacore technology, which relies on the principle of surface plasmon resonance (SPR), was used to investigate and characterize the nuclear receptor CAR. Several drugs selected in the course of a screening performed at the IKP (Dr. Margarete Fischer-Bosch-Institut für Klinische Pharmakologie) were chosen to investigate the influence on CAR with regard to co-activator binding and ligand-dependent activation. For this purpose, the first goal was the soluble expression of both CAR and the co-activators SRC-1 and SRC-2 in *E. coli* cells, and the subsequent purification for binding experiments via SPR. The aim of this work was to investigate to what extent the selected drugs influence the constitutive association of CAR with SRC-1 or SRC-2 by means of SPR. Furthermore, the work aimed to characterize the kinetics of both the association and the dissociation of the receptor – co-activator complex in the presence and absence of ligands. These assays may elucidate which co-activator might be preferred by CAR regardless of physiological factors, and clarify the actual impact of agonist ligands on the kinetics of complex formation and decay. Additionally, the examination of the ligand-free interaction aimed to characterize the constitutive binding of

receptor and co-activator. The selected drugs included among others the indirect activator PB, the inverse agonist Clotrimazole, and the agonist CITCO.

Both the human nuclear receptor CAR as well as the human co-activators SRC-1 and SRC-2 could be expressed solubly in *E. coli* cells which enabled the subsequent purification from the lysate. Binding experiments of immobilized SRC-1 with CAR in the presence of the selected drugs revealed a distinctive ligand-dependent hierarchy in association of receptor and co-activator which allowed a discrimination of the drugs into non- or low, weak, and strong binders of the receptor. As it was expected ligand-induced binding was increased the most for the prototypical CAR agonist CITCO followed by Clofibrate and Arteether. CAR – SRC-2 binding was not as strongly affected by ligands as SRC-1, since increase in binding was low and discrimination of drugs was poor. The association hierarchy included Arteether > CITCO > Triphenylphosphate to be the three most competent agonists. Thus, CAR – SRC-1 interaction appears to be more susceptible to regulation by the selected drugs, especially by the pharmaceutically relevant substances Arteether and Clofibrate. Since ligand-induced binding of CAR and SRC-1 proved to be significantly diminished by Clotrimazole, side effects including cross reactivity caused by the simultaneous taking of the inverse agonist and Arteether or Clofibrate may occur *in vivo*. Yet, Clotrimazole could only be partly confirmed as inverse agonist of CAR since it did not lead to co-activator release in the absence of ligands. Yet, the co-activator SRC-1, unlike SRC-2, revealed to be a powerful tool of identification and characterization of putative agonists which might distinctively influence the constitutive binding with CAR. Further Biacore assays with DRIP 205 (vitamin D-interacting protein 205) as a non-p160 protein would serve as a perfect alternative tool to characterize CAR co-activator binding.

Kinetic binding assays demonstrated that the constitutive binding of CAR with SRC-1 occurred nine times faster than with SRC-2 whereas the stability of both receptor - co-activator complexes revealed to be low but displayed no distinctive differences. Thus, both ligand-induced binding experiments and ligand-free kinetic assays strongly indicate that SRC-1 is the prime co-activator of interest for CAR regardless of expression levels and tissue-specific expression profiles. Consistent with these findings, mammalian two hybrid assays revealed SRC-1 to be the most potent of the p160 co-activators in the presence or absence of CITCO. Additionally, SPR based interactions of ERα (estrogen receptor α) and ERβ with the p160 co-activators revealed SRC-1 to be preferred over SRC-2 for both receptors. When compared to FXR (farnesoid X receptor), however, CAR displayed higher binding affinities with both co-activators.

Surprisingly, equilibrium dissociation constants of ligand-induced kinetic binding assays of CAR and SRC-1 revealed weaker affinities when interactions took place with all agonists, indicating that no ligand was able to accelerate recognition of SRC-1. Thus, more complexes were formed but more slowly than in the absence of ligands. Furthermore, two classes of CAR ligands were revealed. The first class of ligands including Artemether, Triphenylphosphate, and Fenofibrate led to the formation of more complexes, as demonstrated by ligand-induced increase in binding, but could not enhance the stability of the complex. The second class of ligands which comprised CITCO, Clofibrate, Arteether, and Artemisinin furthermore enhanced the stability of the complex but also caused distinctively slower association rates which might be assigned to a two-step association. However, direct CAR – ligand binding assays might furthermore provide characterization of receptor – agonist interactions in a co-activator-independent manner allowing prediction of medical side effects. Unlike the HMG-CoA reductase inhibitor Atorvastatin and its metabolites, Fenofibrate and Clofibrate, were identified as CAR agonists. Atorvastatin induces among others gene expression of *CYP2B6*. Therefore, the HMG-CoA reductase inhibitor is likely to induce CAR activation in a PB-similar way.

1 Introduction

1.1 Detoxification in human liver cells

Every day the human body encounters substances and xenobiotics which could pose serious harm and lead to high toxicity if they accumulated within the human cell (Eichelbaum and Burk, 2001). Hydrophilic substances are hardly able to pass the membrane which is an efficient barrier to these compounds. Lipophilic substances, however, can enter the cell more easily than their hydrophilic counterparts and, thus, require further mechanisms to be neutralized eventually.

Especially lipophilic compounds / xenobiotics pass through two different phases of biotransformation which make them hydrophilic and enhance their polarity in order to be able to be excreted outside both the cell and the human body (Goldstein and Faletto, 1993). These biotransformation reactions can be separated into reactions leading to the addition of functional groups (phase I) and conjugation reactions (phase II) (Conney, 1982). Excretion of the metabolized substances outside the cell / human body by specific transport proteins is often regarded as phase III. The goal of phase I is to add functional groups like hydroxyl or sulphur groups to the lipophilic or non-polar compounds by oxidation, reduction, or hydrolysis in order to prepare them for phase II reactions. As a result of attaching a hydroxyl group to the compound, the once lipophilic compound has been transformed into a substrate for further enzymatic reactions in phase II of the detoxification process. For phase II enzymes the hydroxyl group serves as a reactive group for enzymatic modifications like sulfation, glucuronidation, methylation, *N*-acetylation, conjugation with amino acids or attaching of glutathione molecules. All these conjugation reactions add hydrophilic groups and have, therefore, the only purpose of enhancing the hydrophilicity which was originally introduced in phase I by CYPs. Enhanced hydrophilicity can be reached by modifications carried out by esterases, amidases, or imidases. The next and final step in detoxification is executed by transporter proteins in phase III which are localized directly in the sinusoidal or apical membranes of hepatocytes (Stieger and Meier, 1998; Müller, 2000; Bohan and Boyer, 2002). The activity of transporter proteins is not only limited to the excretion of metabolized xenobiotics, transporters also participate in the reabsorption of compounds from the blood.

The transporter proteins involved in excretion are mostly the ATP-dependent efflux transporters like the multi-drug resistance protein 1 (MDR1) which belongs to the superfamily of ABC transporters (Juliano and Ling, 1976). The originally lipophilic substance is now hydrophilic enough to be excreted by the transporter proteins. The final excretion of the metabolized xenobiotics out of the cell takes place either through the kidneys, the feces or the bile. Taking this course, xenobiotics which, after accumulation, could be toxic to the human body are both made non-toxic and secreted outside the cell. However, there are compounds which exist in a non-toxic precursor form which only after the first metabolization steps inside the liver end up in the final biological and toxic state.

1.2 The cytochrome P450 monooxygenases

Cytochrome P450 monooxygenases (CYPs; E.C.1.14.14.1) belong to the enzyme class of oxidoreductases (E.C.1.14.-.-) and represent one of the largest enzyme families with 11.292 previously known members (http://drnelson.uthsc.edu/CytochromeP450.html; updated August 2009). The CYP enzymes are heme-containing enzymes which, unlike other heme-containing proteins, are linked with a cysteinate ligand. Therefore, reduced CYPs characteristically display an absorption maximum at 450 nm when complexed with carbon monoxide (Klingenberg, 1958; Garfinkel, 1958). The CYPs are enzymes which are responsible for metabolizing a broad spectrum of lipophilic compounds (Nebert and Russell, 2002). They are particularly important for introducing the first phase of detoxification of endogenous and exogenous compounds in the human body (Ziegler, 1994). CYPs are the most important enzymes in xenobiotic metabolism not only because of their high capability as monooxygenases but also because of their ubiquitous occurrence in both tissues and organisms. Among others they are specifically expressed in the liver. The majority of the CYPs expressed in the liver are assigned to metabolizing pharmaceuticals (Shimada *et al*., 1994).

A uniform nomenclature of the cytochrome P450 monooxygenases is based on the amino acid sequence (Nelson *et al*., 1996). The term "CYP" is followed by a number which comprises those enzymes which share more than 40% amino acid sequence homology and are, therefore, assigned to the same family. The subsequent letter designates the enzymes of the same

subfamily which display more than 55% homology in amino acid sequence. The Arabic numeral at the end of the name designates the individual gene.

The *CYP1A*, *CYP2B*, *CYP2C*, *CYP2D*, and *CYP3A* gene subfamilies are induced after exposure to xenobiotics in a distinctive, tissue-specific, dose-dependent, rapid and reversible manner. The cytochrome P450 gene *CYP2B6* is the main target gene of the nuclear receptor CAR (constitutive androstane receptor) in humans (Sueyoshi *et al*., 1999). Expression of *CYP2B6*, subsequent to drug-induced activation of CAR, is caused by exposure to Phenobarbital (Kawamoto *et al*., 1999; Maglich *et al*., 2003). Interestingly, CYP2B6 expression is subjected to significant differences between sexes, ethnic groups and single nucleotide polymorphisms (SNPs) (Lamba *et al*., 2003). Thus, CYP2B6-dependent detoxification can vary to a great extent in individuals. Especially, genetic polymorphism in drug-metabolizing enzymes and other proteins involved in detoxification is linked with interindividual drug potency and toxicity (Evans and Relling, 1999).

1.3 Nuclear receptors

The nuclear receptors constitute a huge family of proteins that are essential to regulate development, metabolism and homeostasis. So far, at least 48 nuclear receptors have been identified in the human genome (Germain *et al*., 2006). One of their most outstanding characteristics is the ability to recognize and bind specific DNA-elements in order to trigger expression of target genes. Therefore, they are primarily bound to a ligand which can be of endogenous or exogenous nature in order to regulate gene expression. For this reason they are considered transcription factors and receptors. The classical nuclear receptor needs to be bound to its specific agonist which results in a conformational change enabling the receptor to bind co-regulators. Nuclear receptors are limited to metazoans and are not to be found in organism like protists, algae, fungi and plants.

The nuclear receptors CAR (constitutive androstane receptor) and PXR (pregnane X receptor) belong to the family of nuclear receptors (Baes *et al*., 1994; Bertilsson *et al*., 1998; Lehmann *et al*., 1998). Both receptors act as xenosensors since they trigger gene expression of specific CYPs after distinctive drug exposure.

Nuclear receptors have a rather conservative composition concerning their modular structure. The receptors are made of four functional modules with two essential domains - the DNA-binding and the ligand-binding domain - constituting the majority of these proteins (figure 1.1) (Mangelsdorf *et al.*, 1995; Enmark and Gustafsson, 1996). The highly variable N-terminal A/B domain contains an activation function (AF-1) in some nuclear receptors. The C domain contains the DNA-binding domain harboring two zinc finger motifs. Considering CAR and PXR, this domain is rather similar in amino acid composition proposing similar DNA motifs for the receptors to bind to. The centrally located D area is a flexible hinge region which is directly followed by the ligand-binding domain (LBD). The LBD contains regions for receptor dimerization, nuclear translocation and binding of nuclear receptors and co-regulators like SRC-1 (steroid receptor co-activator 1). The LBD contains the C-terminal activation function 2 (AF-2). Helix 12 which is located at the C-terminal ending of the LBD is crucial for agonist binding. As a result of a binding event a conformational change takes place which enables interactions with nuclear receptors and co-activators. All of this finally leads to activation of a nuclear receptor's target gene. The activation characteristics of CAR and PXR differ in species which makes it particularly hard to estimate drug-based induction in humans. The C-terminal F domain is not present in both CAR and PXR. Its biological function is still not clear (Germain *et al.*, 2006).

Figure 1.1 Schematic figure depicting the functional domains of a nuclear receptor. The N-terminal region contains the AF-1 domain which is followed by the DBD which posses two zinc finger motifs. The flexible hinge region connects the DBD with the LBD which comprises among other the C-terminal AF-2 essential for co-regulator interactions. The C-terminal F domain is not present in CAR and PXR.
This figure was modified according to Handschin and Meyer, 2003; Pharmacological Reviews, Volume 55: 649-673.

1.4 The constitutive androstane receptor CAR

1.4.1 General properties of CAR

The constitutive androstane receptor CAR (NR1I3) belongs to the family of nuclear receptors (Baes *et al*., 1994). NR1I3 indicates that CAR is assigned to the subfamily 1 and the group I of the nuclear receptor family (Escriva *et al*., 2000). CAR does not belong to the classical nuclear receptors since it is a constitutive active receptor. Human CAR was discovered and characterized for the first time as MB67 to bind and transactivate specific retinoic acid response elements (Baes *et al*., 1994). In mouse, CAR was firstly described only three years later (Choi *et al*., 1997).

The most outstanding property of the nuclear receptor CAR is the ligand-independent, constitutive activity (Suino *et al*., 2004). This characteristic makes CAR rather unique among most other nuclear receptors. The constitutive activity results from a ligand-independent recruitment of transcriptional co-activators.

In most species CAR is predominantly expressed in liver and intestinal epithelium (Baes *et al*., 1994; Wei *et al*., 2002). Identification of many different isoforms of CAR has been reported. Among them many with different functional properties and tissue-specific expression patterns resulting from alternative splicing events (Auerbach *et al*., 2003; Arnold *et al*., 2004). CAR also underlies distinctive species-specific limitations. Mouse CAR, but not human CAR, is strongly activated after direct binding of TCPOBOP (1,4-bis[2-(3,5-dichloropyridyloxy]benzene) (Moore *et al*., 2000; Tzameli *et al*., 2000). The selectivity regarding ligand binding is due to the divergent nature of the ligand binding domain of the same receptor in different species like mouse or man (Moore *et al*., 2000).

1.4.2 Mode of activation

Due to its constitutive activity, the way of activation makes CAR quite unique and extraordinary among most receptors in the nuclear receptor family. CAR is a constitutive active receptor that displays ligand-independent recruitment of co-activators. PXR is activated by direct agonist binding in contrary to co-xenosensor CAR. Additionally, PXR resides in the

nucleus quite passively until exogenous or endogenous ligand binding occurs. CAR, on the other hand, is mostly located in the cytoplasm of non-exposed cells. Figure 1.2 displays the mode of CAR activation in response to induction by Phenobarbital. CAR is sequestered in the cytoplasm of the cell where it is complexed to heat shock protein 90 (hsp90) and the cytosolic CAR retention protein (CCRP) (Yoshinari *et al.*, 2003; Kobayashi *et al.*, 2003). After exposure to Phenobarbital (PB), nuclear translocation of CAR takes place (Kawamoto *et al.*, 1999; Maglich *et al.*, 2003). This translocation is the very first step of CAR activation *in vivo* and, thus, appears to be the pivotal regulating step during CAR activation (Kawamoto *et al.*, 1999). The group of M. Negishi found out that CAR accumulated in the cytoplasm of untreated liver cells in mice. But once treated with PB, the immunohistochemistry revealed CAR to accumulate within one hour in the nucleus of liver cells. PB induces CAR nuclear translocation in man as well as in mouse. TCPOBOP on the other hand, induces CAR nuclear accumulation only in mouse (Moore *et al.*, 2000; Tzameli *et al.*, 2000). The essential step of nuclear translocation, however, is sensitive to inhibition by Okadaic acid (OA). Okadaic acid is a protein phosphatase inhibitor which inhibits PB-induced nuclear translocation of CAR (Kawamoto *et al.*, 1999). The protein phosphatase 2A (PP2A) was discovered to be recruited by CAR due to PB-exposure (Yoshinari *et al.*, 2003). Firstly PP2A is recruited to the hsp90 - CAR complex in PB-treated mice to subsequently dephosphorylate Ser^{202} of mCAR (Hosseinpour *et al.*, 2006). Okadaic acid inhibits the PB-dependent dephosphorylation cascade and, hence, the accumulation of CAR in the nucleus resulting in the inhibition of CAR activation. This way OA enables CAR regulation by retaining it sequestered and complexed in the cytosol.

 Nuclear translocation of CAR is completely independent from the C-terminal AF-2 domain. But PB-dependent nuclear translocation is regulated by the xenobiotic response element (XRS). XRS consists of a 30 amino acid leucine-rich motif at the C-terminal ending of the receptor. It is defined as a LXXLXXL motif essential for drug-induced nuclear translocation in mouse liver *in vivo* (Zelko *et al.*, 2001). Additionally, the p160 transcription factor glucocorticoid receptor interacting protein (GRIP1) seems to help CAR accumulate in the nucleus (Min *et al.*, 2002; Xia *et al.*, 2005). GRIP1, also known as TIF-2 (transcriptional intermediary factor 2) or SRC-2 (steroid receptor co-activator 2) is considered a nuclear receptor co-regulator of transcriptional activity. GRIP1 assists the ligand-independent translocation of CAR into the nucleus by binding the XRS and, thus, enhances nuclear accumulation of the receptor. On the other hand, the transcriptional co-activator PBP

(proliferator-activated binding protein) had also been proposed for assisting CAR in nuclear translocation and, thus, activation (Jia *et al*., 2005).

Once having entered the nucleus, CAR is capable of transactivating target genes. The C-terminal AF-2 region is responsible for the transactivational activity of CAR. The structural basis of the AF-2 domain which is responsible for its activity is still unknown. Inside the nucleus CAR dimerizes with retinoic X receptor (RXR) which is the heterodimerization partner of the majority of all nuclear receptors. Only this way CAR is capable of binding to its specific DNA-regulatory domains like PBREM (PB-responsive enhancer module) which is the enhancer of *CYP2B* genes. CAR, as well as PXR, recognizes DRs (directed repeats) of the binding motif AGGTCA (Whitfield *et al*., 1999). CAR also recognizes DRs of AGG/TTCA, separated by four or five basepairs (DR-4, DR-5). Additionally, the receptor binds DR-2 and DR-3 and recognizes the everted repeats ER-6 and ER-8 (Baes *et al*., 1994; Sueyoshi *et al*., 1999; Kast *et al*., 2002). Transcriptional activation occurs upon CAR binding to PBREM which contains the DR-4 sites NR1 and NR2. CAR complexed with RXR has been found to recognize and bind NR1 (Honkakoski *et al*., 1998). This way CAR recruits co-activator proteins like SRC-1 and still unknown co-regulator proteins.
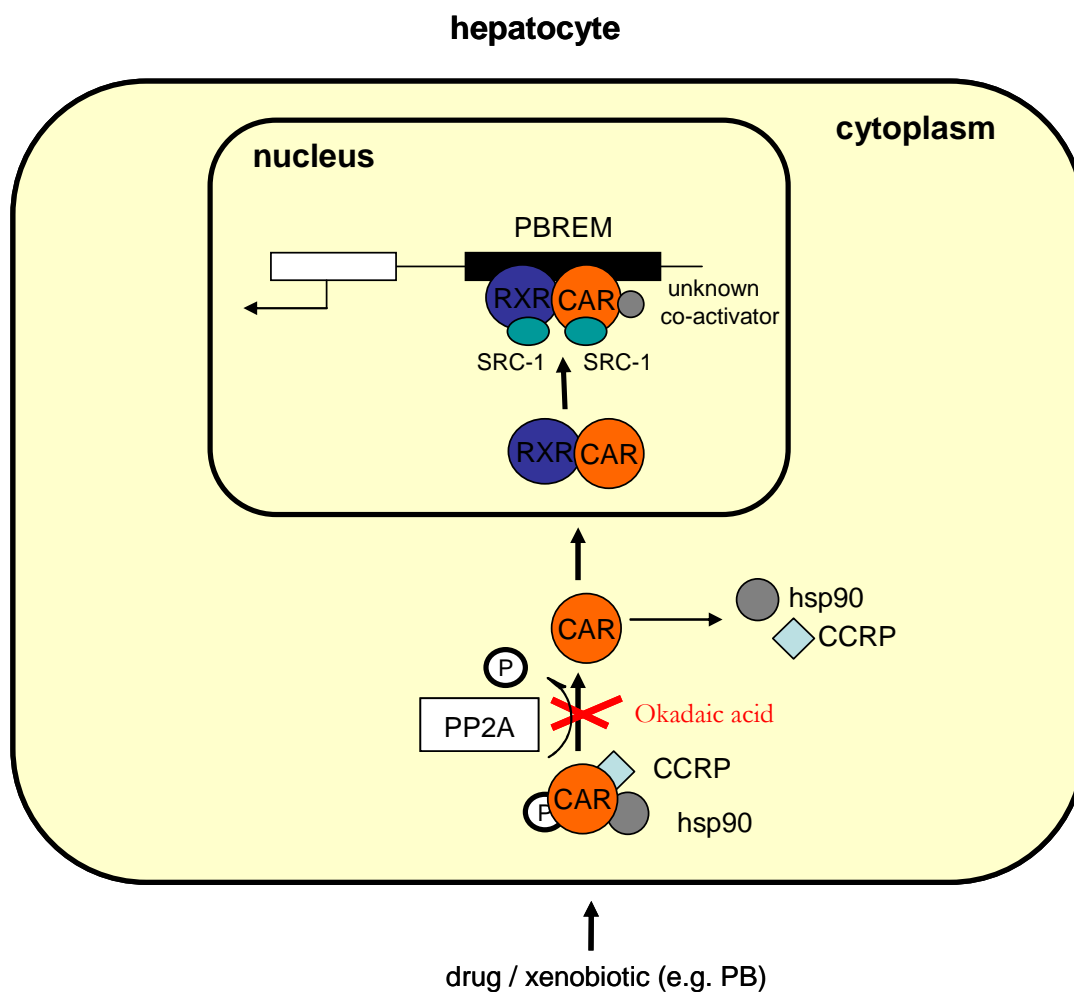
hepatocyte

Figure 1.2 Schematic figure of CAR activation and signaling pathway in liver cells. *In vivo* CAR is sequestered among all in the cytoplasm of hepatocytes. There it is complexed and retained by hsp90 and CCRP. Dephosphorylation of CAR leads to the release of CCRP and hsp90 and nuclear translocation. Dephosphorylation by PP2A and subsequent accumulation of CAR in the nucleus can be inhibited by Okadaic acid. Inside the nucleus CAR heterodimerizes with RXR and binds to specific DNA-regulatory domains of PBREM, recruiting co-activators like SRC-1 to finally initiate expression of target genes.
This figure was adapted from Timsit and Negishi, 2007; Steroids, Volume 72: 231-246.

1.4.3 Target genes

The main target genes of CAR are *cyp2b10* in mouse and *CYP2B6* in humans (Sueyoshi *et al*., 1999; Honkakoski *et al*., 1998). There are also CAR binding sites in the regulatory region of genes encoding human UGT1A1 and both mouse and human transport proteins MDR1 and Mrp2. Exposure to PB leads to the expression of more than 140 genes of which CAR is capable to regulate half of them. It has also been shown that CAR is not necessarily needed for all involved genes to be expressed properly. The PB-induced amino-levulinic acid

synthase 1, an enzyme needed for heme metabolism is both expressed in wild-type and CAR *null* animals suggesting alternative ways for Phenobarbital not involving CAR to reach transcriptional activity (Kakizaki *et al*., 2002; Honkakoski and Negishi, 2000). Additionally, CAR being active can have diverse roles in regulating target genes like sustaining PB-induced genes in a repressive state (Ueda *et al*., 2002).

Crosstalk between CAR and PXR has been proposed for quite a while. This hypothesis is confirmed by several findings. Several groups have already shown that both receptors are also capable of activating each other's target genes (Moore *et al*., 2000; Xie *et al*., 2000; Goodwin *et al*., 2002). The constitutive androstane receptor is probably capable of transactivating expression of *CYP3A4*, both *in vivo* and *in vitro*. This crosstalk between CAR and PXR might be important for CYP3A4 expression since human CAR response elements mediate transactivation of CYP3A4 by human PXR. On the other hand human PXR can initiate crosstalk by transactivating human *CYP2B6* and mouse *cyp2b10* genes through response elements interacting with CAR. The fact that there is cross-talk between CAR and PXR on the DNA level and beyond makes it harder to elucidate metabolism of distinctive drugs of interest concerning CAR's constitutive activity.

Taken together, CAR is involved in the regulation of genes encoding enzymes and proteins responsible for the metabolism of drugs involved in phase I and II, ABC transporter proteins, and among others genes for cholesterol synthesis, ß-oxidation, bilirubin clearance, bile acid and biosynthesis (Ueda *et al*., 2002; Yamamoto *et al*., 2003; Sugatani *et al*., 2001; Beilke *et al*., 2009). It is a positive regulator in the controlling process of hepatic genes in response to PB, even beyond drug and steroid metabolism.

1.4.4 Structural properties

CAR and PXR are nuclear receptors that interact with exogenous compounds more than any other nuclear receptor. As xenosensors they fulfill their ability to bind a broad range of quite diverse ligands. It is striking that classical receptors like ER (estrogen receptor) or GR (glucocorticoid receptor) have a few ligands which they bind with high affinity. Both xenosensors on the other hand, bind a broader and more diverse range of ligands distinctively lower in affinity. Classical nuclear receptors like ER do have a large and rather conserved AF-1 domain whereas CAR and PXR have not been proven to possess a distinct AF-1 domain.

Ligand binding of AF-2 of a classical nuclear receptor usually results in an active conformation that facilitates the binding of a co-activator by its LXXLL motif. Figure 1.3 displays a ribbon diagram of murine CAR complexed with the co-activator SRC-1 and the ligand and activator CITCO (Xu *et al*., 2004). Since CAR does not prove to be a classical nuclear receptor due its ligand-independent constitutive activity, it is not obvious how the capability of CAR to be persistently active is carried out. The AF-2 region of human CAR is stabilized by the residue Ile[330] instead of Cys[357] (Frank *et al*., 2004). Human CAR relies on different amino acids that stabilize its constitutive activity. The constitutive activity of CAR is carried out by at least four contacts among the amino acids of helix 12, co-regulatory amino acids in helices 4 and 11, and a charge clamp between helices 12 and 3. The amino acids in helix 12 comprise Leu[343], Glu[345], Cys[347], and the C-terminus. Both human and mouse orthologs demonstrate enhanced stability through a contact between CAR's C-terminus and the lysine of helix 4 as well as the charge clamp between the glutamate in helix 12 and the lysine in helix 3 (Frank *et al*., 2004).

So, rather unique features about human CAR's helix 12 / AF-2 domain explain CAR's constitutive and species-limited activity (Dussault *et al*., 2002). Regarding CAR's interactions with ligands and their influence on stabilization of the AF-2 / helix 12, there are differences compared to other nuclear receptors. In case of Androstanol, the inverse agonist of CAR, the mode of action or binding is different to that of agonists. Androstanol does not support the active form of CAR by avoiding direct contact of AF-2 and suppresses the interaction between AF-2 and helix 4 which usually promotes the active form to bind co-regulators (Shan *et al*., 2004).
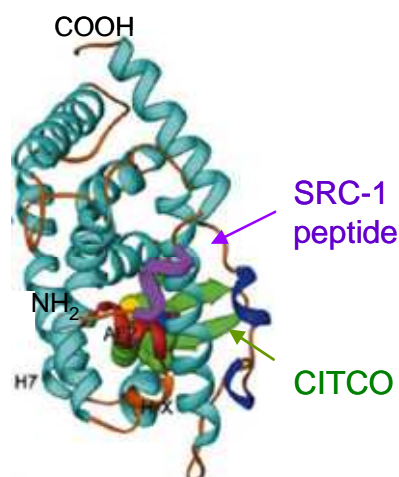
Xu *et al.*, 2004

Figure 1.3 Ribbon diagram of murine CAR (cyan) complexed with CAR agonist CITCO (green) and co-activator SRC-1 (magenta). The AF-2 helices of the ligand-binding domain of CAR are colored in red. Xue *et al*., 2004; Molecular Cell, Volume 6: 919-928

1.4.5 Activators and ligands modulating CAR activity

CAR belonged to the group of orphan nuclear receptors since there had been no distinctive endogenous ligand to it discovered (Enmark and Gustafsson, 1996). The androstane metabolites Androstanol and Androstenol, however, demonstrated to directly bind the receptor and to act as inverse agonists (Forman *et al*., 1998). Thus, CAR needs to be considered as an adopted orphan nuclear receptor. However, CAR is constitutively active even in the absence of any added ligand. Yet, CAR can be activated additionally by ligands.

The ligand binding domain of CAR, as well as PXR, includes a binding pocket which is designed to bind lipophilic substances in the first place. These lipophilic substances mainly belong to the class of small molecules. All these organic molecules have low molecular weights of less than 1 kDa. Both CAR and PXR have a quite similar and overlapping but not identical set of ligands. Most steroid hormone receptors bind their ligands with high affinity and specificity unlike CAR and PXR. One of the most prominent CAR activators is PB (figure 1.4A). Phenobarbital is known as one of the first discovered inducers of CAR activation. PB induces among others genes of the *CYP2B6* subfamily (Waxman and Azaroff, 1992). It is a barbiturate which has sedative and hypnotic characteristics for which it was clinically used until it was replaced by the benzodiazepines. PB is one of the few drugs to

induce CAR in multiple species equally including humans, mice and rats (Sueyoshi *et al*., 1999; Honkakoski *et al*., 1998; Muangmoonchai *et al*., 2001). After exposure of cells to Phenobarbital, translocation of CAR from the cytoplasm to the nucleus takes place. This translocation does not occur due to direct binding of Phenobarbital to CAR but as a result of an indirect activation. Phenobarbital causes a phosphorylation / dephosphorylation cascade that finally leads to dephosphorylation of Ser^{202} of mCAR by PP2A. More than 140 genes can be induced or repressed due to PB exposure. Half of these genes are under control of CAR. Furthermore, PB also stimulates recruitment of co-activators (Min *et al*., 2002).

Another activator of CAR was discovered in a FRET-based drug-assay. In contrast to PB, 6-(4-chlorophenyl)imidazo[2,1-*b*][1,3]thiazole-5-carbaldehyde   *O*-(3,4-dichlorobenzyl)oxime (CITCO), an imidazole derivative, is able to directly bind and activate CAR (figure 1.4B) (Maglich *et al*., 2003). CITCO binds the receptor resulting in nuclear translocation and accumulation of CAR inside the nucleus (Maglich *et al*., 2003). Further characteristics of CITCO as a potent agonist of human CAR are the actitvity in *in vitro* fluorescence-based activation assays, its selectivity for CAR over other nuclear receptors such as PXR, and its capability to induce the CAR target gene *CYP2B6* in primary human hepatocytes. On one hand, the discovery of CITCO is of great importance since it enables a more successful search for additional CAR target genes and further elucidation of CAR translocation and, thus, CAR activation. On the other hand CITCO is a purely synthetic substance without any use as a pharmaceutical drug and might, therefore, not be as important for medical use and the prediction of drug-based side effects.

Artemisinin was discovered to be a potent CAR agonist (figure 1.4B). Artemisinin is a sesquiterpene lactone endoperoxide which is currently the only antimalarial drug which *Plasmodium falciparum* has not yet developed resistance to (White, 2004). It is extracted from the leaves of the Chinese plant *Artemisia annua* (Klayman, 1985). The sesquiterpene derivative showed CAR as well as PXR agonist activity in both human and mouse. CAR agonist activity was demonstrated by inducing transcriptional activity in primary human hepatocytes and in the intestinal cell line LS174T (Burk *et al*., 2005). Artemisinin-induced activation of CAR was also demonstrated in the form of recruitment of the co-activator DRIP 205 (Vitamin D-interacting protein 205) and distinctive induction of *CYP2B6*, *MDR1* and *CYP3A4* (Burk *et al*., 2005). On the other side, the amount of Artemisinin of 100 µM used in reporter gene assays is not comparable to the plasma peak concentration of 2 µM at the most *in vivo* (Svensson *et al*., 1998). This finding also proved to be one of the disadvantages of Artemisinin. In addition to that, long-term monotherapy with Artemisinin leads to high rates

of recrudescence due to its decrease in plasma concentrations to 20 to 30%. Additionally, the extent of activation in the reporter gene assay was rather weak by less than two fold activation. So these findings may suggest possible discrepancy of Artemisinin-induced agonist activity *in vitro* in experiments and *in vivo* in patients. Yet, relevant biological activity depends on the sesquiterpene concentration inside liver cells. Artemether and Arteether are both semi-synthetic pharmaceuticals and derivatives of the originally naturally occurring sesquiterpene Artemisinin (figure 1.4C). Artemether is a methyl ether derivative of Artemisinin. Artether however might be better known using the name Artemotil than ß-Arteether. It is metabolized to Dihydroartemisinin within the human body. This metabolite is therapeutically equally effective as Artemisinin.

Clotrimazole is a substance known as the inverse agonist of human nuclear receptor CAR (Lempiäinen *et al.*, 2005). The structure of Clotrimazole is depicted in figure 1.4D. It reduces basal CAR activity to less than 0.5x of basal activity *in vitro* resulting in values like EC_{50} ~ 0.7 µM (Moore *et al.*, 2000). Clotrimazole is normally used in antifungal treatment. On the other hand it is a mouse CAR agonist stimulating SRC-1 recruitment (Mäkinen *et al.*, 2003). In contrary to the androstane metabolites it can be used as inverse agonist of human CAR in order to force release of co-activators or agonists.

Triphenylphosphate is a human CAR activator. Activation in mouse CAR, however, could not be verified clearly (Honkakoski *et al.*, 2004). Additionally, MD (molecular dynamics) simulations containing CAR and TPP were performed to test putative agonist activity (Jyrkkärinne *et al.*, 2005). Several simulations resulted in TPP always forming a hydrogen bond to His[203] of CAR LBP. TPP is a triester phosphoric acid and phenol (figure 1.4E). It is toxic to fish, shrimps and daphnids since it inhibits their acetylcholine esterase.

Fenofibrate and Clofibrate have already been proven to induce nuclear translocation of CAR in mice (Guo *et al.*, 2007). Fenofibrate as well as Clofibrate are substances of the fibrate class (figure 1.4E). As such they belong to the group of lipid lowering agents. Fenofibrate is a chemical therapeutically used to treat high cholesterol levels in patients with or at risk of cardiovascular disease. Fenofibrate is either alone or in combination with statins administered to fight hypercholesterolemia and hypertriglyceridemia (Sommariva *et al.*, 1984). The benefit of many fibrates is the reduction of low-density (LDL), very low density (VLDL), and high-density lipoproteins (HDL) as well as tryglycerides levels (de la Serna and Cadarso, 1999). Clofibrate enhances lipprotein lipase activity in order to eventually reduce VLDL and LDL.

Bisphenol A is a substance possessing two functional phenol groups (figure 1.4E). In a luciferase transactivation assay screen of 60 mostly non-steroid compounds the diphenyl

compound did not demonstrate ligand activity towards CAR whereas Bisphenol A dimethylacrylate and Bisphenol A dimethylether proved agonist binding to CAR (Dring *et al*., 2010). However, this study also revealed that specific Bisphenol A derived compounds had agonist activity towards one CAR isoform but inverse agonist activity towards the other CAR isoform. The isoforms used in the ligand screens revealing contradictory binding behavior towards the same compound were wildtype CAR (CAR1) and CAR3 which is the ligand-dependent isoform of the receptor (Auerbach *et al*., 2003; Arnold *et al*., 2004; Dring *et al*., 2010).

CAR is known to be deactivated by Androstane metabolites (figure 1.4F). Only the derivatives Androstanol (5α-androstan-3α-ol) and Androstenol (5α-androstan-16en-3α-ol) constitute two endogenous ligands of both murine and human CAR. This means only derivatives which are reduced in position 5 and hydroxylated in position 3 fulfill the essential stereo specificity in order to enable binding. Binding of these hormone derivatives and inverse agonists results in co-activator release from the ligand binding domain (Forman *et al*., 1998). Though they make co-activators dissociate from CAR, these androstanes don't interfere with heterodimerization or DNA-binding. The androstanes derivatives are known to bind both human and murine CAR but act as selective potent mouse but only weak human CAR inhibitors (Moore *et al*., 2000). The co-activator SRC-1 binds RXR, too. Androstenol, however, has no effect on the stability of the SRC-1 – RXR complex (Forman, 1998).

(A
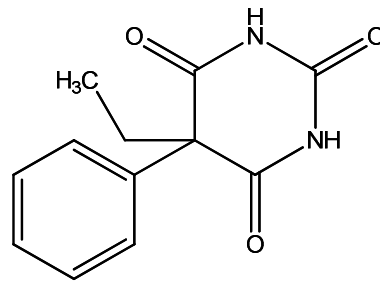
Phenobarbital

(B)

CITCO

Artemisinin

(C)

Artemether

Arteether (Artemotil)

(D)

Clotrimazole
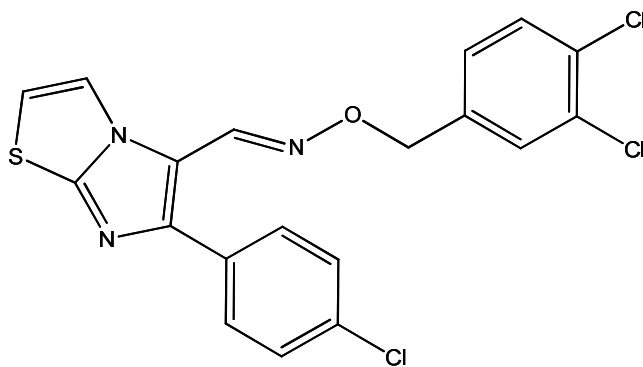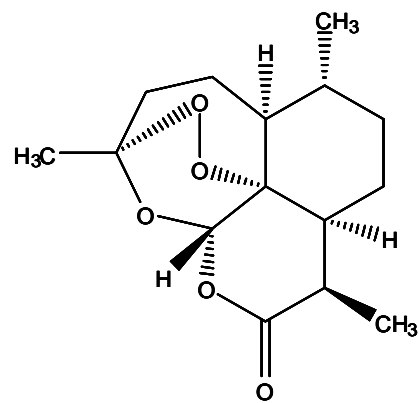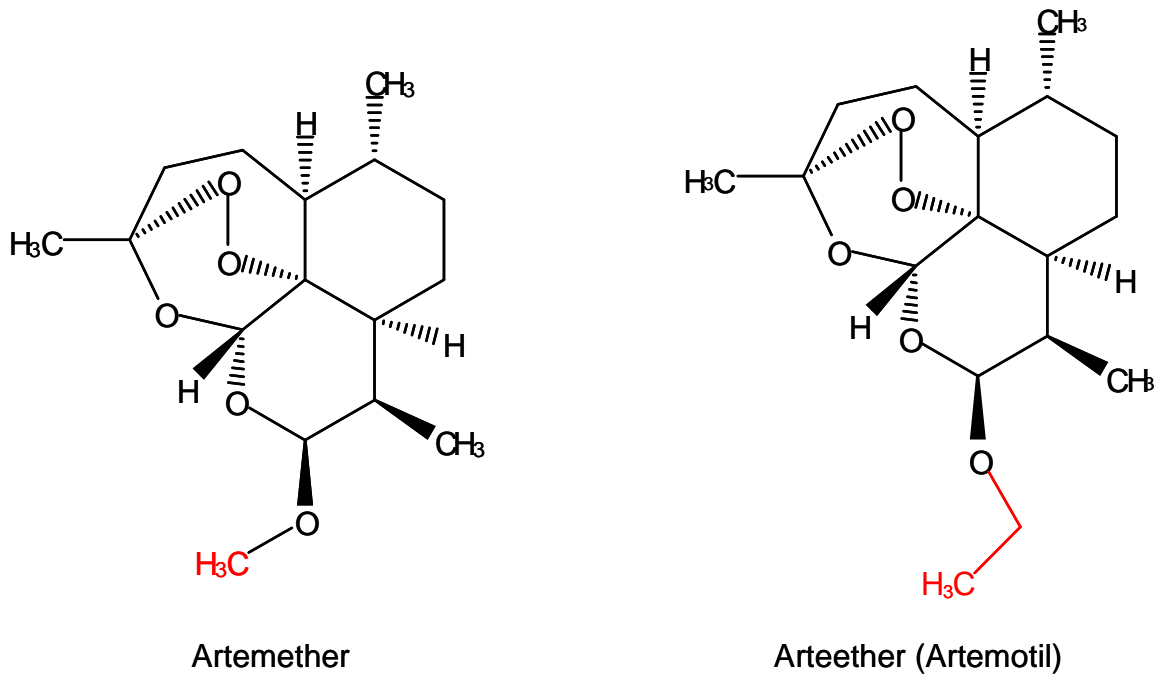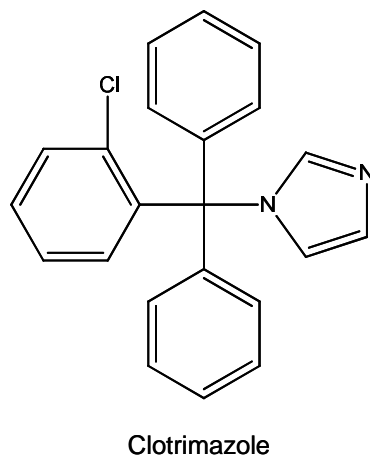
(E)
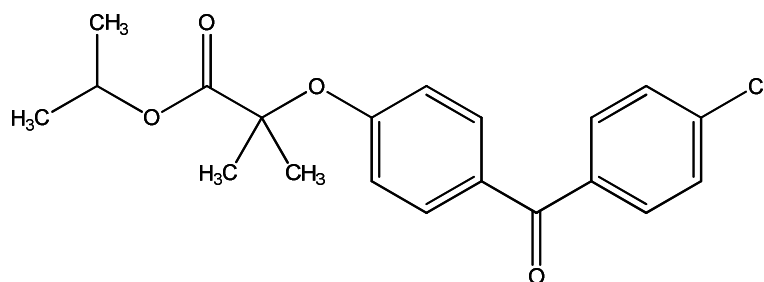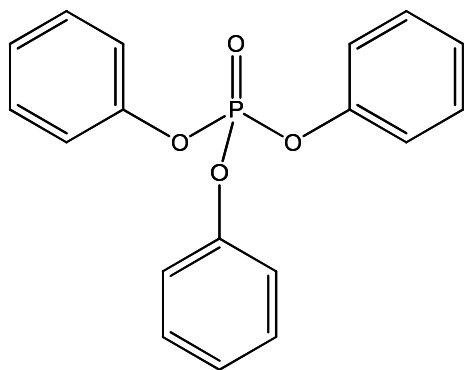
Fenofibrate

Triphenylphosphate

Clofibrate

Bisphenol A

(F)

Androstenol
(5α-androst-16-en-3α-ol)
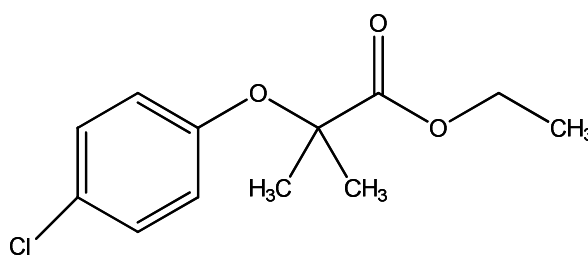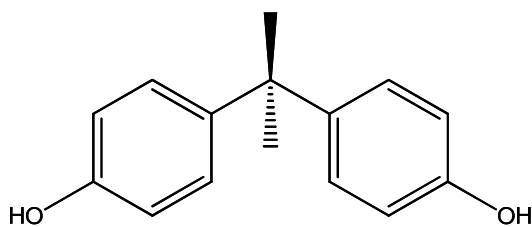
Androstanol
(5α-androstan-3α-ol)
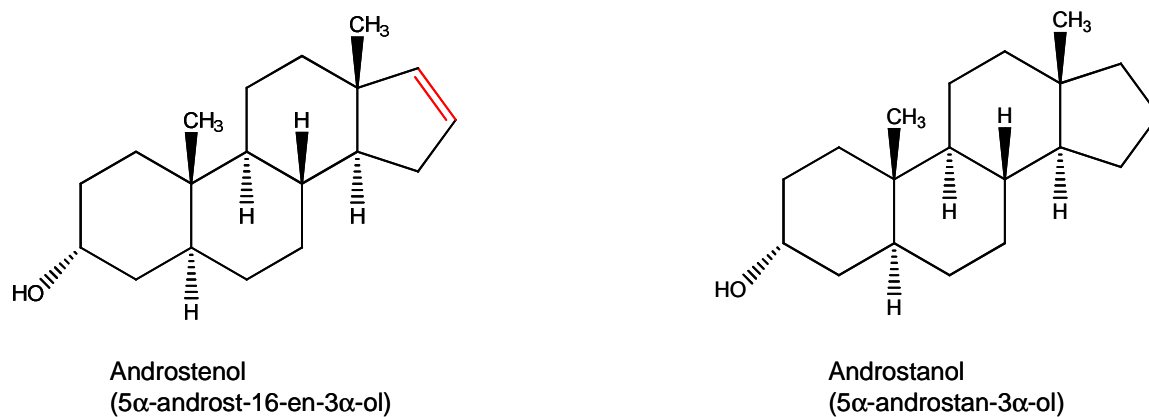
Figure 1.4 Chemical structures of synthetic drugs and naturally occurring compounds. Apart from the androstane metabolites, the compounds and substances depicted belong to the group of small molecules and, thus, have low molecular weights of less than 1 kDa. **A**: inducer, **B**: agonists, **C**: derivatives of the agonist Artemisinin, **D**: inverse agonist of human CAR and agonist of mouse CAR, **E**: putative agonists or compounds with unknown biological activity, and **F**: ligands of human CAR and inverse agonists of mouse CAR. Differences in related structures are highlighted in red.

Table 1.1 summarizes substances and compounds from the group of small molecules which have impact on the activity of human CAR. It includes both direct as well as indirect activators and compounds demonstrating species-specific ligand binding.

Table 1.1 Synthetic drugs or natural compounds regulating human CAR activity.

Synthetic drugs / natural products

Agonists

Artemisinin[a]

CITCO

Indirect activators

Phenobarbital

Phenytoin

Acetaminophen[b]

6,7 - Dimethylesculetin[a]

Activators with unknown biological effect

Atorvastatin

Cerivastatin

Fluvastatin

Simvastatin

Inverse agonists

Clotrimazole[c]

Meclizine[d]

---

[a] naturally occuring compounds

[b] pharmaceutical known under the German brand name of *Paracetamol*

[c] inverse agonist of human CAR

[d] inverse agonist of mouse CAR

1.4.6 Atorvastatin

Cell based reporter assays using FLC7 cells identified Atorvastatin as an inducer of human CAR activity (Kobayashi *et al*., 2005). Additionally, the statin induced *CYP2B6*, the main target gene of CAR, in primary human hepatocyte cultures (Kocarek *et al*., 2002). Consistent with these findings, statins including Atorvastatin were shown to induce the expression of *CYP2B6, CYP3A4*, *CYP2C9* and other CYPs (Feidt *et al*., 2010; Monostory *et al*., 2008).

The statins constitute a class of drugs that is described by its capability to reduce cholesterol levels in the blood (Kocarek *et al*., 1993; Kocarek and Reddy, 1996). One of the statins is Atorvastatin which is sold using diverse brand names like *Sortis* in Germany and *Lipitor* mostly in English-speaking countries (figure 1.5) (Chong and Seeger, 1997; Black *et al*., 1998). It is produced as Atorvastatin calcium and is also known as (3*R*,5*R*)-7-[2-(4-fluorophenyl)-3-phenyl-4-(phenylcarbamoyl)-5-(propan-2-yl)-1*H*-pyrrol-1-yl]-3,5 dihydroxyheptanoicacid (figure 1.5).

Increased cholesterol concentrations can be very critical to the cell. Atherosclerosis is a pathological condition in which cholesterol-containing plaques are formed inside of arteries and block the flow of blood to the tissues the arteries supply. This effect and further consequences can lead to serious harm to the heart. In order to prevent these medical conditions, patients are advised to take statins to minimize the content of cholesterol and, thus, the amount of cholesterol-containing plaques and even minimize the size of already existing plaques. But also patients with a high genetic likelihood to encounter cardiovascular disease are advised to take statins.

Atorvastatin belongs to the family of statins and as such it is a competitive inhibitor of the HMG-CoA (3-hydroxy-3-methylglutaryl - Coenzyme A) reductase (figure 1.6). HMG-CoA reductase catalyzes the reduction of 3-hydroxy-3-methylglutaryl-CoA (HMG-CoA) to mevalonate (figure 1.6) (Nawrocki *et al*., 1995; Marais *et al*., 1997). This reaction is NADPH-dependent and releases CoA. The product mevalonate is an early precursor of squalen which is finally turned into cholesterol. The reduction of HMG-CoA represents the limiting step in cholesterol synthesis in hepatocytes since its synthesis can be inhibited at this very stage. Thus, the use of statins leads to reduced synthesis of cholesterol, a lipid which belongs to the low-density lipoproteins, and lowers cholesterol concentrations in the blood. Inside the human body Atorvastatin is extensively regulated by biotransformation (Jacobsen *et al*., 2000). The HMG-CoA reductase inhinbitor is among others metabolized to both para- and ortho-hydroxy

Atorvastatin lactone and acid derivatives. Atorvastatin metabolization occurs through CYP3A4 and is influenced by *CYP3A5* polymorphism (Park *et al.*, 2008).

Atorvatatin-dependent induction of CAR activity was already shown but agonist activity could not be demonstrated yet (Kobayashi *et al.*, 2005).
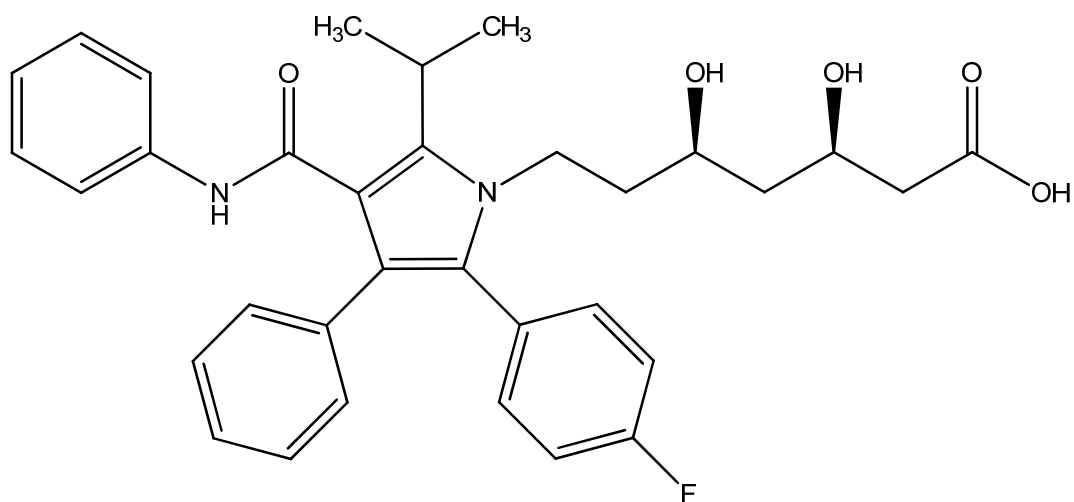
Figure 1.5 Chemical structure of Atorvastatin. Atorvastatin inhibits the HMG-CoA reductase which reduces HMG-CoA to mevalonate. The inhibition of HMG-CoA reductase blocks cholesterol synthesis.

HMG-CoA

HMG-CoA
reductase

2 NADPH

2 NADP$^+$

CoA
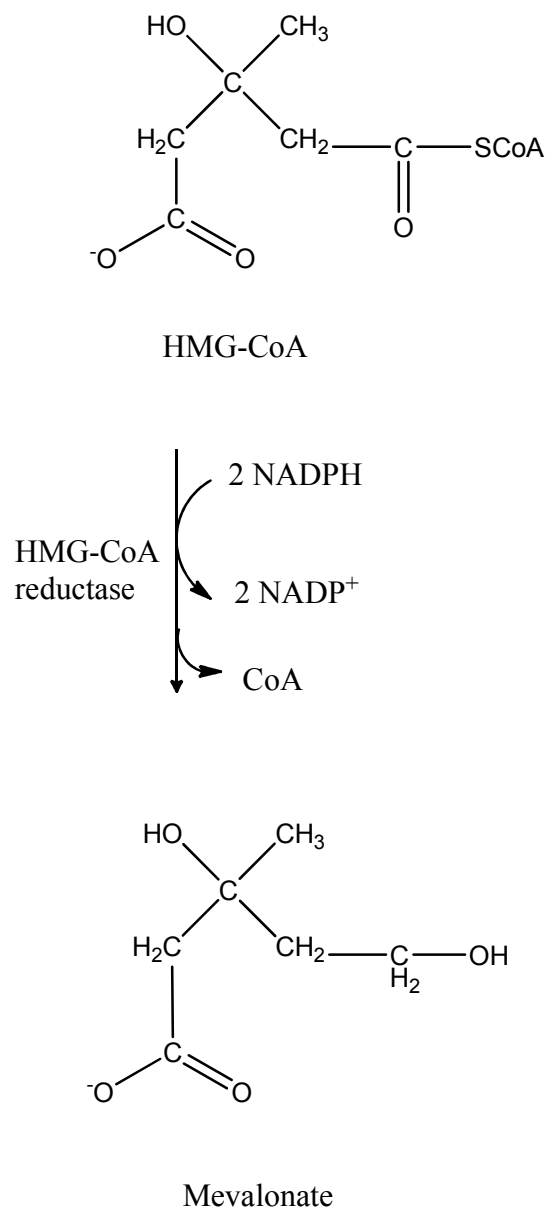
Mevalonate

Figure 1.6 The NADPH-dependent reduction of HMG-CoA to mevalonate. The reduction represents the pivotal step in cholesterol synthesis due to its susceptibility to inhibition.

1.5 The nuclear receptor co-activators SRC-1 and SRC-2

Nuclear receptor co-activators as well as co-repressors belong to the class of nuclear receptor co-regulators. In general, co-regulators assist nuclear receptors with their transcriptional activity. Co-activators enhance, co-repressors however repress transcriptional activity of the receptor.

SRC-1 (steroid receptor co-activator 1) or NCoA1 (nuclear receptor co-activator 1) and SRC-2 (steroid receptor co-activator 2) or NCoA2 (nuclear receptor co-activator 2) belong to the p160 family of co-activators (Onate *et al*., 1995; Voegel *et al*., 1996; Voegel *et al*., 1998). The p160 family consists of SRC-1, SRC-2, and SRC-3 to be complete (Anzick *et al*., 1997).

Members of the p160 family of co-activators are important in hormone metabolism, fertility, and growth development (Xu *et al*., 1998; Gehin *et al*., 2002; Wang *et al*., 2000; Xu *et al*., 2000). Mice which could not express SRC-1 were partly insensitive to diverse steroid hormones to which they could normally respond to when not lacking the co-activator (Xu *et al*., 1998).

Members of the steroid protein family of co-activators display high conservation in their N-termini but also high divergence in their C-termini (Leo and Chen, 2000; Xu and Li, 2003). The conserved N-terminal region of the SRC family harbors the basic helix-loop-helix and Per/ARNT/Sim (PAS) domain which is responsible for homo- and heterodimeric interactions among proteins possessing these motifs (figure 1.7) (Huang *et al*., 1993). Both SRC-1 and SRC-2 possess receptor interaction domains (RID) or nuclear receptor boxes (NR box) which consist of conserved LXXLL motifs (Ding *et al*., 1998). There are three of these domains to each co-activator located in the central part of the proteins. SRC-1, however, is the only p160 member to contain an additional LXXLL motif in the extreme carboxy terminal region. The LXXLL motifs are essential to carry out interactions with mostly liganded receptors. This motif is also located in other co-regulatory protein family members like TRAP (thyroid hormone receptor associated protein) or p300/ CREB (cAMP-response element-binding protein).

The LXXLL motif serves to initiate binding between the receptor's AF-2 region and the co-activator's NR box. A conserved amphipathic helix within the AF-2 region seems to be crucial to interact with the LXXLL motif. However, it has been proposed that human SRC-1 also promotes interaction between the N-terminal AF-1 and the C-terminal AF-2 region of a nuclear receptor (Onate *et al*., 1998).

Apart from the RIDs (receptor interaction domains), SRC-1 also possesses intrinsic histone acetyltransferase activity (EC 2.3.1.48) (Spencer *et al*., 1997). When acetylation takes place the positive charged lysine residues are neutralized and affinity to chromatin sub-structures is lowered, thus, facilitating access to DNA regions.

SRC-1 and SRC-2 co-activate many nuclear receptors among others CAR and ER (estrogen receptor) (Forman *et al*., 1998; Muangmoonchai *et al*., 2001; Min *et al*., 2002). ER has been

proven to bind SRC-1, SRC-2 and SRC-3 by surface plasmon resonance (Cheskis *et al.*, 2003).

Generally, co-activators like SRC-1 bind their distinctive nuclear receptors via their LXXLL binding motif after the receptor has already bound its explicit ligand. Ligand binding of the receptor introduces conformational changes promoting co-activator binding. CAR, on the other hand, is a constitutive active receptor which does not depend on ligand binding to be active and, thus, to bind its distinctive co-activators. Since one of the main functions of ligand binding of nuclear receptors is the recruitment of co-activators, one has to clarify the essential meaning of co-activators to CAR which is ligand independent. Still unanswered questions are whether CAR prefers one co-activator over the other regarding the members of the steroid co-activators for example. Of course, there are natural conditions which force receptors to interact with specific co-activators like tissue-dependent expression profiles and expression levels of both the nuclear receptor and the respective co-activators. All in all, CAR's constitutive activity does depend to a high degree on the ligand independent recruitment of co-activators.
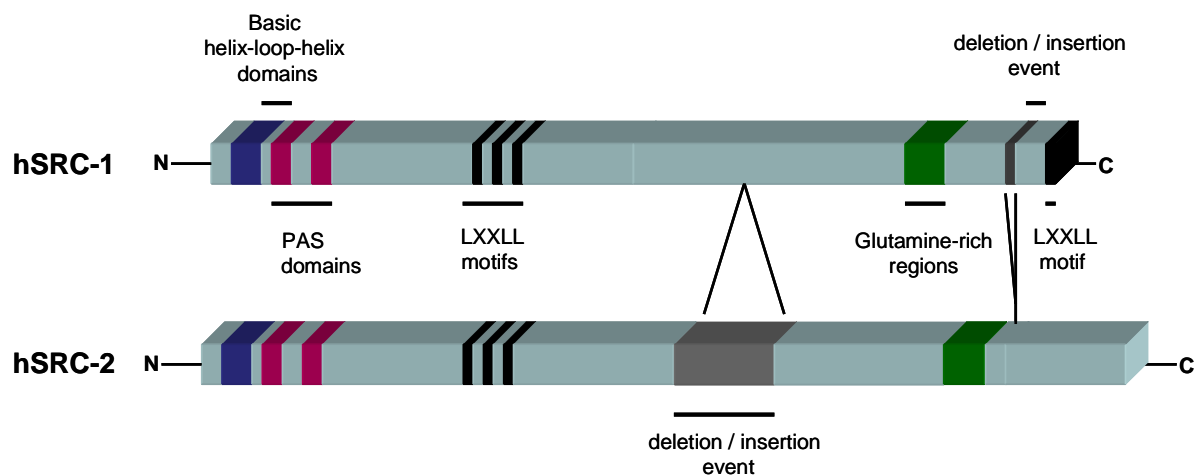
Figure 1.7 Figure depicting the most important functional regions of the co-activators SRC-1 and SRC-2. The co-activators of the p160 family share the N-terminal conserved region and the highly divergent C-terminal region. The characteristic NR boxes consisting of LXXLL motifs are located in the central part of the proteins. SRC-1 is the only member of the p160 co-activator family to harbor an additional LXXLL motif at the extreme part of the C-terminus. PAS: Per/Arnt/Sim domains.
This figure was modified based on Wu *et al.*, 1993; Endocrine Reviews 26 (3): 393-399.

1.6 Surface plasmon resonance (SPR) Technology

1.6.1 Surface plasmon resonance

Biacore technology enables the examination and determination of kinetics, specificity, affinity, thermodynamics, and the concentration of active molecules which are injected free in solution over the surface of a sensor chip (www.biacore.de). Biacore 3000, therefore, allows the determination of parameters which can distinctively characterize the nature of a binding by yielding equilibrium dissociation constants as well as association and dissociation rate constants. With the help of surface plasmon resonance-based technology the interaction between two molecules can be measured in real-time. For this purpose, the molecules don't need to be labeled in order to be detected (Cooper, 2003). Interactions of biomolecules such as proteins, peptides, carbohydrates, lipids, and nucleic acid can be measured. Even substances like small molecules e.g. drug candidates or whole cells can be investigated. Therefore, Biacore technology is widely used in pharmaceutical drug discovery and antibody characterization.

1.6.2 Basics of SPR

Biacore technology is based on surface plasmon resonance (SPR) which was observed for the first time by Turbadar in 1959. After the initial observation, the phenomenon of SPR was investigated (Otto, 1969).

In order to generate the phenomenon of SPR an interface of two media of different refractive index and a thin layer of conducting film is necessary (figure 1.8). Biacore technologies provide a glass layer and a sample solution to act as the necessary different media whereas the conducting film is represented by the gold layer. Surface plasmon resonance occurs when the p-polarized light is reflected at the interface under conditions of total internal reflection (Kretschmann and Raether, 1968; Fägerstam *et al.*, 1992). The electric field which is formed at the interface is referred to as evanescent wave (Ekgasit *et al.*, 2004). The reflected light causes the evanescent wave field, without actually losing energy, to propagate across the interface into the medium of lower refractive index (Raether *et al.*, 1988; Ekgasit *et al.*, 2004).

The beam of visible incident light therefore serves as the trigger for exciting surface plasmons in the gold film to resonate. The excitation by incident light takes place when a certain angle of incidence and wavelength are combined. SPR can then be detected as a drop in the intensity of the reflected light. Additionally, a glass prism is necessary in order to totally reflect the light (Fägerstam *et al*., 1992). Therefore, Biacore systems possess glass sides that are pressed against semi-cylindrical glass prisms using silicone opto-interfaces.

The above quoted plasmons are created when free electrons oscillate against fixed positive ions in a metal like gold. Surface plasmons are plasmons localized to a surface that intensively interact with the photons of the incident light. Due to the coupling of photons with the surface plasmons, energy is released and the intensity of the reflected light drops. The evanescent wave propagates parallel to the interface. Since the wave occurs and spreads across the interface SPR is very sensitive to changes in the sample solution at the interface. Changes in the solution are measured as changes in the refractive index of the solution and, therefore, as changes in the SPR signal. Interactions of the immobilized protein and the drug or protein that is passed over in the sample solution cause an increase in sample concentration and, thus, a representative increase in refractive index. This enhancement changes the angle of incidence which is necessary to form the surface plasmon resonance and the SPR angle (figure 1.8 and 1.9). SPR is detected as a function of time and, hence, displayed in a Biacore sensorgram as time plotted against change in the refractive index depicted as resonance units (RU).

The amplitude of the evanescent wave field decreases as a function of distance from the interface (Ekgasit *et al*., 2004). Thus, only changes in refractive index close to the interface influence the SPR signal and are detected as changes in the sensorgram (Homola *et al*.,1999).
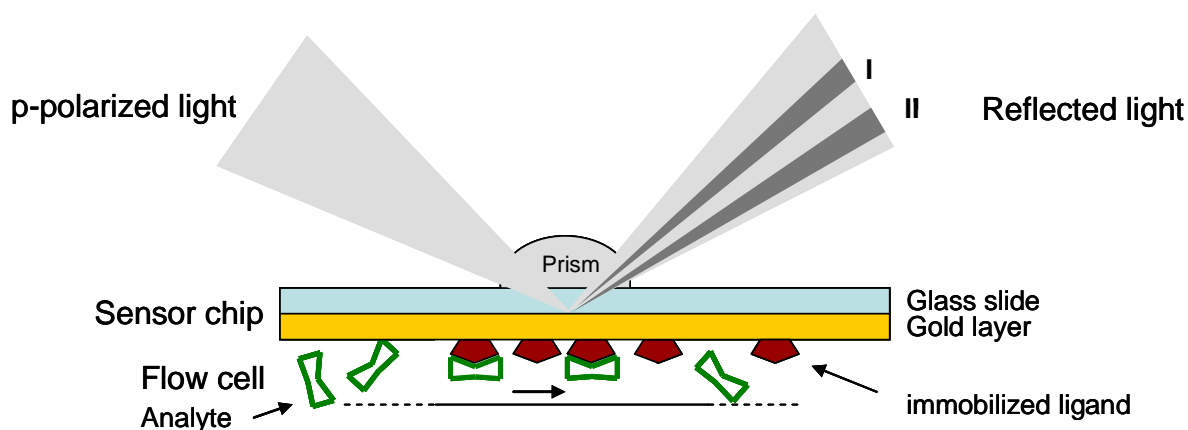
Figure 1.8 The principle of surface plasmon resonance. p-polarized light is reflected under conditions of total internal reflection. Due to the coupling of photons with the plasmons of the evanescent wave, the reflected light loses intensity. This drop of intensity leads to a drop of reflected light which is measured as change in the refractive index. **I**: angle I; **II**: angle II. This figure was modified according to Biacore Sensor Surface Handbook, version AA.
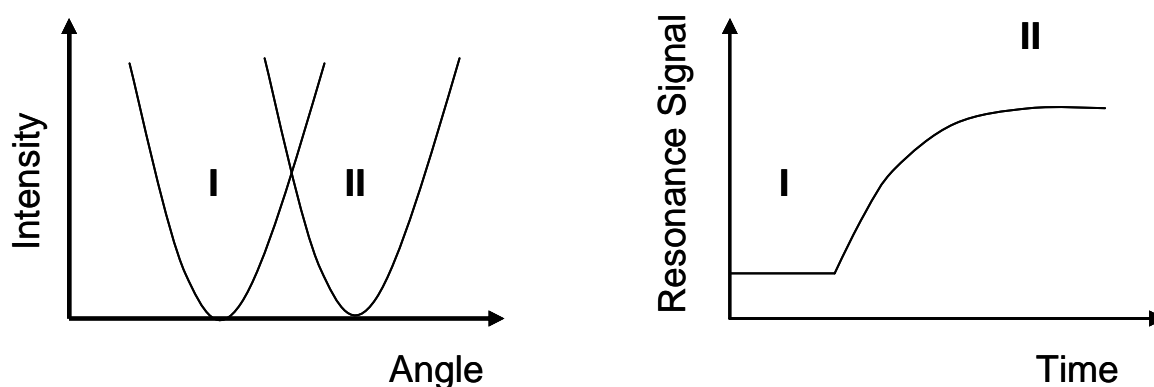
Figure 1.9 SPR detection. The increase in sample concentration at the surface of the sensor chip leads to an adequate change in refractive index which finally changes the angle of incidence which is necessary to actually form surface plasmon resonance and the SPR angle. **I**: angle I; **II**: angle II.
This figure was modified according to BIAtechnology Handbook.

1.6.3 Biacore terminology

In order to measure direct interactions using Biacore technology (e.g. Biacore 3000), one of the interaction partners is covalently immobilized on the sensor surface. It is referred to as the "ligand" which relies on the terminology used in affinity chromatography (figure 1.10). The binding partner which is free in solution and passed over the sensor surface to bind the ligand is referred to as the "analyte". The binding of the analyte to the immobilized ligand is

depicted in a sensorgram of response against time. The analyte is carried in running buffer and injected to pass over the sensor surface. Before and after analyte injection, running buffer continuously flows over the sensor surface (Biacore Getting Started 28-9384-71 Edition AC).
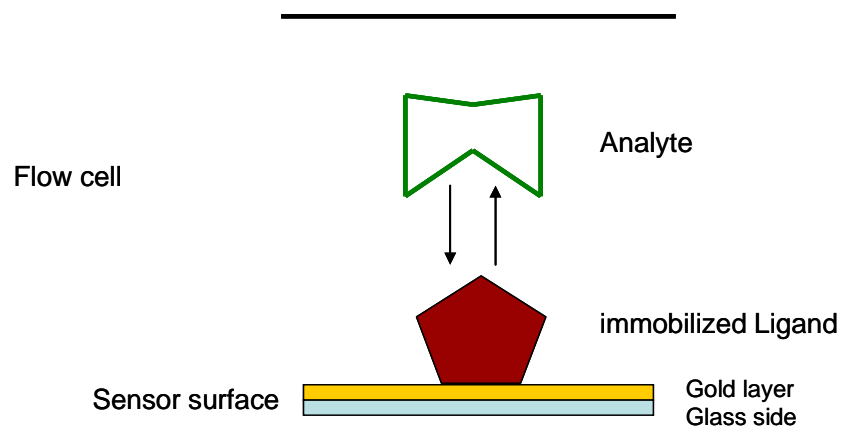
Figure 1.10 Biomolecular interactions on a Biacore CM5 chip. The molecule which is covalently immobilized on the chip surface is referred to as the "ligand" whereas the molecule which is passed in free solution over the sensor surface is referred to as the "analyte".
This figure was modified according to Biacore Sensor Surface Handbook, version AA.

1.7 Objective of this thesis

The nuclear receptor CAR is a constitutive active receptor which recruits co-activators in a ligand-independent manner. Yet, it has been shown that after ligand binding the constitutive activity of CAR can be further enhanced or inhibited (Maglich *et al*., 2003; Burk *et al*., 2005). Since CAR is responsible for regulation of genes encoding enzymes and proteins involved in detoxification, most of the selected drugs are pharmaceutically relevant compunds which were examined in screenings performed at the IKP. The HMG-CoA reductase inhibitor Atorvastatin and its metabolites, among others, were chosen to investigate ligand-dependent activation or deactivation of CAR. In addition, binding of CAR to its co-activators SRC-1 and SRC-2 was aimed to be characterized. Therefore, the first aim of this thesis work was to express both the nuclear receptor CAR and the co-activators SRC-1 and SRC-2 solubly and purify the proteins to a high degree from *E. coli* cell lysate in order to investigate interactions by means of surface plasmon resonance.

One main goal of the presented work was to investigate to what extent the selected ligands influence the complex formation of CAR and SRC-1 or SRC-2. Another main goal was the kinetic characterization of receptor – co-activator binding regarding association and dissociation in the presence and absence of ligands. Since kinetic assays do not only yield equilibrium dissociation constants but also association and dissociation rate constants, which are able to characterize both the constitutive binding and the ligand-induced binding more detailed, qualitative information of the influence of ligands on the receptor was expected. These SPR experiments may answer the question which co-activator might be preferred by CAR regardless of tissue-dependent expression profiles and expression levels.

Clofibrate and Fenofibrate as well as Atorvastatin were demonstrated to be activators of CAR but could not be confirmed as agonist ligands so far (Guo *et al*., 2007; Kobayashi *et al*., 2005). Thus, another goal of this thesis work was to examine whether these drugs regulate CAR by direct agonist binding or indirect activation.

2 Materials and Methods

2.1 Materials

2.1.1 Lab material

Lab material which was used on a daily basis is listed in the following table.

Table 2.1 Lab material for daily use

Material	Company
pipette tips, petri dishes (9.4 cm Ø), microtiter plates (96 wells)	Greiner, Frickenhausen
0.5, 1.5, and 2.0 ml vials	Eppendorf, Hamburg
1.5 ml cuvettes, semi-micro, PS	Ratiolab, Dreieich-Buchschlag
Spectra/Por® Dialysis membrane	Spectrum Laboratories, Inc., Breda, the Netherlands

2.1.2 Chemicals

The chemicals used during the work are listed in table 2.2 and grouped according to the company they were purchased from.

Table 2.2 Chemicals

Chemical	Company
Ethanol 98% for analysis, 2-Propanol	Riedel-deHaën, Seelze
Acryamide / Bisacrylamide 30%, Bacto-Peptone	Roth GmbH, Karlsruhe
Agar, Ammonium Peroxide Sulfate (APS),	Fluka Chemie, Buchs, Switzerland

Ampicillin (sodium salt), Bromophenol Blue, Coomassie Brilliant Blue R250, Dimethyl sulfoxide (DMSO), Disodium hydrogen phosphate, Ethidium bromide, Glycine, Yeast extract, Imidazole, Isopropyl β-D-thiogalactopyranoside (IPTG), ß-Mercaptoethanol, Sodium dihydrogen phosphate, Sodium Dodecyl Sulfate (SDS), Sodium hydroxide, Rubidium chloride	
Agarose, 1kb DNA ladder	Carl Roth, Karlsruhe
Unstained protein ladder (SDS-PAGE) SM#0661 SM#0431	Fermentas, St. Leon-Rot
Tryptone	DIFCO, USA, Detroit
Methanol	Roche, Mannheim
Talon® His-Tag Purification Resins	Clontech, Heidelberg
EDC (1-ethyl-3-(3-dimethylaminopropyl) carbodiimide)	Biacore / GE Healthcare, München
NHS (N-hydroxysuccinimide)	
Ethanolamine	

2.1.3 Drugs

Drugs and endogenous compounds used for interaction analysis via surface plasmon resonance were donated from Oliver Burk from the Dr. Margarete Fischer-Bosch-Institut für Klinische Pharmakologie (IKP Stuttgart).

Table 2.3 Drugs and endogenous compounds

Drugs and endogenous compounds	Company
Artemisinin, Artemether and Arteether	Dafra Pharma, Oud-Turnhout, Belgium
CITCO, Clotrimazole, Phenobarbital, Triphenylphosphate, Bisphenol A, 5α-Androstan-3α-ol, 5α-Androstan-16en-3α-ol, Clofibrate, Fenofibrate, Atorvstatin, Atorvstatin lactone and acid as well as their respective para- and ortho metabolites	Sigma-Aldrich, Schnelldorf

2.1.4 Kits

The kits were used at DNA or protein level for analytical and preparative purposes.

Table 2.4 Kits

Kits	Company
GenElute^{TM} Plasmid Miniprep Kit	Sigma-Aldrich, Taufkirchen
QIAquick® Gel Extraction Kit	Qiagen, Hilden
QIAquick® PCR Purification Kit	Qiagen, Hilden
BCA Protein Assay Kit	Pierce, Rockford (USA)
Silver staining Kit	Fermentas, St. Leon-Rot
Biacore Amine Coupling Kit	Biacore / GE Healthcare, München

2.1.5   Bacterial strains

Table 2.5 Bacterial strains

Species	Strain	Genotype	Reference
Escherichia coli	DH5α	*supE*44 Δ*lac* U169 (Φ80 *lac*ZΔM15) hsdR17 recA1 endA1 gyrA96 thi-1 relA1	Clontech, Heidelberg
Escherichia coli	BL21(DE3)	*hsdS* *gal* (I*ts*857 *ind*1 Sam7 *nin*5 *lac*UV5-T7 *gene* 1)	Novagen, Bad Soden

2.1.6   Plasmids

Table 2.6 Vectors

Plasmids	Company
pET28a(+)	EMD Biosciences (Novagen), San Diego, USA
pET22b(+)	EMD Biosciences (Novagen), San Diego, USA

2.1.7   Enzymes

Enzymes were used for introduction of restriction sites, digestion of DNA and ligation of digested DNA.

Table 2.7 Enzymes

Enzyme	Company
Restriction enzymes	
BamHI	Fermentas, St. Leon-Rot
NdeI	Fermentas, St. Leon-Rot
PCR	
Pfu **DNA polymerase**	Fermentas, St. Leon-Rot
Ligation	
T4 DNA Ligase	Fermentas, St. Leon-Rot

2.1.8 Synthetic Oligonucleotides

Synthetic oligonucleotides were purchased from Metabion (Martinsried) and used for amplification of DNA.

Table 2.8 Synthetic oligonucleotides

Name	Sequence (5' → 3')	Application
CAR LBD for 105aa (*Nde*I)	GGAATTCCATATGCAACTGAGTAAGGAGCAAGAAG	Synthesis of the ligand-binding domain (LBD) of CAR
CAR rev 348aa (*Bam*HI)	CGCGGATCCTCAGCTGCAGATCTCCTGGAG	Synthesis of the ligand-binding domain (LBD) of CAR
SRC1 for 617aa (*Nde*I)	GGAATTCCATATGGACAGACTTTCAGATGGAGACAG	Synthesis of the receptor interaction domains (RID) of SRC-1 without his-tag
SRC1 rev 769aa (*Bam*HI)	CGCGGATCCTTAGGATCCTCAATCAGGCTCAG	Synthesis of the receptor interaction domains (RID) of SRC-1 without his-tag
SRC1 for 617aa	GGAATTCCATATGCATCATCATCA	Synthesis of the receptor

10xhis-tag (*Nde*I)	TCATCATCATCATCATCATGACAG ACTTTCAGATGGAGACAG	interaction domains (RID) of SRC-1 introducing a 10x his-tag at the N-terminus
SRC-2 583aa for (*Nde*I)	GGAATTCCATATGAAAGACTGTT TGGACTATAT	Synthesis of the receptor interaction domains (RID) of SRC-2
SRC-2 779aa rev (*Bam*HI)	CGCGGATCCTCATGTGTTACTGGC AGGATCTGT	Synthesis of the receptor interaction domains (RID) of SRC-2

2.1.9   Sample material for PCR

Sample material which served as template for amplification via PCR was obtained from Oliver Burk from the IKP (Dr. Margarete Fischer-Bosch-Institut für Klinische Pharmakologie, Stuttgart).

2.1.9.1 Sample material for amplification of human CAR

The human nuclear receptor CAR was amplified by PCR from individual human liver cDNA and cloned into the pcDNA3 vector (Invitrogen) (Burk *et al*., 2002; Genbank accession number NM_005122 / GI 32189358). This vector served as a template for the amplification of the ligand binding domain (LBD) of human CAR. The oligonucleotides *CAR LBD for 105aa (Nde*I*)* and *CAR rev 348aa (Bam*HI*)* were used in the PCR to amplify the base sequence comprising amino acids 105 to 348. The oligos also introduced the restriction sites *Nde*I and *Bam*HI which were used for restriction and ligation of the PCR products.

2.1.9.2 Sample material for amplification of the human co-activators SRC-1 and SRC-2

The receptor interaction domains (RID) of the human co-activators SRC-1 and SRC-2 were amplified by PCR from individual human liver cDNA and cloned into vector pM (Arnold *et al*., 2004). These vectors served as templates for the amplification of the RID.

The oligonucleotides *SRC1 for 617aa (Nde*I*)* and *SRC1 rev 769aa (Bam*HI*)* served to amplify the base sequence comprising amino acids 617 to 769 of the human co-activator SRC-1. The oligos also introduced the restriction sites *Nde*I and *Bam*HI which were used for restriction and ligation of the PCR products. Furthermore, the reverse oligo introduced a stop codon to inhibit the expression of a C-terminal his-tag provided by the pET22b(+) vector. In order to produce an SRC-1 protein, possessing an N-terminal tag of 10 histidines, a different forward oligo (*SRC1 for 617aa + 10x his-tag (Nde*I*)* was used for amplification via PCR.

The oligonucleotides *SRC-2 583aa for (Nde*I*)* and *SRC-2 779aa rev (Bam*HI*)* were used in the PCR to amplify the base sequence comprising the amino acids 583 to 779. The oligos also introduced the restriction sites *Nde*I and *Bam*HI which were used for restriction and ligation of the PCR products.

2.1.10 Equipment

Table 2.9 Equipment

Instruments and equipment	Company
Agarose gel electrophoresis device **Mini-Sub^{TM} DNA Cell, Mini-Sub^{TM} DNA Cell GT**	BioRad, München
Power supply for gel electrophoresis	
BioRad Power PAC 3000 / 300	BioRad, München
Analytical Balances	
Precision Advanced	Ohaus Waagen, Giessen,
Basic	Sartorius, Göttingen
Incubator	
Multitron shaking incubator	Infors, Botmingen, Switzerland
SDS PAGE	
Gel dryer	BioRad, München
PCR	
Mastercycler epgradient S	Eppendorf, Hamburg
pH meter	
Digital pH meter pH525	WTW, Weilheim
Photometer	
Nanodrop ND-1000 spectrophotometer	Nanodrop Technologies, Delaware, USA
Western blot device	
Trans-Blot SD SEMI **DRY Transfer Cell**	BioRad, München
Centrifuges	
Eppendorf centrifuge 5417 R	Eppendorf, Hamburg
Eppendorf centrifuge 5810 R	Eppendorf, Hamburg
Sonifier ultrasonic cell disruptor	
Branson sonifier 250	Branson, Danbury, USA
Surface plasmon resonance	

Biacore 3000	Biacore / GE Healthcare, München

2.1.11 Complex media

Luria-Bertani (LB) Media (Sambrook *et al.*, 1989)

Bacto-Tryptone	10 g
Bacto-Yeast Extract	5 g
NaCl	10 g
H_2O_{bidest}	ad 1 l
pH 7.5 (NaOH)	

LB media was autoclaved at 121°C for 20 minutes. Antiobiotics were added to liquid media directly before use. For the preparation of LB agar plates, 16 g/l agar was added to the liquid media directly before autoclaving. Antibiotics were added when media reached around 50°C. Kanamycin was used at concentrations of 30 µg/ml and Ampicillin at 50 µg/ml.

2.1.12 Buffers

TE buffer	10 mM Tris
	1 mM EDTA
	pH 8.0
TAE buffer	242g Tris
(50x concentrated)	57 ml acetic acid 100%
	ad 1 l H_2O_{dest}
	pH 8.0
DNA loading buffer	12.01 g urea
	0.21 g EDTA
	25 ml glycerine
	50 mg bromphenol blue
	ad 1 l H_2O_{dest}

TfbI buffer	0.59 g KOAc
(Transformation buffer I)	2.42 g RbCl
	0.29 g $CaCl_2$
	2.0 g $MnCl_2 \cdot 4\ H_2O$
	30 ml glycerine
	200 ml H_2O_{dest}
	pH 5.8 (HOAc)

TfbII buffer	0.21 g MOPS
(Transformation buffer II)	1.1 g $CaCl_2$
	0.12 g RbCl
	15 ml glycerine
	100 ml H_2O_{dest}
	pH 6.5 (NaOH)

SDS gel electrophoresis buffer	30 g Tris
	144 g glycerine
	10 g SDS
	ad 2 l H_2O_{dest}

Lower Tris buffer	36.34 g Tris
	0.8 g SDS
	200 ml H_2O_{dest}
	pH 8.8 (HCl)

Upper Tris buffer	12.11 g Tris
	0.8 g SDS
	200 ml H_2O_{dest}
	pH 6.8 (HCl)

SDS sample buffer	500 mM Tris-HCl pH 6.8
	10% (v/v) glycerine
	20% (v/v) SDS

| | 2% (w/v) β-Mercaptoethanol |
| | 0.05% (m/v) Bromophenol blue |

Destaining solution	300 ml methanol
	100 ml acetic acid (100%)
	ad 1 l H_2O_{dest}

| **Staining solution** | 100 ml destaining solution |
| | 250 mg Coomassie Brilliant Blue |

Sonication buffer	5 mM imidazole
(Equilibration buffer)	50 mM Tris-HCl
	150 mM NaCl
	0.1% Tween 20
	1 mM Mercaptoethanol
	pH 7.5

| Washing buffer (IMAC) | Sonication buffer |

| Elution buffer (IMAC) | Sonication buffer |
| | 250 mM imidazole |

Western Blot

Transfer buffer	25 mM Tris
	142 mM glycine
	20% (v/v) methanol
	ad 1 l H_2O_{dest}

TBST buffer	50 mM Tris
(Tris buffered Saline – Tween 20)	150 mM NaCl
	0.1% (v/v) Tween 20
	ad 1 l H_2O_{dest}

Blocking buffer   4% (w/v) non-fat dried milk

ad 100 ml TBST buffer

Primary antibody solution   10 µl monoclonal anti-poly histidine

clone MIS-1 in mouse from Sigma

Aldrich M1029[n]

9.99 ml Blocking buffer

Secondary antibody solution   10 µl anti-mouse IgG-alkaline

phosphatase conjugate

9.99 ml TBST buffer containing 1% (w/v)

non-fat dried milk

Buffer A   5 mM $MgCl_2$ x $6H_2O$

100 mM $NaCl_2$

100 mM Tris

ad 100 ml H_2O_{dest}

Reaction solution   30 ml Buffer A

200 µl of 5% (w/v) NBT (4-nitroblue-
tetrazoliumchloride) in 70% DMF (N,N-
dimethylformamide)

100 µl of 5% (w/v) BCIP (5-bromo-4-
chloro-3-indolyl-phosphate) in 70% DMF

Detection solution   33 µl BCIP in 70% DMF

40 µl NBT

20 ml Reaction solution

Immobilization buffer (Biacore)*   10 mM sodium acetate

pH 5

Immobilization running buffer (Biacore)* 10 mM HEPES

150 mM NaCl

70

	3 mM EDTA
	0.005% (v/v) Surfactant P20
	pH 7.4
Running buffer (Biacore)*	50 mM sodium phosphate
	150 mM NaCl
	0.1% Tween 20
	1 mM β-Mercaptoethanol
	pH 7.5
Regeneration solution (Biacore)*	10 mM NaOH
	150 mM NaCl
	0.3% SDS

* All Biacore buffers were degassed and filter-sterilized before use.

2.1.13 Stock solutions

Ampicillin (sodium salt):	25 mg/ml in H_2O_{bidest}, filter-sterilized and used at 50 μg/ml.
Kanamycin (sulfate):	30 mg/ml in H_2O_{bidest}, filter-sterilized and used at 30 μg/ml.
IPTG	1M in H_2O_{bidest}, filter-sterilized.

(Isopropyl β-D-thiogalactopyranoside):

Stock solutions were stored at -20°C.

2.2 Methods

2.2.1 Methods in Molecular Biology

2.2.1.1 Polymerase Chain Reaction (PCR)

The Polymerase Chain Reaction was used to amplify highly diluted specific DNA fragments of target template DNA or cDNA. The PCR is able to amplify even the lowest concentrations of template DNA in order to produce millions of copies (Mullis *et al*., 1986).

Principle:

1. *Denaturation*

During denaturation temperatures of 95°C cause the DNA to melt in order to produce single-stranded DNA templates.

2. *Annealing*

For annealing the temperature is lowered to usually 3 to 5°C lower than the melting temperature of the oligonucleotides. Now, the primers are able to bind the complementary single-stranded DNA molecules and the polymerase can bind the primer – DNA hybrid.

3. *Elongation*

The temperature for elongation depends on the DNA polymerase used for PCR. For the *Pfu* polymerase from *Pyrococcus furiosus* 72°C are used for the extension step. A new strand complementary to the template DNA strand is synthesized by the DNA polymerase in 5' to 3' direction.

A new cycle starts after heating and the subsequent denaturation of the double-stranded DNA molecules. Up to 35 cycles were run yielding an exponential amplification of the template DNA.

The following compounds were used to amplify target DNA via PCR:

> 2 µl template cDNA or DNA*
>
> 5 µl dNTPs
>
> 5 µl 10x Pfu polymerase buffer
>
> 1 µl oligo forward
>
> 1 µl oligo reverse
>
> 1 µl Pfu DNA polymerase
>
> 35 µl H_2O_{dest}

* Before dilution samples contained bewteen 30 ng/µl and 120 ng/µl DNA or cDNA. Subsequently, the purified template was diluted 1:100 and used as the template for amplification.

Table 2.10 PCR program for amplification of target DNA

Temperature [°C]	Time [min]	Number of cycles
95	5	1
95	0.5	
55 - 60	0.5	35
72	2	
72	5	1

2.2.1.2 Purification of PCR products

The purification of PCR products was performed using the QIAquick® PCR Purification Kit from Qiagen. For detailed description of the purification steps see the instruction manuals.

2.2.1.3 Purification of plasmid DNA

The purification of plasmid DNA from *E. coli* cells was performed using the GenElute™ Plasmid Miniprep Kit from Sigma-Aldrich. For detailed description of the purification steps see the instruction manuals.

2.2.1.4 Agarose gel electrophoresis

The agarose gel electrophoresis was performed to visualize PCR products and to separate digested plasmid DNA. In the applied electric field, DNA is separated due to its negative charge. Short DNA molecules move faster through the pores of the gel matrix than longer molecules which enables the separation of DNA molecules according to their size.

Agarose (1%) was solubilized and heated in 40 ml TAE buffer and mixed with 5 µl of ethidium bromide solution (1%) before polymerization. The samples were mixed with 60% (v/v) of DNA loading buffer. Gels were run at 90 – 120 V for 30 – 50 min and subsequently visualized by UV light.

2.2.1.5 Gel extraction of DNA fragments

The purification of digested plasmid DNA was performed using the QIAquick® Gel Extraction Kit from Qiagen. For detailed description of the purification steps see the instruction manuals.

2.2.1.6 Restriction of plasmid DNA and PCR products

The oligonucleotides used for PCR were designed to introduce restriction sites of the enzymes *Nde*I and *Bam*HI. *Nde*I which introduces the start codon ATG was introduced by the forward primer and *Bam*HI was brought in by the reverse primer.

Incubation of the PCR product and the plasmid DNA with the enzymes occurred for at least 3-4h or over night at 37°C.

The following compounds were mixed for restriction:

> 5-9 µl DNA
>
> 1µl *Bam*HI
>
> 1µl *Nde*I
>
> 4 µl 10x Buffer Tango^{TM} (with BSA)
>
> 5-9 µl H$_2$O$_{dest}$

After restriction digestion PCR products were purified using the QIAquick® PCR Purification Kit from Qiagen. Digested Plasmid DNA was separated by gel electrophoresis and subsequently purified by gel extraction using the QIAquick® Gel Extraction Kit.

2.2.1.7 Ligation

After purification of the digested PCR product and the vector DNA, both fragments were ligated using T4 DNA ligase. The ligation mix contained a 1:2 molar ratio of digested vector DNA versus digested insert DNA. Digested vector DNA reached at least a concentration of 8 ng/µl. The ligation mix was incubated at 16°C overnight.

The following compounds were mixed for ligation:

> 1 µl T4 DNA ligase
> 1 µl T4 10x ligase buffer
> 4-6 µl digested vector DNA
> 2-4 µl digested insert DNA
> 0-2µl H_2O_{dest}

2.2.2 Methods in Microbiology

2.2.2.1 Preparation of competent *E. coli* cells

Chemically competent *E. coli* cells were prepared with the RbCl method for transformation with DNA. For this purpose 50 ml of LB media was inoculated with an overnight culture and cultivated at 37°C until an OD_{600} of 0.5 was reached. The culture was centrifuged for 10 min at 4000 rpm and 4°C and the harvested cells were resuspended in 20 ml cold TfbI buffer. After incubation on ice for 15 min, the suspension was centrifuged again and the cell pellet was resuspended in 2 ml cold TfbII buffer. The cells were then incubated on ice for another 15 min and aliquoted in volumes of 200 µl to be immediately stored at -80°C.

2.2.2.2 Transformation of *E. coli* cells with plasmid DNA

Competent *E. coli* DH5α cells were transformed with ligated plasmids. Five µl of ligation mixture was gently resuspended with a 200 µl aliquot of competent cells and incubated on ice for 20 min. The mix was then heated at 42°C for 45 sec and incubated on ice for another 20 min. Afterwards 650 µl of LB media was added to the mix and and incubated at 37°C under shaking conditions for 30 min. Subsequently, the cells were centrifuged at 6000 rpm for 5 min at room temperature and spread on a plate containing LB medium and, depending on the plasmid, either Ampicillin or Kanamycin. After the cell solution had soaked into the agar, plates were kept at 37°C overnight.

For protein expression competent *E. coli* BL21(DE3) cells were transformed with the purified and diluted plasmid after sequencing.

Both *E. coli* DH5α and BL21(DE3) cells harboring plasmids were grown in LB medium containing antibiotic and used for the preparation of glycerol stocks. Glycerol stocks were prepared with sterile 50% (v/v) glycerol and stored at -80°C.

2.2.2.3 Heterologous protein expression in shaking flasks

The expression of the target proteins was performed in *E. coli* BL21(DE3) containing pET vector constructs. The pET expression system is still one of the most powerful tools for expressing target genes in *E. coli* since it relies on the strong T7 promoter and strains containing T7 RNA polymerase. As a result the host cells can produce the target protein in

levels up to 50% of the total protein. In addition, pET vectors encode N- or C-terminal his-tags comprising 6-10 histidines which allow the purification of the overexpressed recombinant proteins by immobilized metal affinity chromatography (IMAC). Protein expression was always performed in 1 l shaking flasks. In order to ensure optimal oxygen supply flasks were filled with not more than 200 ml of LB media.

2.2.2.3.1 Protein expression of the nuclear receptor CAR

The CAR LBD gene was cloned into the pET28a(+) vector which harbors a Kanamycin resistence gene. Thus, LB media was constantly prepared with 30 µg/ml of Kanamycin. Five ml LB medium was inoculated with a single colony picked from an agar plate and incubated at 37°C and 180 rpm over night. The next day 200 ml LB media was inoculated with 2 ml of the overnight culture and incubated at 37°C and 180 rpm until an OD_{600} between 0.4 and 0.6 was reached. In order to produce CAR protein two different expression protocols were performed:

Protein expression was induced with 0.2 mM IPTG and the culture was incubated at 25°C and 180 rpm for 4 hours.

Protein expression was induced with 0.2 mM IPTG and the culture was incubated at 16°C and 120 rpm for 20 hours.

After protein expression cells were harvested by centrifugation at 4°C and 4000 rpm for 15 minutes. The media supernatant was discarded and the pelleted cells were stored at -20°C.

2.2.2.3.2 Protein expression of the co-activators SRC-1 and SRC-2

The receptor interaction domains (RID) of SRC-2 were cloned into the pET28a(+) vector whereas the RID of SRC-1 were cloned into the pET22b(+) vector harboring an Ampicillin resistence gene. Hence, LB media were constantly prepared by adding 30 µg/ml of Kanamycin for SRC-2 and 50 µg/ml Ampicillin for SRC-1 expression.

The following protocol was performed for both SRC-1 and SRC-2 expression:

5 ml LB medium was inoculated with a single colony picked from an agar plate and incubated at 37°C and 180 rpm over night. The next day 200 ml LB media was inoculated with 2 ml of the overnight culture and incubated at 37°C and 180 rpm until an OD_{600} between 0.4 and 0.6 was reached. Protein expression was started by adding 0.2 mM IPTG and incubation at 25°C and 140 rpm for 4 hours. After protein expression cells were harvested by centrifugation at

4°C and 4000 rpm for 15 minutes. The media supernatant was discarded and the pelleted cells were stored at -20°C.

2.2.3 Methods in Biochemistry

2.2.3.1 Cell disruption of *E. coli* cells

2.2.3.1.1 Cell disruption by heat shock

When protein expression was performed for the first time 1 ml samples of the respective culture were taken 0, 1, 2, 3, and 4 hours after expression. These samples were harvested by centrifugation at 4°C and 6000 rpm for 10 minutes. The pelleted *E. coli* cells were then resuspended in phosphate buffered saline (PBS) dependent on their optical density considering equation (1):

$$(1) \qquad V \;=\; \frac{1000}{OD_{600}} \; x \; 0.25$$

V: volume of PBS [µl]

For SDS-PAGE analysis samples were diluted 1:1 in SDS sample buffer and subsequently heated at 95°C for 5 minutes for cell disruption by heat shock.

2.2.3.1.2 Cell disruption by sonication

Harvested and frozen *E. coli* cells from protein expression in 1 l shaking were thawed carefully on ice and resuspended in sonication buffer with 1 mM PMSF. Sonication was performed with a sonifier ultrasonic cell disruptor. In order to disrupt the cells cycles of 2 minutes at 35% duty cycle (constant) and at an output control of 4 were performed. Each cycle was followed by a break of 2 minutes. During the process of sonication and pausing the cells were always kept on ice. After cell disruption cell debris was harvested by centrifugation at 4°C and 4000 rpm for 45 minutes. The supernatant cell lysate and cell debris were separated and either stored at -20°C or immediately prepared for SDS-PAGE, protein purification or Western blot. The cell lysate but not the cell debris was used for protein purification.

2.2.3.2 Protein purification by Immobilized Metal Affinity Chromatography (IMAC)

Expressed proteins were purified from *E. coli* cell lysate by means of cobalt-based immobilized metal affinity chromatography (IMAC) using the Talon his-Tag Purification Resins from Clontech. SRC-2 and CAR were expressed harboring an N-terminal histidine tag by using the pET28a(+) vector. SRC-1 was expressed with a 10x his-tag which is localized at the N-terminus too. The histidine tag of the target proteins binds the Co^{2+} ions of the purification resins with high affinity and therefore enables isolation of the human proteins from the *E. coli* lysate. One ml of the his-Tag Purification Resins may bind up to 5 mg of his tagged protein. Additionally, cobalt-based affinity chromatography demonstrates very low co-purification of *E. coli* housekeeping proteins.

For purification of the target proteins from cell lysate *E. coli* cells were already sonified in the equilibration buffer. All purification steps were performed at 4-8°C in order to ensure protein stability. The column bed volume (0.5 ml) was pre-equilibrated four times with four column volumes (CV) of equilibration buffer (sonication buffer). The cell lysate was then applied to the resin and the flow through sample was collected and reloaded onto the column to increase target protein yield. The column was subsequently washed four times with five CV of equilibration buffer. The target protein was then eluted with 0.5 to 1 ml elution buffer containing 250 mM imidazole. After purification the resins were regenerated with 20 mM MES (2-(N-morpholine)-ethanesulfonic acid) and stored in 20% ethanol and at 4°C before reuse.

2.2.3.3 Determination of protein concentration

Target protein concentration was determined with the help of the BCA Assay Kit from Pierce. The principle relies on the reduction of Cu^{2+} to Cu^{1+} ions by protein in an alkaline medium and the subsequent colorimetric detection of Cu^{1+} by bicinchoninic acid (BCA). The complex of two molecules of BCA with one Cu^{1+} ion demonstrates a strong linear absorbance at 562 nm with the increase of protein concentration. For detailed description of the assay protocol see the instruction manuals.

2.2.3.4 Sodium Dodecyl Sulfate Polyacrylamide Gel Electrophoresis (SDS-PAGE)

The overexpressed target proteins were examined before and after purification by means of sodium dodecyl sulfate polyacrylamide gel electrophoresis (SDS-PAGE) (Laemmli, 1970). For this purpose the protein buffer solution was diluted in SDS sample buffer in a ratio of 1:1 and heated at 95°C for 5 minutes. The denaturated proteins were subsequently added to the

wells of the gel. Due to the electric field applied across the gel the negatively-charged proteins migrate to the anode and are separated according to their size. The gel was run at 20 mA for 70 minutes. For visual examination the gel was stained for at least one hour at room temperature and destained overnight using the respective staining and destaining solutions.

For SDS-PAGE analysis 12.5% acrylamide resolving gels were prepared and cast over by the stacking gel. Detailed composition of the gels is provided in the following table.

Table 2.11 Detailed composition of the resolving and the stacking gel.

	Resolving gel	Stacking gel
Rotiphorese® Gel 30	2.67 ml	0.52 ml
Upper Tris buffer pH 6.8	-	1 ml
Lower Tris buffer pH 8.8	2 ml	-
H_2O_{dest}	3.33 ml	2.47 ml
10% (m/v) APS (Ammonium persulphate)	40 µl	40 µl
TEMED	4 µl	4 µl

2.2.3.5 Silver staining

Additionally to the Coomassie staining method, the Silver staining Kit from Fermentas was used to visualize the overexpressed and purified target proteins. The advantage of the silver staining in comparison to the common Coomassie staining is its high sensitivity to better highlight co-purified *E. coli* housekeeping proteins. This staining procedure can detect up to 0.05 ng of protein per band and, therefore, reveals a >100x higher sensitivity. During silver staining the silver ions interact with the negatively charged amino acid residues of the proteins. The reduction of these bound silver ions to metallic silver enables the detection of the proteins.

For detailed description of the single steps of silver staining see the instruction manuals.

2.2.3.6 Western Blot

Western Blot analysis is a tool used to verify the presence of the overexpressed target protein among all *E. coli* housekeeping proteins. In contrast to Coomassie staining, Western Blot only detects his-tagged proteins.

2.2.3.6.1 Semi-dry Protein Transfer for Western Blotting

Target proteins were separated in a polyacrylamide gel and then transferred on a nitrocellulose (NC) membrane. The transfer of the proteins was carried out in a semi-dry blotting device with the help of an electric field (figure 2.1).

For the transfer the NC membrane and 6 Whatman papers were cut to the size of the gel. The membrane and the gel were then incubated in transfer buffer for 15 minutes at room temperature. The Whatman papers were only equilibrated for a few seconds. For the blot the Whatman papers, the gel, and the NC membrane were set as depicted in the following figure:
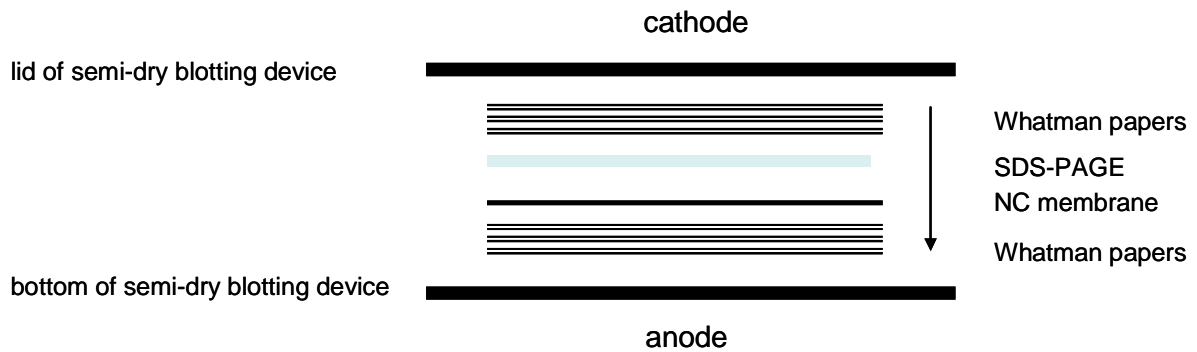
Figure 2.1 Protein transfer in a semi-dry blotting device. The arrow indicates the blotting direction of the proteins migrating towards the anode of the blotting device and, thus, to the NC membrane.

Since the anode of the blotting device was positioned on the bottom, the NC membrane was assembled under the SDS-PAGE to ensure that the proteins migrate in the right direction (figure 2.1, arrow). The blot was run at 15V for 45 minutes.

The successful transfer of the prestained marker bands matching the target protein in size indicated that the protein of interest migrated too. After the transfer the membrane was washed with TBST buffer twice for 10 minutes at room temperature.

2.2.3.6.2 Immunodetection of blotted proteins on Nitrocellulose Membranes

Once on the NC membrane the blotted proteins can be detected by the primary monoclonal anti-poly histidine antibody and the secondary anti-mouse IgG-alkaline conjugate. In order to maintain a weak background by reducing the binding of non-specific proteins, putative binding sites were saturated with non-fat dried milk provided in the blocking buffer for one hour at room temperature. All washing and incubation steps were performed in a plastic container gently agitated at room temperature. Each washing step included 50 ml of TBST

buffer. Immediately after blocking the membrane was incubated with the monoclonal anti-poly histidine antibody for one hour or overnight at 8°C. Afterwards, the membrane was washed three times for 10 minutes, followed by incubation with the anti-mouse IgG-alkaline conjugate for one hour or overnight at 8°C. Both antibodies were diluted in a ratio of 1:1000 in blocking buffer. After incubation, the membrane was washed twice for 10 minutes. Visualization of the Western Blot was carried out by incubating the membrane in 20 ml detection solution for about 7 minutes. The alkaline phosphatase of the secondary anti-mouse antibody catalyzes the hydrolysis of BCIP to phosphate and 5-bromo-4-chloro-3-indolyl which due to oxidation and dimerization is turned to the blue dye 5,5'-dibromo-4,4'-dichloro-indigo. NBT, on the other hand, is reduced to the blue dye di-formazane. After washing with water the detection reaction was stopped.

2.2.4 Methods in Surface Plasmon Resonance

2.2.4.1 Sensor surface properties of a CM5 Biacore Chip

The Biacore sensor chip consists of two solid layers: a gold and a glass layer (figure 2.2). The glass layer is coated with a 50 nm-thick gold layer to fulfill conditions for surface plasmon resonance which occurs under total internal reflection at thin layers of several conducting materials. The glass layer acts as a carrier of the gold layer. Gold provides many advantages which make it preferable for scientific use. Gold fulfils SPR conditions at easily handled visible light wavelengths and can be covalently attached to surface matrix layers. Additionally, it is suitable for biomolecular interactions in physiological buffers due to its inert feature (Produktinformation Biacore 3000; Biacore Getting Started 28-9384-71 Edition AC).

Since the gold layer itself is not able to act as immobilization ground, it is covered with the matrix of carboxymethylated dextran. On a CM5 sensor chip the dextran layer is approximately 100 nm thick (Fägerstam *et al.*, 1992). This polymer consists of unbranched carbohydrates forming a thin layer for covalent immobilization of the ligand. Additionally, it offers a hydrophilic environment for biomolecular interactions. Due to the negatively-charged carboxyl groups of the dextran matrix the ligand needs to be charged positively during the process of immobilization. There are four flow cells (Fc) on the CM5 chip on which proteins can be immobilized. Typically, Fc 1 and 3 are used as reference flow cells. A reference flow cell is not immobilized with a ligand. After binding or kinetic analysis the response measured on the reference flow cell is subtracted from the response signal measured on the immobilized flow cell in order to neglect non-specific binding of the analyte to the dextran matrix. This subtraction enhances the quality of the binding and response signal and, thus of the obtained information, measured on the immobilized flow cell. When Fc1 and 3 are used as reference flow cells the Biacore sensorgrams illustrate the response signals of Fc 4-3 and Fc 2-1. Alternatively, Fc 1 can be used as the only reference flow cell on the chip. Therefore, the flow cells 2, 3, and 4 are immobilized with the ligand. Hence, three assays can be measured by performing one assay in which the analyte is injected over all flow cells simultaneously. The Biacore sensorgrams then depict the response signals of Fc 4-1, Fc 3-1, and Fc 2-1 (Produktinformation Biacore 3000; Biacore Getting Started 28-9384-71 Edition AC).
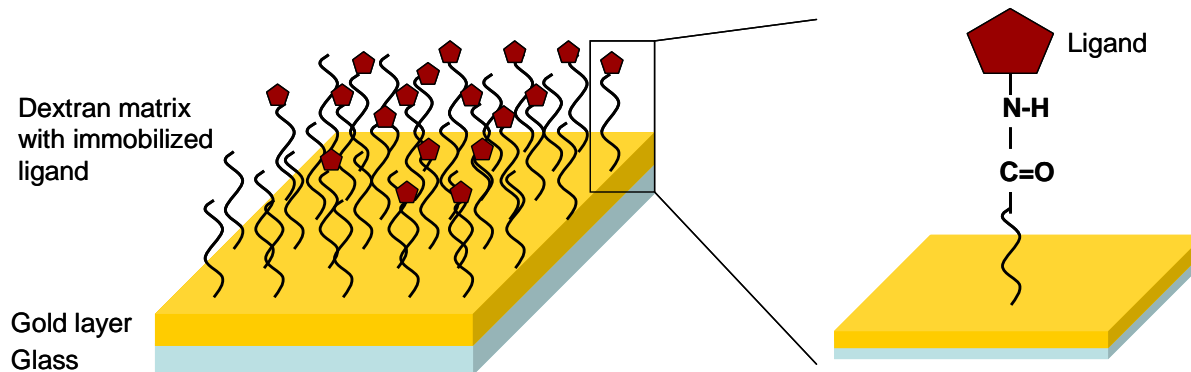
Figure 2.2 Sensor surface properties of a Biacore CM5 chip. The glass layer is coated with a 50 nm gold layer which is covalently attached to a carboxymethylated dextran matrix. The ligand is covalently attached to the dextran matrix during immobilization.
This figure was modified according to Biacore Getting Started 28-9384-71 Edition AC.

2.2.4.2 Immobilization of proteins on a CM5 Biacore chip

For binding and kinetic analyses, using SPR overexpressed and purified proteins had to be immobilized on the dextran matrix of a CM5 chip. The covalent immobilization of a protein to the dextran matrix represents the common procedure to enable direct and measurable interactions between the stable bound ligand and the analyte protein or drug. Amine, thiol and aldehyde coupling are different approaches for covalent immobilization of proteins. Amine coupling is one of the most used immobilization procedures. Immobilization of both the nuclear receptor CAR and the co-activators was done using the Biacore Amine Coupling Kit. However, prior to the actual attachment of the protein, the chip surface had to be activated (figure 2.3). During all steps of activation, immobilization, and blocking a flow rate of 10 µl/min was set. The carboxymethylated dextran surface was activated by injecting a mixture of 30 µl of both EDC (1-ethyl-3-(3-dimethylaminopropyl) carbodiimide) and NHS (N-hydroxysuccinimide) for 3-5 minutes in order to provide reactive succinimide esters. After activation was finished, the ligand was injected to covalently bind to the surface. The provided esters react with amino groups and other nucleophilic groups to attach the injected ligand to the dextran. As a condition for immobilization, the protein needs to be pre-concentrated at the surface. Due to the negatively-charged dextran matrix, the ligand needs to be positively charged in order to be pre-concentrated at the matrix surface. For this purpose the pH of the immobilization buffer needs to be between the pK of the dextran matrix (pK: 3.5) and the isoelectric point of the protein to be immobilized. For the nuclear receptor CAR as well as the co-activators SRC-1 and SRC-2, the immobilization buffer with a pH of 5.0 was

chosen to attach the proteins to the surface. One molar ethanolamine (pH 8.5) was subsequently passed for 6.5 minutes over the surface to deactivate remaining active esters. The amount of covalently-bound ligand on the dextran matrix after blocking is referred to as the immobilization level R_L (Biacore Getting Started 28-9384-71 Edition AC; Produktinformation Biacore 3000).
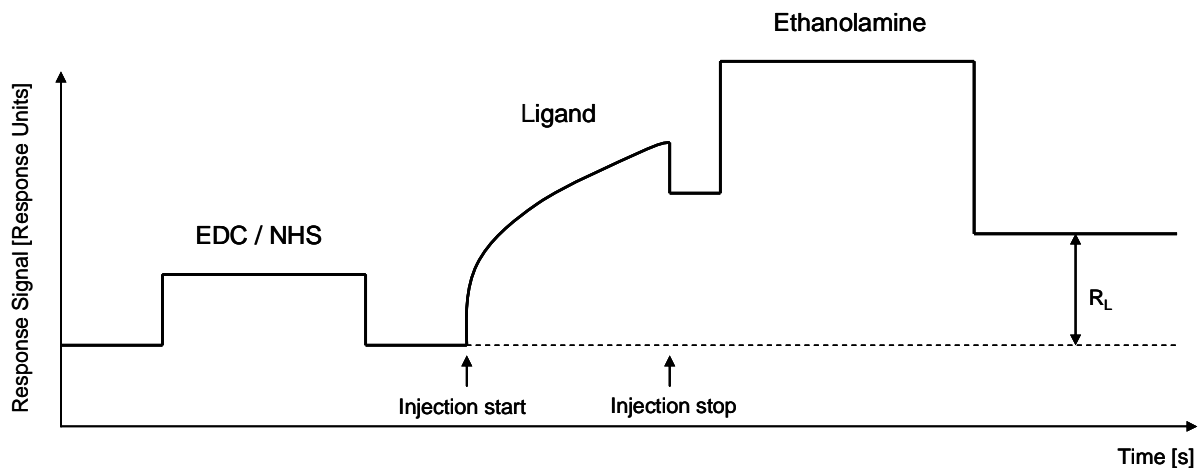

Figure 2.3 Immobilization of proteins. The goal of immobilization is to irreversibly bind the protein of interest to the carboxymethylated dextran matrix. Before immobilization the surface is activated by a mix of EDC and NHS. The protein is then injected over the modified dextran matrix. After ligand injection the surface is blocked with ethanolamine. R_L represents the immobilization level and therefore the amount of covalently bound ligand.

2.2.4.2.1 Immobilization of the co-activators SRC-1 and SRC-2 for binding analysis

In order to investigate the association of CAR with its co-activators under the influence of drugs the flow cells of a CM5 chip were immobilized with either SRC-1 or SRC-2. The distinctive flow cells on CM5 chips were immobilized with the same target protein at different densities which correspond to different R_L values (figure.2.4 and 2.5, table 2.12). The number of flow cells used for examination of binding or kinetic analysis varied from one flow cell to three flow cells. Fc1 was constantly used as the only reference flow cell to subtract non-specific binding of the analyte to the carboxymethylated dextran matrix. Therefore, the Biacore sensorgrams depict the response signals of both the binding and kinetic assays as Fc 4-1, Fc 3-1 and / or Fc2-1. For binding analysis the analyte was passed over the surface of the respective flow cells. All immobilization levels which were achieved on different CM5 chips are summarized in table 2.12.

Table 2.12 Immobilization levels on distinctive flow cells of CM5 chips. These chips were used to investigate ligand-dependent association of CAR and its co-activators. Each row comprises three flow cells of a single chip immobilized with the same ligand. Fc1 was constantly used as the reference flow cell.

Ligand	Analyte	Immobilization levels (R_L) in the respective flow cells (Fc) of a CM5 chip [RU]		
		Fc2	Fc3	Fc4
SRC-1	CAR with drug of interest [a]	131	85	161
	CAR with drug of interest [b]	258	297	172
SRC-1	CAR with drug of interest and Clotrimazole [c]	160	239	191
SRC-2	CAR with drug of interest [d]	657	228	378

[a] Phenobarbital, CITCO, Fenofibrate, Clotrimazole, the Artemisinin drugs and Triphenylphosphate.

[b] Atorvastatin drugs, androstanes, Clofibrate and Bisphenol A.

[c] Drugs listed in [a] and Clofibrate respectively in the presence of Clotrimazole.

[d] Drugs listed in [a] and Clofibrate.

Selective immobilizations were depicted to demonstrate every step during the process of covalent immobilization of the ligand on the sensor surface (figure 2.4 and 2.5). Figure 2.4 represents the attachment of SRC-1 to the dextran matrix in order to investigate CAR – SRC-1 binding under the influence of the Atorvastatin drugs and the androstanes. The second immobilization demonstrates the covalent attachment of SRC-1 in order to examine drug-dependent CAR – SRC-1 association under the influence of the inverse agonist Clotrimazole (figure 2.5).
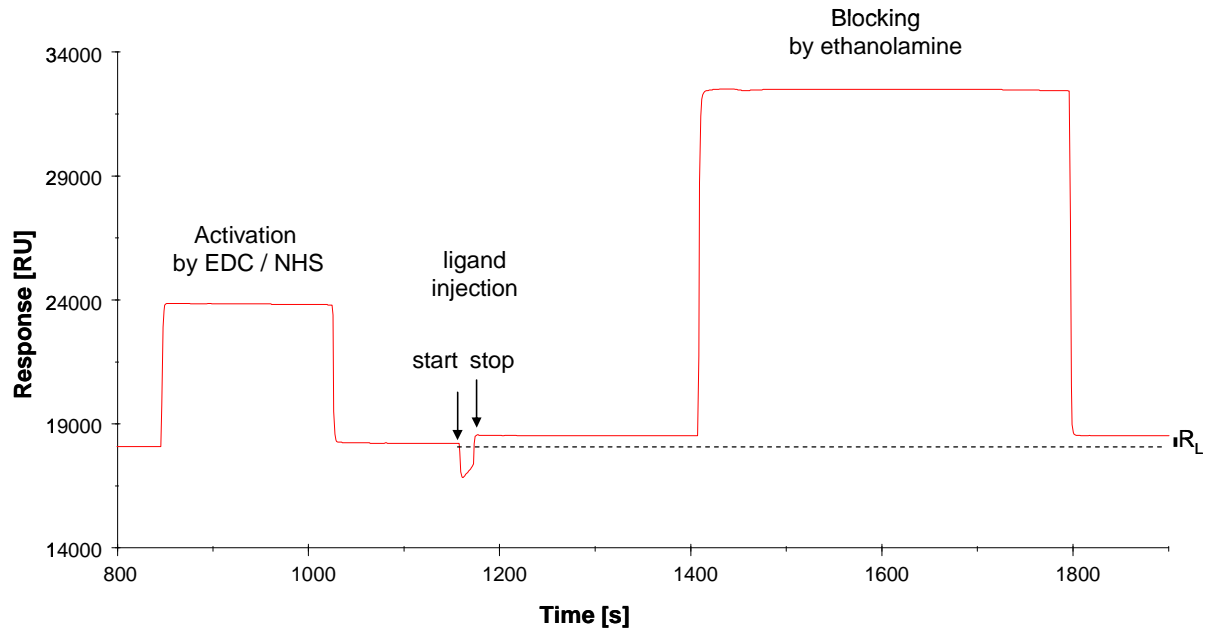
Figure 2.4 Immobilization of SRC-1 for binding analysis with CAR under the influence of androstanes and Atorvastatin drugs.
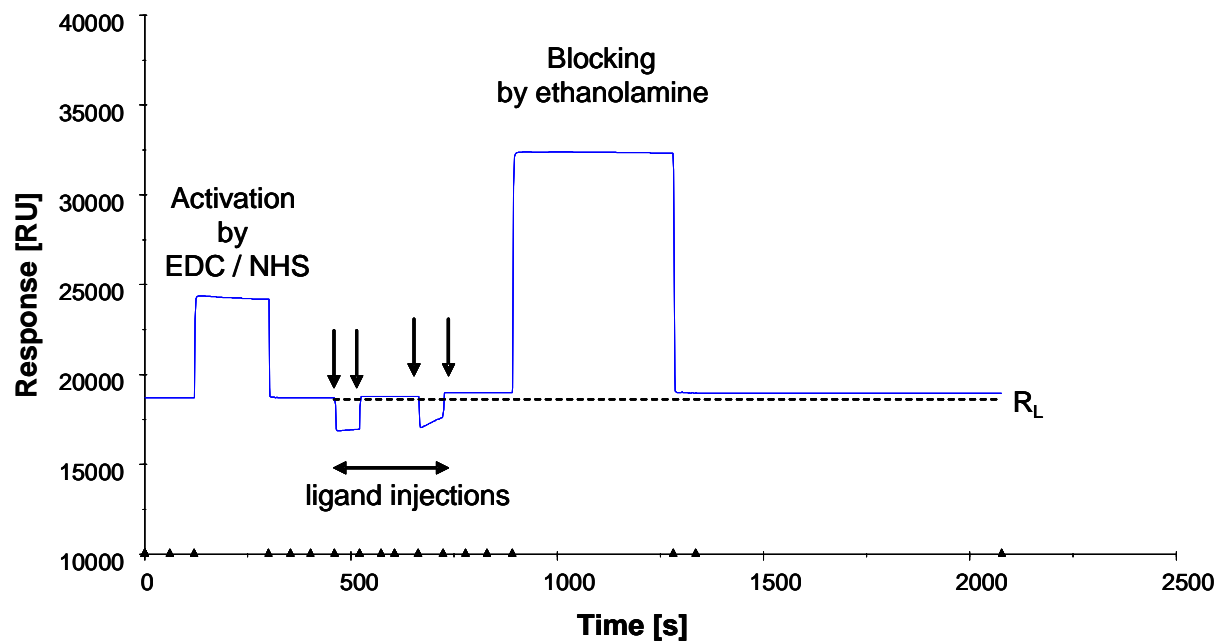
Figure 2.5 Immobilization of SRC-1 for drug-dependent binding analysis with CAR after pre-incubation with Clotrimazole.

2.2.4.2.2 Immobilization of the nuclear receptor CAR for kinetic binding analysis

In order to investigate and evaluate kinetic binding assays CAR was immobilized on Biacore CM5 chips. Set-up and reference subtraction was performed as described before. All immobilization levels which were achieved on different flow cells of CM5 chips are summarized in table 2.13.

88

Table 2.13 Immobilization levels on distinctive flow cells of CM5 chips. These chips were used to investigate ligand-dependent and ligand-free kinetics of CAR - co-activator binding. Each row comprises three flow cells of a single chip immobilized with the same ligand. Fc1 was constantly used as the reference flow cell.

Ligand	Analyte	Amount of immobilized ligand (R_L) in the respective flow cells (Fc) of a CM5 chip [RU]		
		Fc2	Fc3	Fc4
CAR	SRC-2 [a]	-	1650	3234
	SRC-1 – drug of interest [b]			
CAR	SRC-1 [c]	-	737	-

[a] drug-free kinetic analysis

[b] CITCO, Artemisinin drugs, Triphenylphosphate and Fenofibrate

[c] drug-free kinetic analysis

Selective immobilizations were depicted to demonstrate the covalent immobilization of the ligand on the sensor surface (figure 2.6 and 2.7). Figure 2.6 represents the attachment of CAR to the sensor surface in order to perform kinetic binding analysis of the receptor and SRC-1. Figure 2.7 demonstrates the immobilization of CAR to perform kinetic binding analysis of the receptor and SRC-1 under the influence of drugs as well as drug-free kinetic binding analysis with SRC-2.
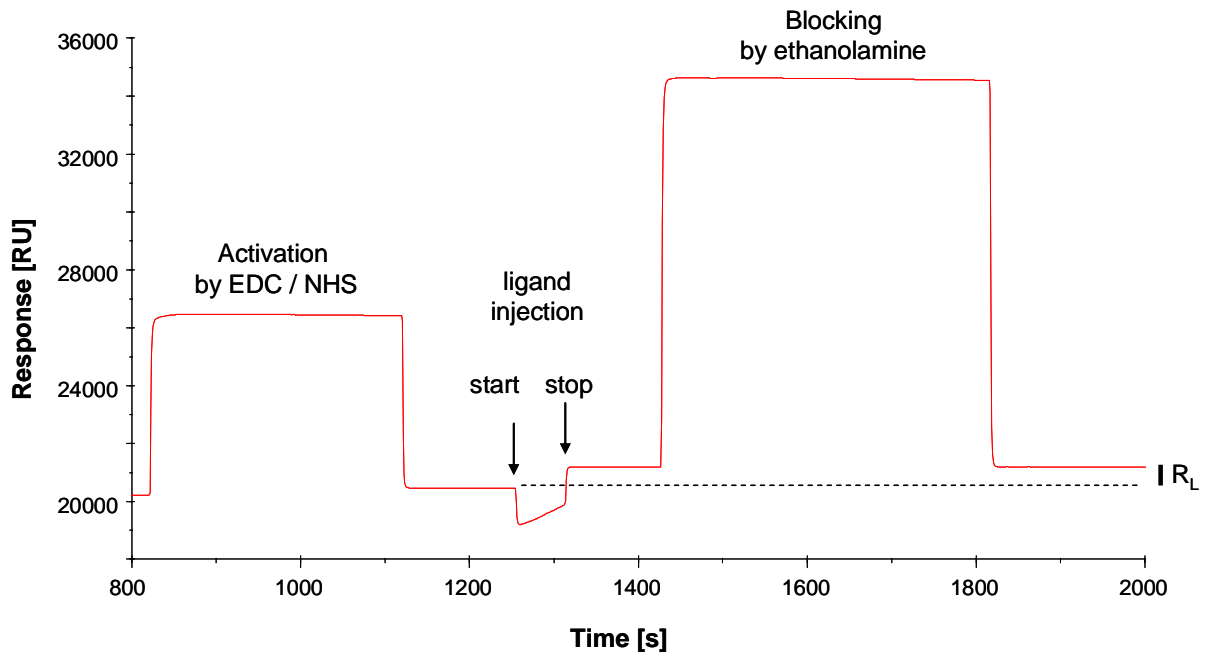
Figure 2.6 Immobilization of CAR for ligand-free kinetic binding analysis with SRC-1.
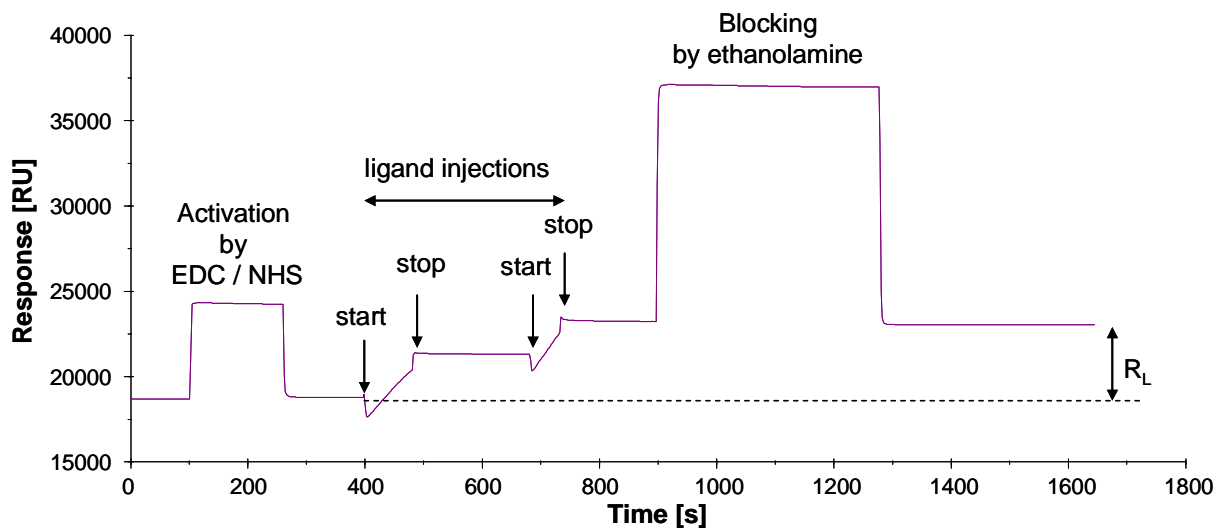
Figure 2.7 Immobilization of CAR for ligand-free kinetic binding analysis with SRC-2 or ligand-dependent kinetic binding analysis with SRC-1.

2.2.4.3 Experimental set-up for binding assays

The aim of the binding assay was to find out whether drugs might have a direct influence on complex formation of CAR with its co-activators and, thus, might be a tool of manipulating CAR activity. For measuring these interactions by means of SPR, the surface of a CM5 Biacore sensor chip was immobilized with one of the co-activators. Being the analyte, CAR

90

was injected either on its own or after pre-incubation of at least 30 minutes at room temperature with one of the drugs of interest. The ligand–free interaction was performed twice per assay and considered factor 1 (mean out of CAR mock 1 and 2) to constitute the association for the constitutive binding between receptor and co-activator. As the analyte CAR was injected over the co-activator surface with or without drugs. The change in response caused by samples of liganded CAR was calculated as x – fold responses. The focus was to examine the x – fold response caused by ligand - protein interactions relative to the drug-free binding. Thus, the absolute response value of the association was not the prime focus but the relative enhancement. One hundred micromolar of each drug or 10 µM CITCO respectively were pre-incubated with 210 nM CAR for at least 30 minutes at room temperature and afterwards injected in the flow cell over the immobilized co-activator. Considering the interaction with immobilized SRC-2 CAR was diluted to a final concentration of 50 nM only. The drugs used for investigating CAR – SRC-1 interactions were CITCO, Phenobarbital, Clofibrate, Fenofibrate, Clotrimazole, Artemisinin, Arteether, Arthemether, Triphenylphosphate, Androstanol and Androstenol. For inhibition assays containing Clotrimazole, 100 µM of the inhibitor was added to the CAR – drug mix. Running buffer contained 50 mM sodium phosphate pH 7.5, 150 mM sodium chloride, 0.1% Tween 20, 1 mM ß-mercaptoethanol and 1% DMSO. Compounds were diluted for the first time in a ratio of 1:100 with running buffer without DMSO in order to match the DMSO content of the running buffer. The next dilution steps were performed with the DMSO-containing runnig buffer to yield a final concentration of 100 µM of the specific drug or 10 µM of CITCO.

For the examination of the influence of HMG (3-hydroxy-3-methylglutaryl) - CoA reductase inhibitors on complex formation of CAR and SRC-1, Atorvastatin acid and lactone as well as their particular ortho- and para-OH- derivatives were also pre-incubated with CAR.

For investigation of CAR – SRC-2 interactions the same drugs apart from the Atorvastatin drugs, Clofibrate and Bisphenol A were used.

A common binding cycle depicted in a Biacore sensorgram consists of several steps that include association, dissociation, and the regeneration of the ligand surface to ensure binding between analyte and ligand in the next cycle (figure 2.8). The baseline before injection of the analyte illustrates the running buffer flowing over the ligand surface. It sets the basis for the association. After the cycle has reached a stable baseline, the analyte is injected. The time period between injection start and stop is considered as the association and describes the binding between ligand and analyte. The association is characterized by an increase in response. After injection stop of the analyte, only running buffer runs over the surface. The

time span between injection stop of the analyte and regeneration of the surface is therefore regarded as the dissociation of the complex. Depending on the stability of the complex formed, it is characterized by a decrease in response. In order to prepare the ligand surface for the next binding cycle, the remaining bound analyte has to be removed from the surface. The regeneration step leads to the release of the binding partners so that the analyte can be washed away without harming the ligand. Usually, the regeneration step is not depicted in the sensorgram. The Biacore sensorgram illustrates the association and dissociation phase. After the extraclean step, which is also not depicted in the sensorgram, a new cycle can begin.
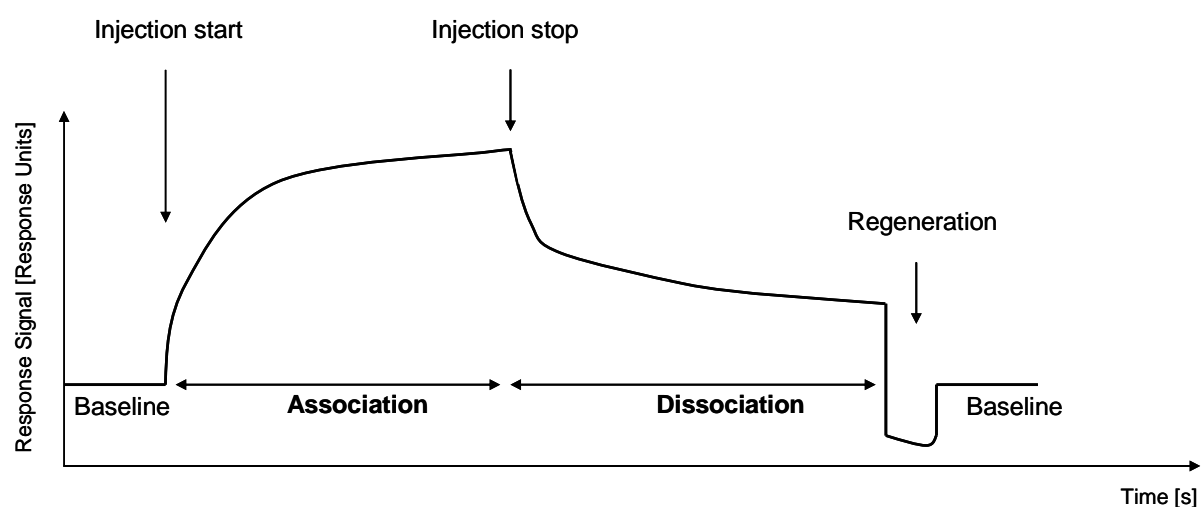
Figure 2.8 Illustration of a typical binding cycle depicted in a Biacore sensorgram. The sensorgram depicts the baseline before analyte injection, the association and dissociation of the analyte – ligand interaction and the regeneration of the ligand surface. After evaluation of the binding and kinetic data the regeneration and washing steps are not depicted in the sensorgram.

All steps of binding as well as kinetic assays were run at 25°C and using a flow rate of 50 µl/min to minimize mass transfer. Before the analyte was injected, running buffer equilibrated the ligand surface for more than 1.5 minutes to ensure a stable baseline which is pivotal for data analysis. Both association and dissociation were measured for 1 minute. Ten seconds after dissociation had finished, regeneration was carried out. The regeneration of the surface comprised two steps. During the first step the analyte was separated from the bound ligand with the regeneration solution containing 10 mM NaOH, 150 mM NaCl, and 0.3% SDS. During the second step remaining SDS was washed away from the surface to ensure binding of the proteins in the next cycle. The first step of regeneration was performed for 1 min, the second step for 30 sec. After regeneration an extra-clean step, washing the surface with running buffer, was performed. After this step a new cycle of binding started.

Before each assay the system was equilibrated at least three times and three injections of running buffer and regeneration solution respectively were performed to optimize baseline stability. Each cycle depicted the interaction of the respective co-activator and CAR pre-incubated with one of the drugs of interest. Two cycles depicted the ligand-free interactions (CAR mock 1 and 2). Each assay also contained at least 3 cycles of running buffer, protein-free drugs and DMSO solvent control injections. Prior to injection each cycle was able to establish a stable baseline for at least 90 seconds.

2.2.4.4 Experimental set-up for kinetic binding assays

The kinetic binding assays investigated the interactions of CAR and its co-activators. In comparison to the ligand-dependent association experiments, kinetic data may reveal more detailed and crucial information on both association and dissociation.

The nuclear receptor CAR was immobilized at low densities on a Biacore CM5 chip. The co-activators SRC-1 and SRC-2 were injected over the receptor surface to examine the protein binding. In order to cover a broad spectrum of sample concentrations the co-activator was injected over the receptor with the highest concentration being ten times higher than the lowest. Each assay contained five different concentrations of analyte comprising 0.75, 2, 4, 6 and 8 μM of the respective co-activator. The goal of this experiment was to yield kinetic data describing the nature of kinetics achieved by CAR binding to either SRC-1 or SRC-2. In order to address the question which of the co-activators might be favored by their receptor CAR, binding experiments were performed in the absence of drugs. These assays were performed in running buffer without DMSO. The ligand-dependent kinetic assays examined the binding between immobilized CAR and SRC-1 only. These assays were performed using the running buffer with 1% DMSO including the drugs Clofibrate, Artemisinin, Arteether, Artemether, Triphenylphosphate, and Fenofibrate.

After the assay was run, experimental curves were evaluated using the Biacore Evaluation Software. This software provides diverse different binding models matching the different modes of binding. For evaluation of the ligand-dependent kinetic binding assays the 1:1 Langmuir binding model was used for most of the drugs. The ligand-dependent binding assays with Fenofibrate and Triphenylphosphate as well as the ligand-free interactions of CAR and its co-activators were fitted with the 1:1 Langmuir binding fitting model with drifting baseline. All kinetic binding assays were depicted as fits of the chosen models. Additionally, the residual plot of the fit was depicted. The residual plot serves as an alternative tool of demonstrating the quality of the fit.

3 Results

3.1 Overexpression of the recombinant human nuclear receptor CAR and the recombinant human co-activators SRC-1 and SRC-2 in *E. coli*

The human constitutive androstane receptor was described for the first time in the mid 1990s (Baes *et al*., 1994). In order to characterize the interactions of CAR with the human co-activators SRC-1 and SRC-2 properly, the respective functional domains of the target proteins need to be expressed. For this purpose the ligand binding domain (LBD) of CAR and the receptor interaction domains (RID) of the co-activators were cloned into pET expression system vectors and expressed in *E. coli*. The respective cDNA which served as the template for the molecular cloning of the specific constructs was donated from Dr. Oliver Burk from the IKP (Dr. Margarete Fischer-Bosch-Institut für Klinische Pharmakologie) and is derived from individual liver.

3.2 Overexpression of the human CAR protein in *E. coli* and optimization of cultivation conditions

CAR protein expression was performed using 1l shaking flasks which contained 200 ml of LB media. The culture was kept under conditions of 37°C and 180 rpm until it reached an OD_{600} value between 0.4 and 0.6. Protein expression was induced with 0.2 mM IPTG. After induction CAR was expressed at 25°C and 140 rpm for 4 hours.

Figure 3.1A displays the expression of protein during four hours. The left hand side shows the culture which was induced with IPTG. The right hand side shows the culture which served as the negative control since it was not induced. The latter does not show any significant overexpression of target protein. On the other hand the induced culture clearly demonstrates a protein band which was overexpressed in a time dependent-manner. This band, which represents the overexpressed CAR, ran visibly above the 20 kDa and below the 29 kDa protein marker band. The ligand binding domain (LBD) of CAR has a molecular weight of 29.2 kDa.

Lanes 1 and 2 of figure 3.1B represent the lysate and pellet samples of the non–induced culture after three hours of protein expression. Lane 3 and 4 illustrate the lysate and pellet samples of the induced culture. It is obvious that the overexpression of the target protein CAR occurred properly. On the other hand, it is evident, too, that this selective expression happened mostly in the insoluble cell fraction of *E. coli* and not in the lysate. CAR was produced into insoluble inclusion bodies of *E. coli* cells. This is a wide and common problem among overexpressed proteins. Being in inclusion bodies, it is very difficult to use CAR for analyzing purposes without having to denature and renature the protein again. Especially one has to consider that the process of denaturation and renaturation can lead to partly irreversibly damaged and, thus, to non-functional proteins. On the other side, proteins which have been expressed into inclusion bodies are of very high purity. Since there is no activity test for nuclear receptors to verify their structural and functional integrity after de- and renaturing the protein, an alternative way was chosen to produce soluble CAR protein.
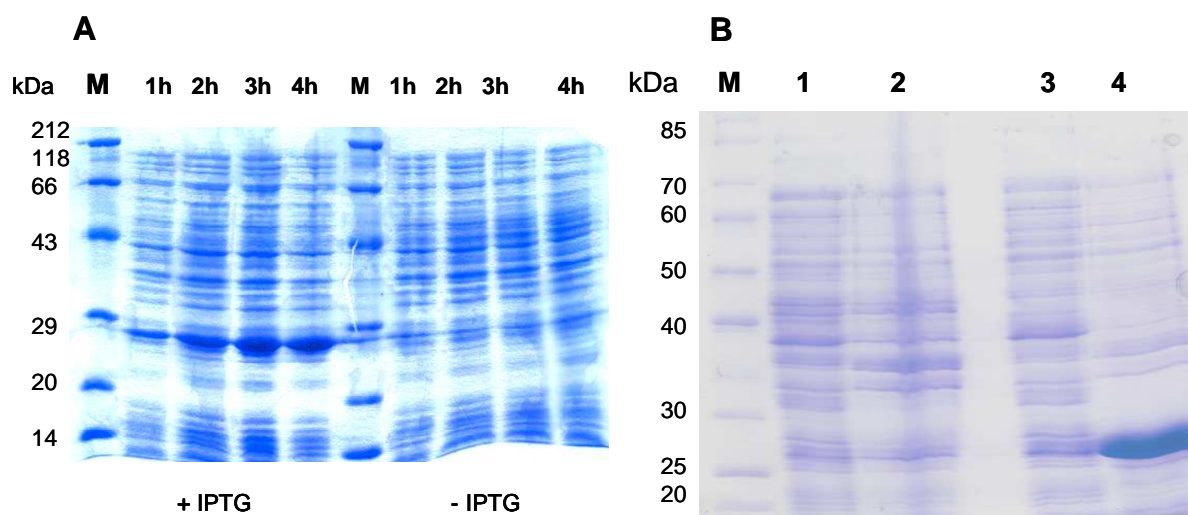
Figure 3.1 Overexpression of CAR protein (SDS-PAGE 12.5%). Protein expression was induced by 0.2 mM IPTG. **A** Time-dependent overexpression of human CAR in *E. coli* BL21 (DE3). On the left hand side, samples of the induced culture are depicted, on the right hand side, samples of the non-induced cell culture are shown. M: unstained protein ladder. **B** Human CAR after 3h of protein expression in *E. coli* BL21(DE3). The LBD of CAR has a molecular weight of 29.2 kDa. M: unstained protein ladder, 1: lysate and 2: pellet of the non-induced culture; 3: lysate, and 4: pellet of the induced culture.

It is a fact that co-expression of nuclear receptors with co-activators or other binding partners can improve the receptors expression pattern in *E. coli.* Being expressed on their own, nuclear receptors are mostly produced in inclusion bodies. On the other hand, especially when co-

expressed with their partner proteins, the receptors can be produced solubly (Li *et al.*, 1997). For this reason the aim was to co-express CAR with one of its binding partners like SRC-1 which is one of its co-activators (Vincent *et al.*, 2004).

Competent *E. coli* BL21 (DE3) cells that already carried the *CAR LBD* gene in the pET28a(+) vector were transformed with pET22b(+) containing the *SRC-1 RID* gene. Afterwards inoculation was performed to express protein at 25°C and 140 rpm for four hours. Figure 3.2A illustrates samples of the induced (arrows) and non-induced *E. coli* cultures after four hours and samples of time-dependent protein expression of the induced culture. Whole cell samples digested by heat shock demonstrated that the negative control did not show any distinctive overexpression of target proteins (figure 3.2A). On the other hand, the induced culture showed overexpression of CAR and SRC-1 represented as broader protein bands running between the 20 and 29 kDa marker band of the protein ladder (figure 3.2A, arrows). The LBD of CAR has a molecular weight of 29.2 kDa whereas the RID (receptor interaction domains) of SRC-1 has a molecular weight of 16.9 kDa. The protein bands of CAR and SRC-1 indeed showed increase in expression within four hours. Cells of the induced culture were then disrupted by sonication. Subsequently, the purification of the proteins from the lysate was carried out (figure 3.2B, arrows). CAR was purified using its histidine-tag for IMAC. The SRC-1 protein did not carry a histidine-tag. Thus, purification of SRC-1 occurred by binding to CAR. The purified CAR and SRC-1 proteins are displayed in lane 6 of figure 3.2B. Thus, CAR could be expressed solubly in the presence of its co-activator SRC-1. Even though the receptor was expressed in the lysate, the protein partly remained in inclusion bodies of *E. coli*, too (figure 3.2B, arrow lane 2). The pET22b(+) vector carried one histidine-tag of six residues at the C-terminus of the inserted SRC-1 sequence. Since this sequence was cloned into pET22b(+) with a C-terminal stop codon, the co-activator was not attached to a his-tag. As a result, SRC-1 could not be purified using affinity chromatography via his-tag. Given that SRC-1 was captured in the eluate fraction of the purification, it must have bound to its receptor CAR. Furthermore, this purification is a proof of the structural and, hence, functional integrity of both the CAR and the SRC-1 protein.
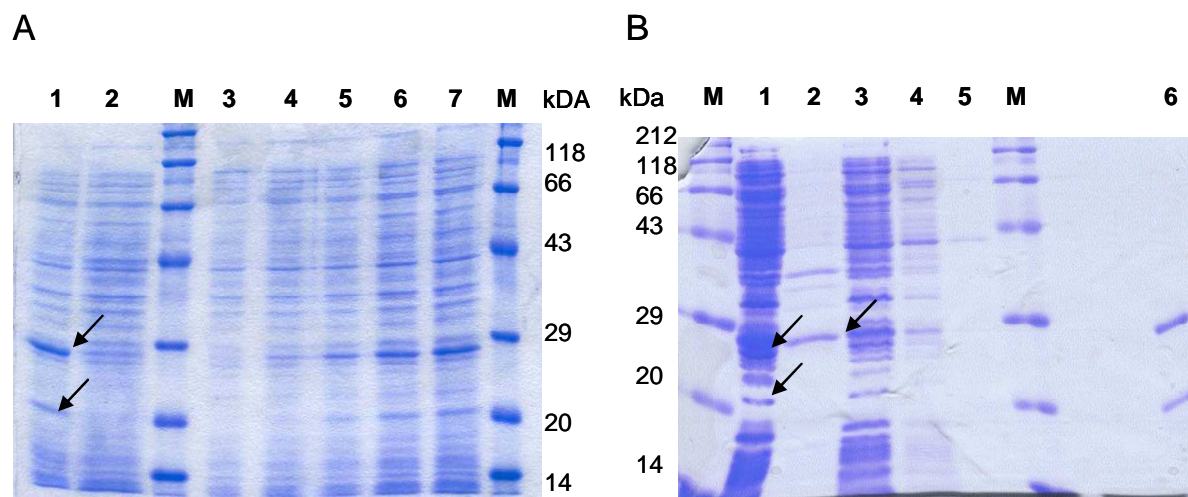
Figure 3.2 Co-expression (A) and purification (B) of CAR and SRC-1 via IMAC from *E. coli* BL21 (DE3) cell lysate (SDS-PAGE 16%). A Protein induction was carried out with 0.2 mM IPTG. The LBD of CAR has a molecular weight of 29.2 kDa whereas the RID of SRC-1 has a molecular weight of 16.9 kDa. 1: sample of the induced culture after 4h and 2: sample of the non-induced culture after 4h. M: unstained protein ladder; sample of the induced culture after 0h (lane 3), 1h (lane 4), 2h (lane 5), 3h (lane 6), and 4h (lane7) of protein expression. **B** M: unstained protein ladder, 1: lysate, 2: pellet, 3: flow through, 4: washing step 1, 5: washing step 5, 6: eluate

This expression demonstrates that the soluble overexpression of CAR protein was possible. Yet, since separation of the co-expressed proteins by means of anion exchange chromatography and elution via enhanced salt concentrations was not successful (results not shown), and one of the interactions to be examined was the very binding between receptor and co-activator, a different approach was chosen to yield soluble CAR protein. This approach included lowering temperature from 25° to 16°C, variation of both expression duration from 4 hours to 20 hours and shaking velocity from 140 rpm to 120 rpm. Optimization of expression conditions yielded soluble CAR protein (figure 3.3, arrow, lane 3) The negative controls did not exhibit overexpression of the target protein . However, by comparing figure 3.3 to figure 3.1B it is evident that altering the conditions of expression led to a partly shift of CAR protein from inclusion bodies to the lysate of the expressing *E. coli* cells (arrows, figure 3.3). Thus, CAR could be expressed solubly. Yet, there was still target protein left insolubly in the pellet fraction. Protein expression in 100 ml LB media yielded between 0.1 and 0.2 mg/ml of CAR protein.
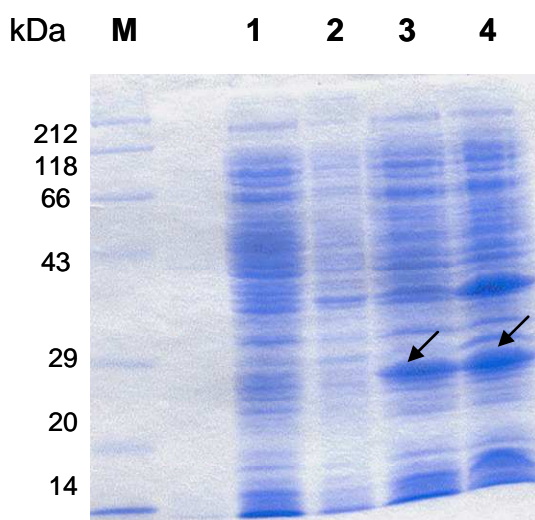
Figure 3.3 Overexpression of CAR protein under optimized conditions (16°C, 20h, 120 rpm) in *E. coli* BL21 (DE3) (SDS-PAGE 12.5%). Cell culture was induced with 0.2. mM IPTG. The LBD of CAR has a molecular weight of 29.2 kDa. M: unstained protein ladder, 1: lysate and 2: pellet of the non-induced culture; 3: lysate, and 4: pellet of the induced culture.

3.3 Overexpression of the human co-activators SRC-1 and SRC-2 in *E. coli*

Protein expression of SRC-1 and SRC-2 was performed using 1l shaking flasks which contained 200 ml of LB media. After transformation of the pET22b(+) vector containing the *SRC-1 RID* gene and the pET28a(+) vector containing the *SRC-2 RID* gene into *E. coli* BL21 (DE3), the cells were inocculated via 5 ml of over night culture. In contrast to the SRC-1 protein co-expressed with CAR, this SRC-1 protein was expressed with an N-terminal tag containing 10 histidine residues. The culture was kept under conditions of 37°C and 180 rpm until they reached an OD_{600} value between 0.4 and 0.6. Protein expression was induced with 0.2 mM IPTG. After induction both co-activators were expressed at 25°C and 140 rpm for four hours. There was no distinctively stronger expressed protein band especially when compared to the non-induced samples of *E. coli* (figure 3.4A, arrows). The SDS-PAGE illustrating the protein expression over time revealed that there was SRC-1 protein expressed in rather low concentrations (figure 3.4B, arrow) running between 18.4 and 25 kDa. The RID of SRC-1 carrying a 10x his-tag has a molecular weight of 18 kDa. However, SRC-1 protein could be detected in the lysate as well as the pellet of the *E. coli* cells.

Figure 3.4 Overexpression of the co-activator SRC-1 in *E. coli* BL21 (DE3) (SDS-PAGE 16%). The cell culture was induced with 0.2 mM IPTG. The RID of SRC-1 carrying a 10x his-tag has a molecular weight of 18 kDa. **A** 1: lysate and 2: pellet of non-induced culture, 3: lysate and 4: pellet of induced culture. M: unstained protein ladder. **B** M: unstained protein ladder, whole cell sample of the induced culture after 0h (lane 1), 1h (lane 2), 2h (lane 3), and 3h (lane 4) of protein expression.

SRC-2 protein expression as well did not yield a significant overexpression of target protein (figure 3.5A, arrow). But when compared to the non-induced culture, it is visible that protein expression took place depicted by SRC-2 running between 25 and 35 kDa. The RID of SRC-2 has a molecular weight of 24 kDa. Figure 3.5B illustrates both the lysate and the pellet after sonication of the cells. The overexpressed SRC-2 is visible in the lysate of the cell (figure 3.5B, arrow). Protein expression in 100 ml LB media yielded between 0.2 and 0.3 mg/ml SRC-1 and 0.1 and 0.2 mg/ml SRC-2.
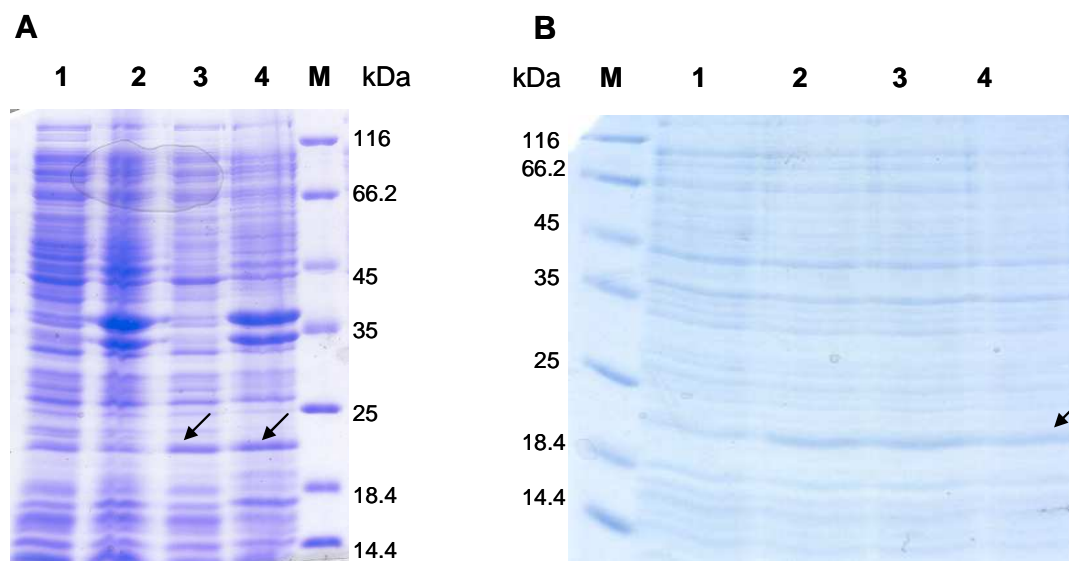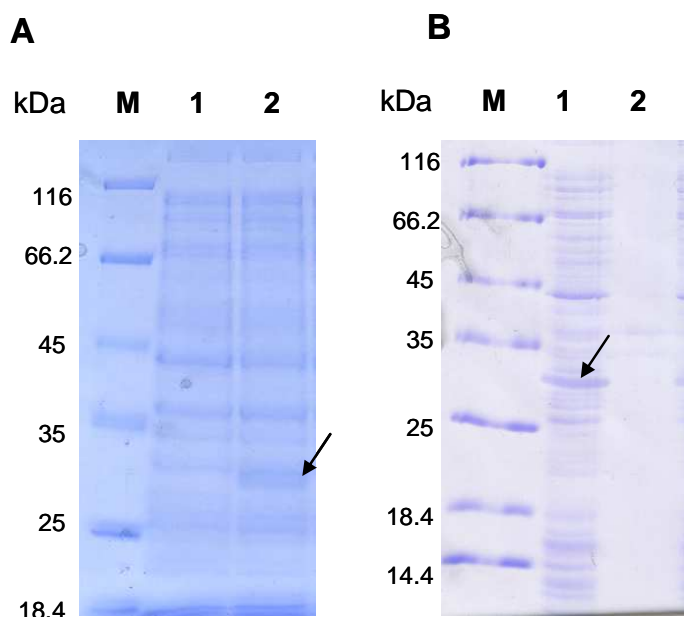
Figure 3.5 Overexpression of the co-activator SRC-2 in *E. coli* BL21 (DE3) (SDS-PAGE 16%). The cell culture was induced with 0.2 mM IPTG. The RID of SRC-2 has a molecular weight of 24 kDa. **A** M: unstained protein ladder. Whole cell samples of 1: non-induced culture and 2: induced culture. **B** M: unstained protein ladder, 1: lysate and 2: pellet of induced culture.

3.4 Detection of target proteins by Western Blot

Due to protein expression at 25°C and 140 rpm for four hours CAR was produced mainly in the pellet fraction of the *E. coli* cells (figure 3.6A, black arrow, lane 2). The Western Blot confirmed that CAR under these conditions was over expressed into inclusion bodies of *E. coli* cells. Minor part of CAR was expressed into the lysate (figure 3.6A, black arrow, lane 1). In contrary to the SDS-PAGE, the Western Blot reveals that CAR was not only insoluble but also degraded as one can see by the minor bands running below the undamaged protein (figure 3.6A, lane 2, red arrow). These smaller pieces of the original protein were to be found primarily in the pellet fraction of the cells. The pellet illustrates truncated CAR which visually seemed to make up to at least 50% of all proteins. Additionally, these degraded proteins have a broad range of different sizes up to less than 17 kDa. Apart from CAR itself, the lysate only displayed one additional slight band of protein running on half way between 17 and 26 kDa (figure 3.6A, lane 1, red arrow). Figure 3.6B depicts his-tagged eGFP running between 26 and 34 kDa which served as a positive control in the Western Blot. In the same figure one can see

CAR, expressed at 16°C and 120 rpm for 20 hours, purified from the lysate of *E. coli* cells which were induced with IPTG. It only consists of one band running slightly above 26 kDa (figure 3.6B, lane 2, black arrow). Contrary to CAR in inclusion bodies, the solubly expressed and purified CAR depicted in figure 3.6B (lane 2) illustrates that there were no degradation products any more, once eluated from the lysate of *E. coli* cells. This fact reveals that optimizing expression conditions by lowering temperature and shaking velocity as well as prolonging expression time led to CAR being produced into the soluble part of the *E. coli* cells. CAR expressed under non-modified conditions demonstrated degradation both in the lysate and the pellet whereas changing conditions led to enhanced stability. Expressing the receptor solubly provided two important advantages which are the easy purification from the lysate and the stability and integrity of the receptor not being truncated or damaged like in the pellet of *E. coli* cells.
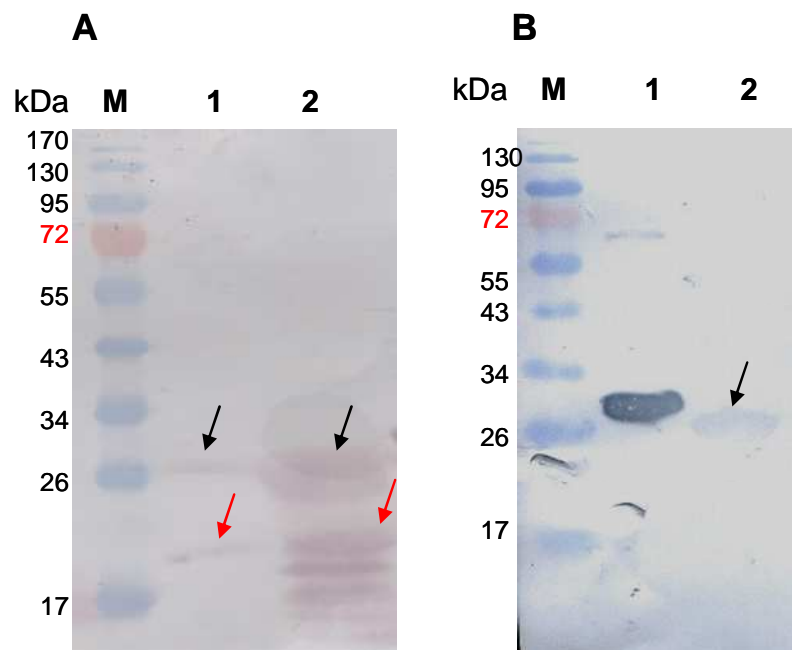
Figure 3.6 Western Blot of the nuclear receptor CAR. A M: prestained protein ladder, 1: lysate and 2: pellet of insoluble CAR. CAR was expressed at 25°C and 140 rpm for 4 hours. CAR protein is marked by black arrows. Degradation products are marked by red arrows. **B** M: prestained protein ladder, 1: his-tagged eGFP and 2: soluble CAR purified from the lysate of *E. coli* cells. CAR was expressed at 16°C and 120 rpm for 20h. CAR protein is marked by black arrows.

Figure 3.7 displays the Western Blot of SRC-1 from the lysate and pellet fraction of *E. coli* cells. SRC-1 running between 17 and 26 kDa is visibly expressed in the soluble as well as in the insoluble part of the cells. By contrast to insoluble CAR, the co-activator does not show any signs of protein degradation, neither in the lysate nor in the pellet.
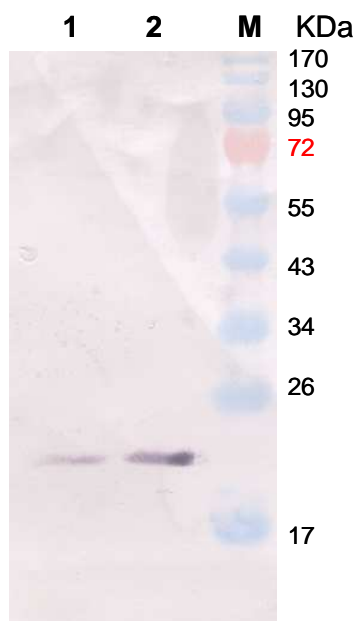
Figure 3.7 Western Blot of the co-activator SRC-1. SRC-1 was expressed with an N-terminal his-tag. 1: lysate, 2: pellet, and M: prestained protein ladder.

3.5 Purification via immobilized metal ion affinity chromatography (IMAC)

The purification of solubly expressed CAR was performed via immobilized metal ion affinity chromatography (IMAC). As a pre-condition for IMAC, it is necessary that the recombinant protein is attached to a tag of six histidine residues. Being cloned into the pET28a+ vector CAR is linked to an N-terminal his-tag of six residues. The purification of target proteins was illustrated by Coomassie and silver staining of SDS-PAGEs. Since the purity of the protein is crucial for interaction analysis in the Biacore system, silver staining was carried out in order to illustrate and emphasize the purity of the eluate. CAR visibly running between 25 and 30 kDa was purified from the lysate (figure 3.8A, lane 1). The Coomassie staining of the purification depicts that the eluate consisted of only one protein band. The silver staining, however, reveals that apart from the target protein, there was another not identified protein

running along with it (figure 3.8B, lane 9). This protein was only visible as a slight band of much weaker intensity. Therefore, it was not supposed to be of any major importance or interference.
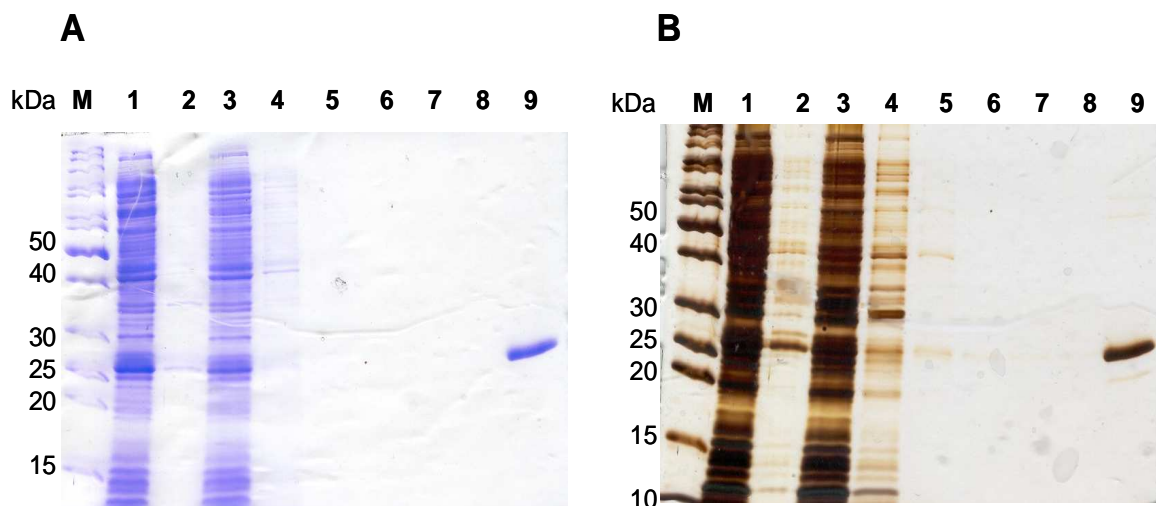
Figure 3.8 Purification of CAR protein via IMAC from *E. coli* cell lysate (SDS-PAGE 12.5%). A Coomassie staining, **B** silver staining; M: unstained protein ladder, 1: lysate, 2: pellet, 3: flow through, 4: washing step 1, 5: washing step 2, 6: washing step 3, 7: washing step 4, 8: washing step 5, and 9: eluate.

SRC-1 and SRC-2 were purified by performing the same IMAC purification protocol which was used for CAR. In order to be purified via IMAC, SRC-1 was amplified via PCR with 10 histidine residues. Subsequently, *10x His – SRC-1* was cloned into pET22b+. Being cloned into the pET28+ vector, SRC-2 is linked to an N-terminal his-tag of six residues. Both co-activators were found to be well expressed in the lysate of *E. coli* cells from which they were purified. The protein band of SRC-1 running between 18.4 and 25 kDa is depicted in figure 3.9A (lane 6). Obviously, the eluate was of high purity. Yet, there was another weak band of unknown protein running higher than SRC-1. SRC-2 running between 25 and 35 kDa is illustrated in figure 3.9B. The silver staining proves that SRC-2 was also of high purity (lane 6). As in the case of SRC-1 and CAR there was an additional weak band of protein visibly running higher than SRC-2. Since the silver staining of SRC-2 was slightly overdeveloped, both SRC-2 and the other protein band are of stronger intensity.

Taken together the nuclear receptor CAR as well as the co-activators SRC-1 and SRC-2 could be purified with the high purity necessary for SPR (surface plasmon resonance) analysis.
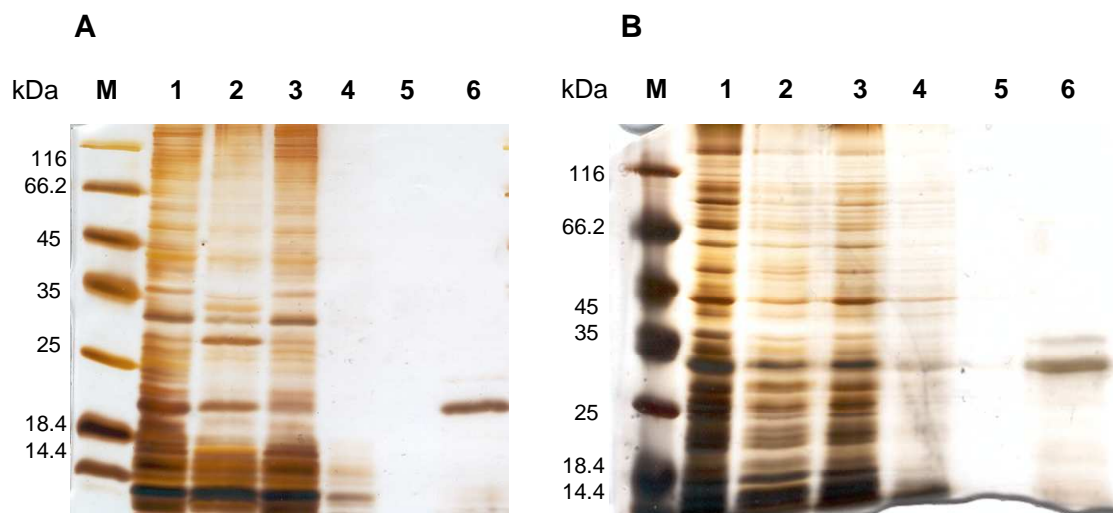
Figure 3.9 Purification of the co-activators SRC-1 (A) and SRC-2 (B) via IMAC from *E. coli* BL21 (DE3) cell lysate (SDS-PAGE, 12.5%). Silver staining containing following samples: M: unstained protein ladder, 1: lysate, 2: pellet, 3: flow through, 4: washing step 1, 5: washing step 5 and 6: eluate.

3.6 Investigation of CAR interactions using Surface plasmon resonance (SPR)

3.6.1 The influence of ligands on the association of the receptor – co-activator complex

Unlike the majority of the nuclear receptors, CAR is active in a ligand – independent manner (Moore *et al.*, 1998; Qatanani and Moore, 2005). Thus, the interaction between CAR and its co-regulators like SRC-1 and SRC-2 occurs even in the absence of a ligand. The activity of the receptor can be modified positively by the prominent CAR activator CITCO (Maglich *et al.*, 2003). CITCO (6-(4-chlorophenyl)imidazo[2,1-*b*][1,3]thiazole-5-carbaldehyde *O*-(3,4-dichlorobenzyl)oxime) by contrast to PB, a known CAR inducer, acts as an agonist and direct binder of the receptor. Hence, this process can be monitored as a real time event using surface plasmon resonance (Biacore 3000).

In the course of a screening performed at the IKP (for more details see diploma thesis of Jeanette Fait) several drugs could be verified as agonists and / or activators of the nuclear receptor CAR investigating the ligand-dependent interactions with the RID (receptor interaction domains) of DRIP205 (Vitamin D Receptor interacting protein 205) in mammalian

two-hybrid assays. These drugs were chosen for investigating the influence of ligands on the association of the receptor – co-activator complex using SPR.

In the following assays the analyte CAR was injected either on its own or after pre-incubation of at least 30 minutes with one of the drugs of interest. The ligand–free interaction represents the constitutive binding between receptor and co-activator and was therefore considered factor 1 (mean from CAR mock 1 and 2). The change in association response caused by samples of liganded CAR was calculated as x – fold responses. The focus was to examine the x – fold enhancement caused by liganded protein interactions relative to the drug-free binding. Thus, the absolute response value of the association was not the prime focus but the relative enhancement. One hundred micromolar of each drug or 10 µM CITCO respectively were pre-incubated with 210 nM CAR for at least 30 minutes at room temperature and afterwards injected in the flow cell over the immobilized co-activator. Considering the interaction with immobilized SRC-2 CAR was diluted to a final concentration of 50 nM only. For a better overview all the control samples are not demonstrated in the sensorgram. The controls include samples of running buffer, drugs without CAR and a diluted DMSO solution.

Regarding the assays the co-activator SRC-1 serves as the protein ligand and was, therefore, immobilized on Biacore CM5 chips. In this case, the term ligand designates the protein which was immobilized on the CM5 flow cell. One out of the 4 flow cells of each chip was not immobilized with the ligand but kept blank and was, therefore, used as the reference cell. Fc1 was used as the reference cell.

Eight different drugs were chosen from the screening which was performed at the IKP. The goal was to discover drugs which enhanced the constitutive binding between the nuclear receptor CAR and its co-activators using the Biacore 3000 system. The drugs which were chosen for the Biacore assays are CITCO, Phenobarbital, Clofibrate, Fenofibrate, Clotrimazole, Artemisinin, Arteether, Artemether, Triphenylphosphate, Androstanol, and Androstenol. Phenobarbital for example is known to induce CAR activation without binding it (Negishi et al., 1999). Clotrimazole is proven to act as an inverse agonist of human but not mouse CAR (Lempiäinen *et al*., 2005; Moore *et al*., 2000; Mäkinen *et al*., 2003). Enhancing the binding between receptor and co-activator is supposed to serve as a tool of identifying putative drugs strengthening the activation of the nuclear receptor CAR.

3.6.1.1 The influence of drugs on the association of CAR and SRC-1

The binding of non-liganded CAR to SRC-1 (CAR mock 1 and 2) yielded the lowest association curves of all curves demonstrated (figure 3.10). CAR liganded with clotrimazole achieved a binding response that almost matched the constitutive binding between CAR and SRC-1. So did CAR liganded with Phenobarbital. The only drugs that led to a significant higher association response are CITCO and Fenofibrate.

Figure 3.10 Sensorgram of the ligand-dependent binding between the immobilized co-activator SRC-1 and the nuclear receptor CAR. Before injection of the analyte over the co-activator surface, 0.21 µM CAR was pre-incubated with 100 µM of each drug respectively but with 10 µM of CITCO. Drugs used: PB: Phenobarbital, Feno: Fenofibrate, Clot: Clotrimazole and CITCO. CAR mock 1 and 2 represent the constitutive and ligand-independent receptor – co-activator binding.

Unlike the first assay depicted in figure 3.10, the pre-incubation of CAR with all putative ligands of the second assay led to a distinctive enhancement of the constitutive binding between the two proteins (figure 3.11). Binding of CAR liganded with Artether yielded the highest response curve whereas the pre-incubation of Artemisinin, Triphenylphosphate and Artemether with CAR yielded significantly lower but similar increase in association with SRC-1 while complex formation.

Figure 3.11 Sensorgram of the ligand-dependent binding between the immobilized co-activator SRC-1 and the nuclear receptor CAR. Before injection of the analyte over the co-activator surface, 0.21 µM CAR was pre-incubated with 100 µM of each drug respectively. Drugs used: TPP: Triphenylphosphate, ART: Artemisinin, AM: Artemether and AE: Arteether. CAR mock 1 and 2 represent the constitutive and ligand-independent receptor – co-activator binding.

Another set of drugs was tested including Clofibrate, Bisphenol A, Androstanol, and Androstenol. All these putative ligands resulted in a binding curve higher than the one caused by CAR binding the co-activator only, depicted as red and green curves (figure 3.12, CAR mock1 and 2). Again three of the drugs namely Bisphenol A, Androstanol, and Androstenol achieved comparable but less high association curves compared to Clofibrate which reached one of the highest association responses of CAR to SRC-1 of all drugs.
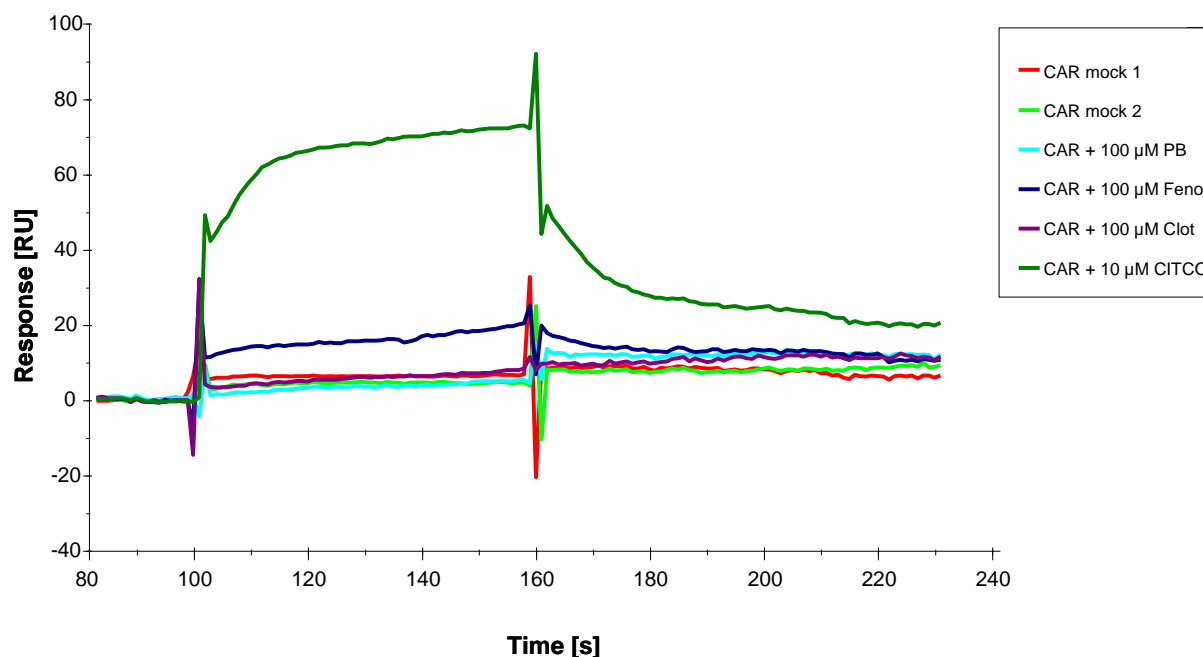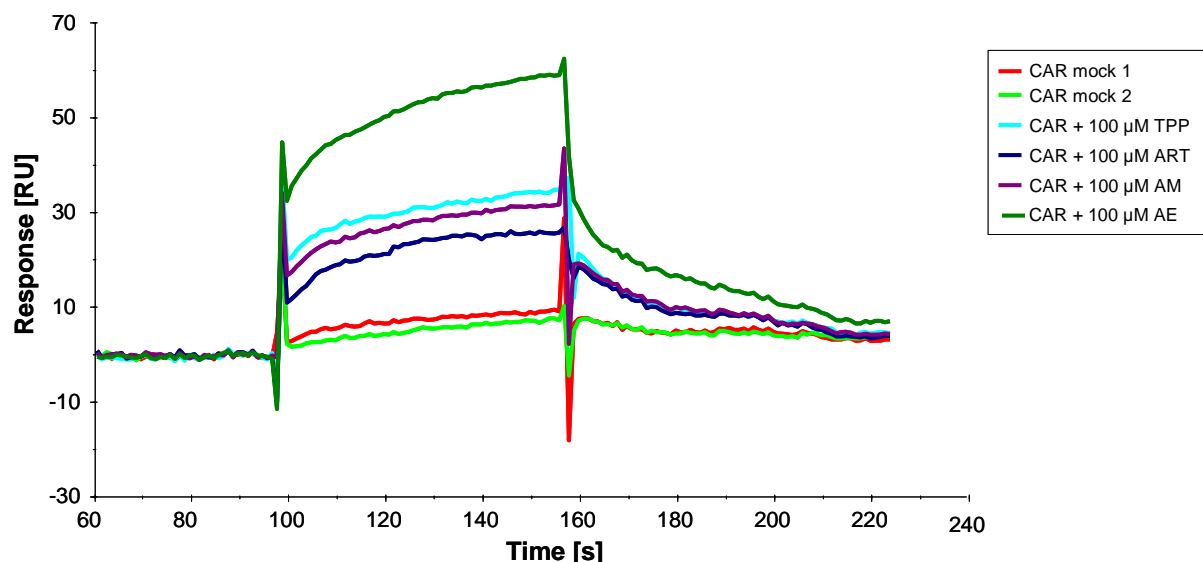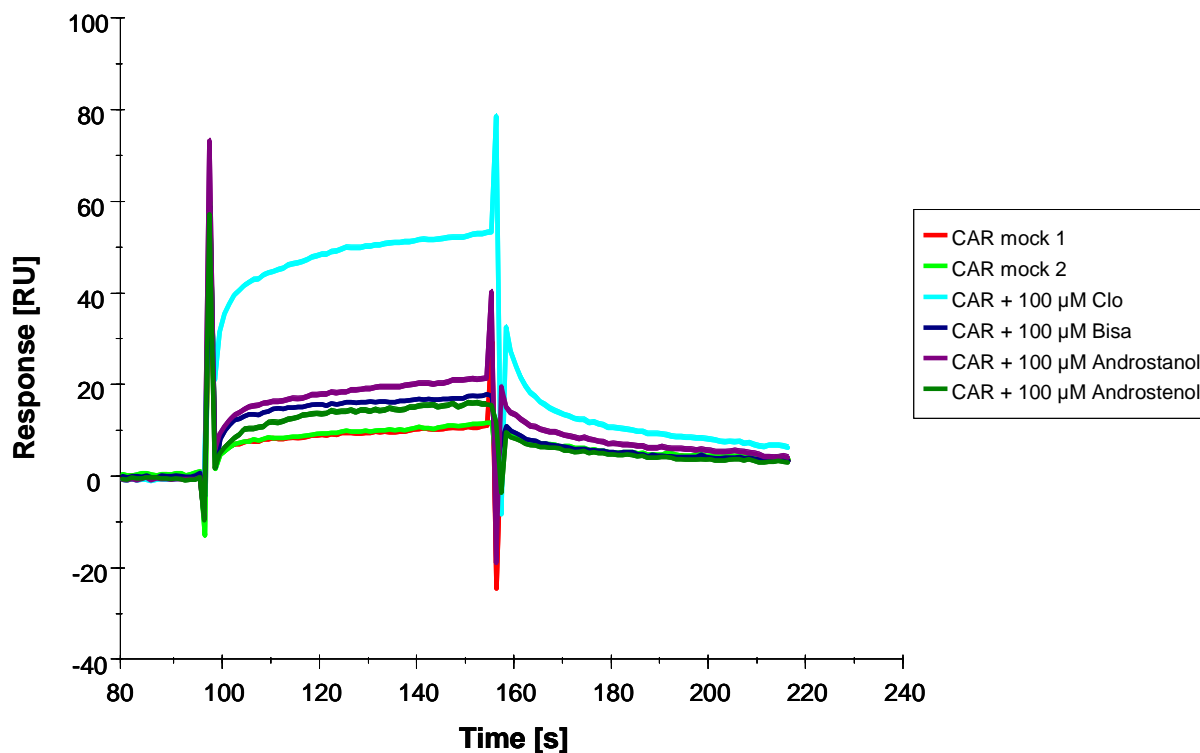
Figure 3.12 Sensorgram of the ligand-dependent binding between the immobilized co-activator SRC-1 and the nuclear receptor CAR. Before injection of the analyte over the co-activator surface, 0.21 µM CAR was pre-incubated with 100 µM of each drug respectively. Drugs used: CLO: Clofibrate, Bisa: Bisphenol A, Androstanol and Androstenol. CAR mock 1 and 2 represent the constitutive and ligand-independent receptor – co-activator binding.

The above-quoted assays of liganded CAR binding its co-activator SRC-1 resulted in a hierarchy of association as follows:

CITCO > AE > CLO > AM > TPP > ART > Feno > Bisa A > PB > Clot

The hierarchy is based on the enhanced association responses of ligand-dependent CAR – SRC-1 interactions relative to ligand-free interactions designated as CAR mock 1 and 2. The pre-incubation of CAR to a set of putative ligands caused a hierarchy of association that can be divided into three categories: low, medium and high association regarding the achieved value of response at the final point of the association phase. Figure 3.13 demonstrates that CAR pre-incubated with Clotrimazole, Phenobarbital and Bisphenol A achieved low association responses which yielded only a 1.2x, 1.4x and 1.5x higher response than the constitutive binding between the receptor CAR and its co-activator SRC-1. The drugs leading to a distinctive increase in binding when pre-incubated with CAR are Fenofibrate (2.2x),

Artemisinin (2.5x), Artemether (3.3x) and Triphenylphosphate (3.3x). The highest association responses achieved Clofibrate (5.3x). Arteether (5.3x) and CITCO belonged to the strong inducer category. Thus, in the presence of CITCO CAR displayed the most intense interaction with its co-activator SRC-1 reaching an association level 7.3x higher than the constitutive binding.

Figure 3.13 Ligand-dependent binding between the immobilized co-activator SRC-1 and the nuclear receptor CAR. Blue bars depict the ligand-dependent interaction, black bars constitute the negative controls of injected drugs without CAR. The blue bar named CAR displays the binding between CAR and SRC-1 in the absence of any ligand. The association responses yielded from ligand-dependent interactions were depicted as x-fold responses of the ligand-free binding. Data represent the standard deviation of three (drugs) and six (DMSO) individual binding analyses.

CAR was furthermore tested for binding SRC-1 after being incubated with either Androstanol or Androstenol. The interaction curves of liganded receptor binding its co-activator displayed that both substances led to a slightly increased association response compared to the constitutive binding. Androstanol yielding a 1.6x higher association value bound inconsiderably more intense to SRC-1 than Androstenol did with a 1.5x higher value (figure 3.14).
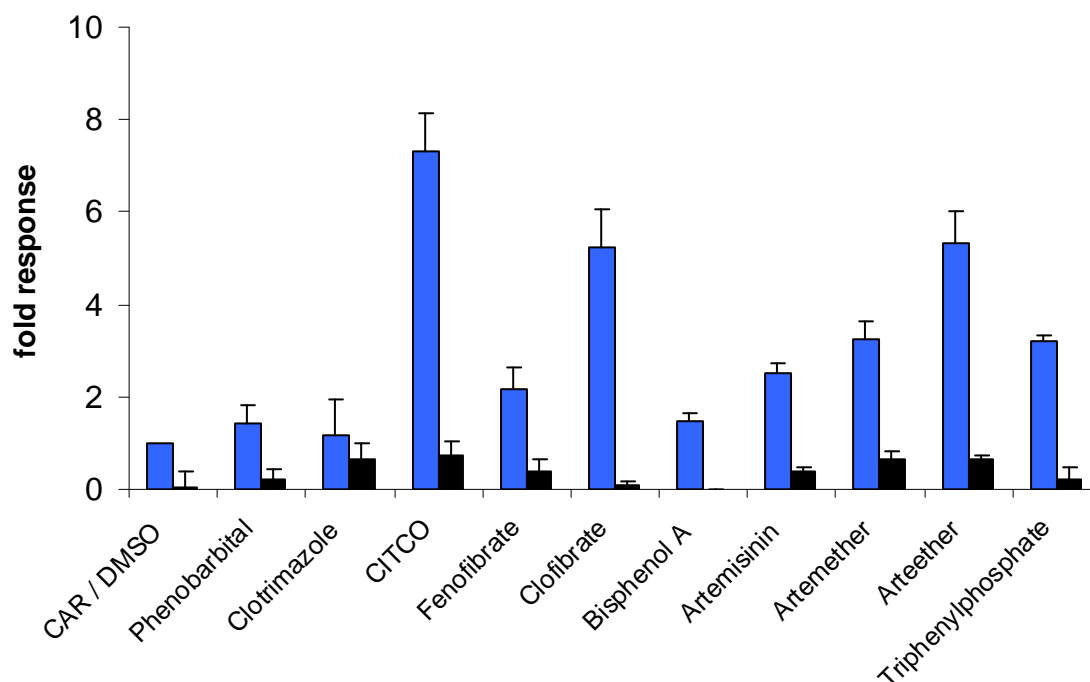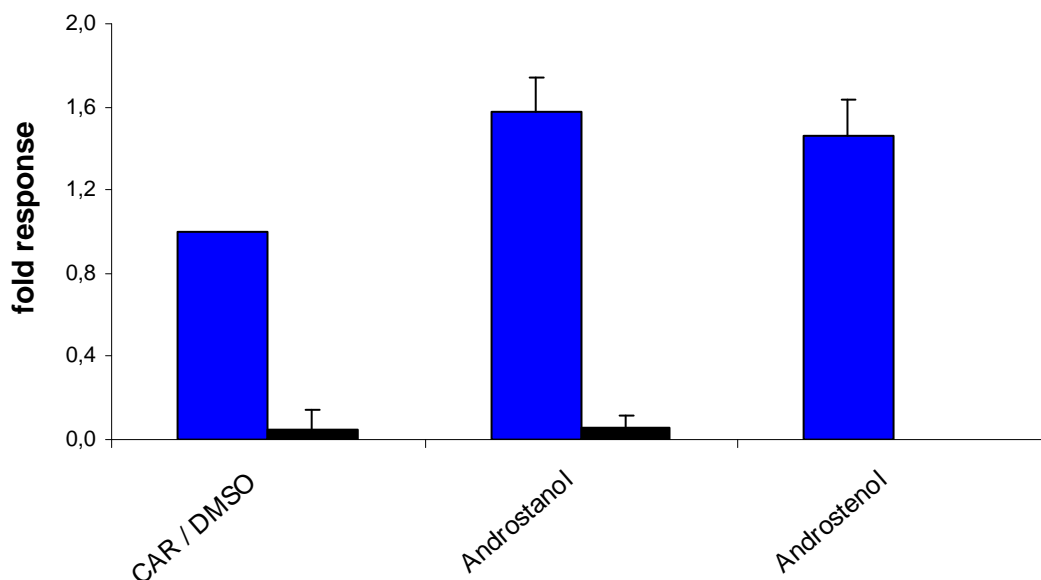
Figure 3.14 Ligand-dependent binding between the immobilized co-activator SRC-1 and the nuclear receptor CAR. Blue bars depict the ligand-dependent interaction, black bars constitute the negative controls of injected drugs without CAR. The blue bar named CAR displays the binding between CAR and SRC-1 in the absence of any ligand. The association responses yielded from ligand-dependent interactions were depicted as x-fold responses of the ligand-free binding. Data represent the standard deviation of four (Androstanol), five (Androstenol) and nine (DMSO) individual binding analyses.

3.6.1.2 Drug-dependent association of CAR and SRC-1 under the influence of the inverse agonist Clotrimazole

A further series of assays served to examine whether the ligand-induced enhancement of the CAR – SRC-1 association could be fully or at least partially be reversed by an inverse agonist. For this purpose association of the receptor and the co-activator was examined under the influence of both the ligand as well as 100 µM Clotrimazole at the same time. Clotrimazole is the inverse agonist of human CAR but not mouse CAR and is used for antifungal medication (Lempiäinen *et al*., 2005; Moore *et al*., 2000; Mäkinen *et al*., 2003).

CAR incubated with Clotrimazole was demonstrated to alter the constitutive binding only to a 1.2x higher response for the association and, thus, yielding the lowest change in response (figure 3.10 and 3.13). Similar to the inhibitor-free assays it was still CITCO yielding one of the highest bindings followed by Phenobarbital and Fenofibrate (figure 3.15).

Figure 3.15 Sensorgram of the ligand-dependent binding between the immobilized co-activator SRC-1 and the nuclear receptor CAR co-incubated with the inverse agonist Clotrimazole. Before injection of the analyte over the co-activator surface, 0.21 µM CAR was pre-incubated with 100 µM of each drug respectively and 100 µM of clotrimazole at the same time. Drugs used: PB: Phenobarbital, Feno: Fenofibrate, Clotrimazole und CITCO. CAR mock 1 and 2 represent the constitutive and ligand-independent receptor – co-activator binding.

Figure 3.16 depicts the sensorgram with curves of the only drug Clofibrate and the non-liganded proteins. This small molecule seems to be one of the drugs on which the inhibitor had the highest impact. The enhanced association which happened when there was no inhibitor (figure 3.12 and 3.13) seems to be almost completely abolished resulting in no distinctive enhancement of CAR - SRC-1 association. Hence, this interaction resembles more the ligand-free protein – protein interaction.

Figure 3.16 Sensorgram of the ligand-dependent binding between the immobilized co-activator SRC-1 and the nuclear receptor CAR co-incubated with the inverse agonist Clotrimazole. Before injection of the analyte over the co-activator surface, 0.21 µM CAR was pre-incubated with 100 µM of each drug respectively and 100 µM of clotrimazole at the same time. Drugs used: Clo: Clofibrate. CAR mock 1 and 2 represent the constitutive and ligand-independent receptor – co-activator binding.

In figure 3.17 one can see another assay of the inhibitor-based binding curves of both Artemisinin and its derivatives Arteether and Artemether as well as the curve of Triphenylphosphate. The highest association curve in this sensorgram was the result of CAR being co-incubated with Arteether. Artemether and Artemsinin demonstrated lower responses but still enhanced association relative to the drug-free binding of the proteins. Triphenylphosphate, however, demonstrated distinctively decreased binding.
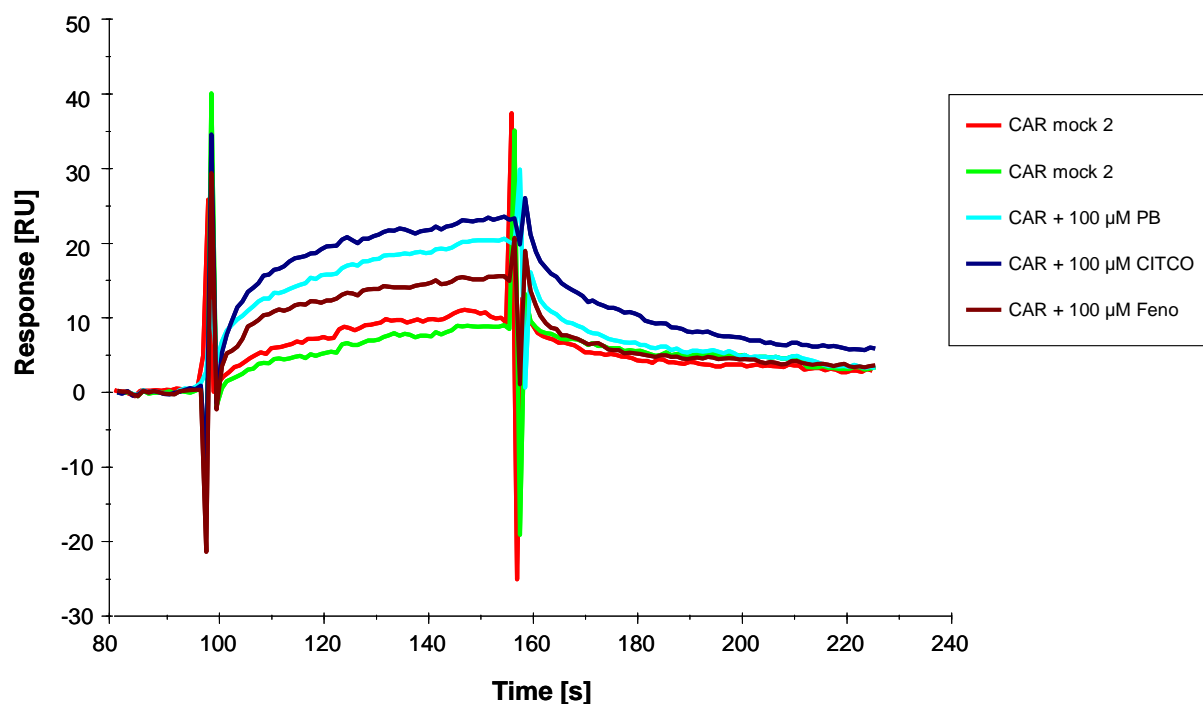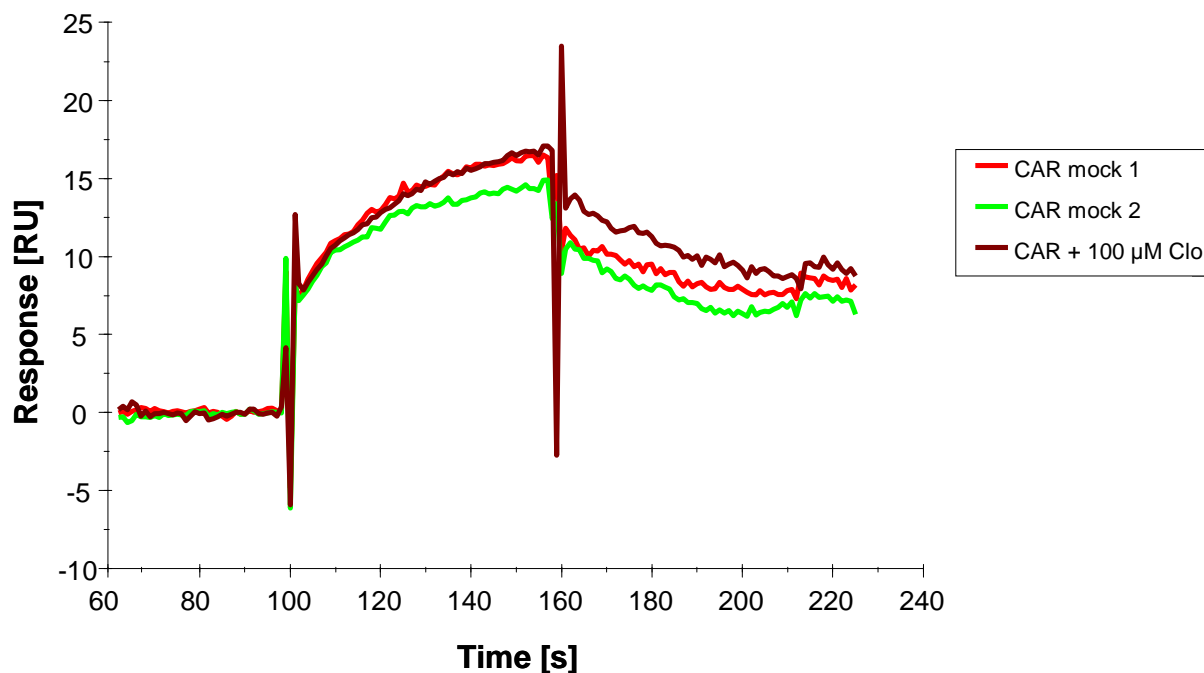
Figure 3.17 Sensorgram of the ligand-dependent binding between the immobilized co-activator SRC-1 and the nuclear receptor CAR co-incubated with the inverse agonist Clotrimazole. Before injection of the analyte over the co-activator surface, 0.21 µM CAR was pre-incubated with 100 µM of each drug respectively and 100 µM of clotrimazole at the same time. Drugs used: TPP: Triphenylphosphate, ART: Artemisinin, AM: Artemether and AE: Arteether. CAR mock 1 and 2 represent the constitutive and ligand-independent receptor – co-activator binding.

Figure 3.18 shows the chart of the ligand-induced interaction between CAR and SRC-1 with or without the inverse agonist Clotrimazole. It is obvious that adding Clotrimazole to the drug – protein mix (yellow bars) decreased the former increased association (blue bars) in each and every ligand-based binding event of the receptor and its co-activator apart from Phenobarbital. Though being co-incubated with the specific inhibitor, all drugs still led to an enhanced response relative to the non-liganded interactions (CAR mock 1 and 2). Without the inhibitor there is a broad range of enhanced association events of the different drugs ranging from 1.4x for Phenobarbital to 7.3x stronger association for CITCO. CITCO yielding a value of 2.3x higher response proves to be the strongest inducer among all drugs despite the presence of the inverse agonist. On the other hand, it was CITCO of which the original enhancement was decreased the most from 7.3x dropping to 2.3x fold response. The second highest response was measured for the drugs Arteether and Phenobarbital. Both chemicals lead to 2x higher association values compared to the constitutive ones. Thereby the intensity of association dropped from 5.3x to 2x for Arteether whereas Phenobarbital is the only drug displaying an

increase of response from 1.4x to 2x higher in binding once being co-incubated with Clotrimazole. The next highest response values were measured for Artemether (1.7x), Fenofibrate (1.4x), Artemisinin (1.3x), Clofibrate (1.2x) and finally Triphenylphosphate reaching the lowest binding response with 1.1x higher binding than the proteins solely.

Even Clofibrate causing one of the highest association responses dropped considerably from 5.3x to 1.2x when Clotrimazole was added. The remaining drugs' association responses dropped but this decrease was significantly lower compared to the one of Arteether, CITCO and Clofibrate.

The addition of Clotrimazole led to an association varying from 1.1x to only 2.3x higher association responses. As a result, CAR being co-incubated with both Clotrimazole and the respective drug seems to lower the binding capability of the proteins to similar values of association responses regardless of how strong or weak the ligand was in the absence of the inverse agonist. Thus, there was no distinctive hierarchy of association responses as there was for the ligand-based interactions without the inverse agonist Clotrimazole.

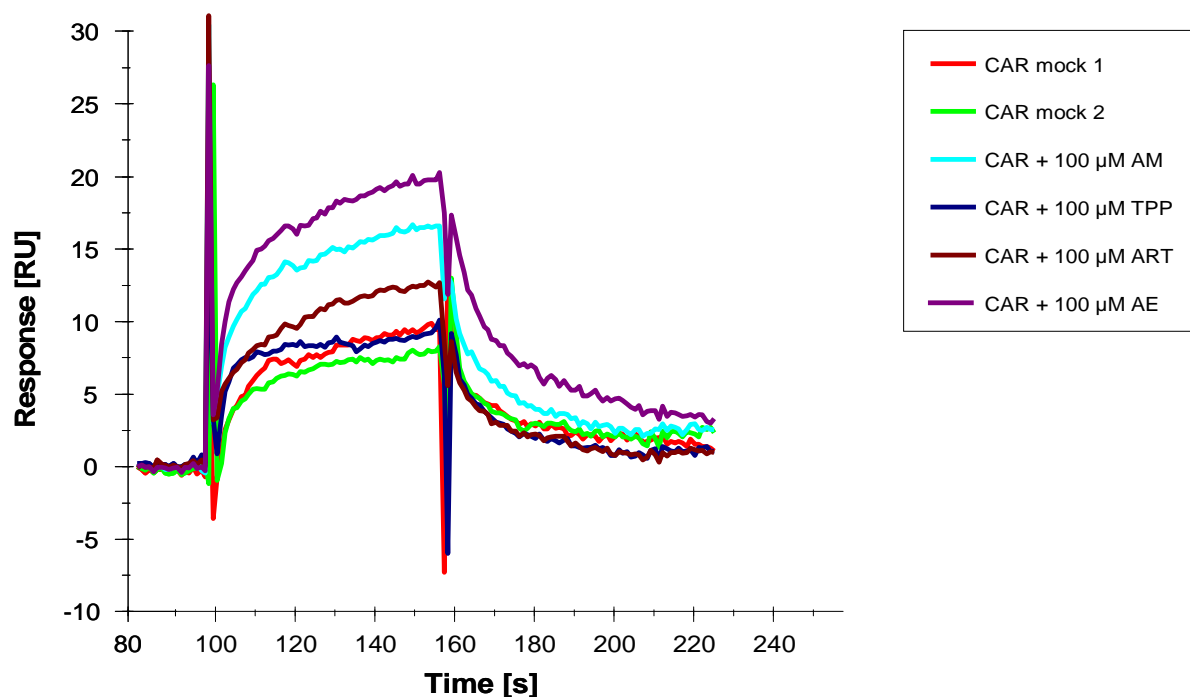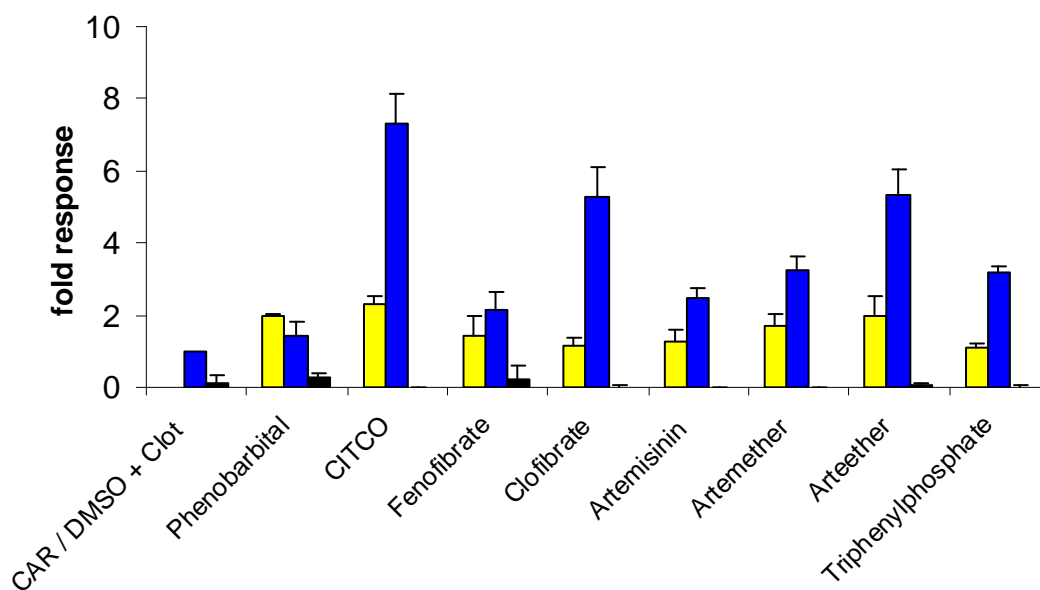**Figure 3.18 Ligand-dependent binding between the immobilized co-activator SRC-1 and the nuclear receptor CAR co-incubated with Clotrimazole.** Blue bars depict the ligand-dependent interaction without Clotrimazole, yellow bars represent the ligand-dependent interaction with Clotrimazole, and black bars constitute the negative controls of injected drugs without CAR. The blue bar named CAR displays the binding between CAR and SRC-1 in the absence of any ligand. The association responses yielded from ligand-dependent interactions are depicted as x-fold responses of the ligand-free binding. Data of the inhibition assays represent the standard deviation of three (Phenobarbital and CITCO), seven (Fenofibrate), thirteen (DMSO + Clotrimazole) and four (remaining drugs) individual binding analyses. Data of the Clotrimazole-free assays represent the standard deviation of three individual binding assays for each drug.

3.6.1.3 The influence of Atorvastatin and its metabolites on the association of CAR and SRC-1

HMG (3-hydroxy-3-methylglutaryl) - CoA reductase inhibitors which increase the expression of P450s, are commonly used to treat hypercholesterolemia. These inhibitors comprise statins like Atorvastatin which is a cholesterol-lowering drug.

After the immobilization of SRC-1, Atorvastatin and its metabolites were tested for increase in association the same way as the drugs above mentioned.

The sensorgrams of the CAR – SRC-1 interaction under the influence of Atorvastatin acid and lactone as well as their particular ortho- and para-OH- derivatives are shown in figures 3.19 and 3.20. Both the precursors and their derivatives did not deviate strongly from the

116

constitutive binding of the non-liganded proteins. On one hand, the binding curve of Atorvastatin lactone ran higher than the CAR mock 2 curve, on the other hand the acid of Atorvastatin ran lower than CAR mock 1. There was no significant increase or decrease in response shown for para-OH Atorvastatin both acid and lactone. Ortho-OH Atrovastain acid ran underneath while Atorvastatin ortho-OH lactone ran above the constitutive binding curves.

Figure 3.19 Sensorgram of the Atorvastatin-dependent binding between the immobilized co-activator SRC-1 and the nuclear receptor CAR. Before injection of the analyte over the co-activator surface, 0.21 µM CAR was pre-incubated with 100 µM of each drug respectively. Drugs used: Acid: Atorvastatin acid, Lac: Atorvastatin lactone. CAR mock 1 and 2 represent the constitutive and ligand-independent receptor – co-activator binding.

Figure 3.20 Sensorgram of the Atorvastatin-dependent binding between the immobilized co-activator SRC-1 and the nuclear receptor CAR. Before injection of the analyte over the co-activator surface, 0.21 µM CAR was pre-incubated with 100 µM of each drug respectively. Drugs used: para Acid: Atorvastatin para-OH acid, para Lac: para-OH Atorvastatin lactone, ortho acid: Atorvastatin ortho-OH acid and ortho Lac: ortho-OH Atorvastatin lactone. CAR mock 1 and 2 represent the constitutive and ligand-independent receptor – co-activator binding.

Figure 3.21 demonstrates that altered binding between CAR and SRC-1 as the result of being liganded could hardly be detected since the intensity of the interaction ranged from only 1.3x for Atorvastatin lactone to 0.6x of the constitutive binding for Atorvastatin acid. These drugs marked the maximum and minimum levels of binding after incubation with the described set-up of drugs. The para- and ortho-OH acid metabolites both yielded 0.9x of the constitutive binding. The para- and ortho-OH lactone metabolites also matched the non-liganded interaction with values of 1x and 1.1x relative to drug-free interaction. Thus, CAR in the presence of either Atorvastatin acid, lactone or each of their respective derivatives did not show any significantly enhanced or decreased binding to SRC-1.
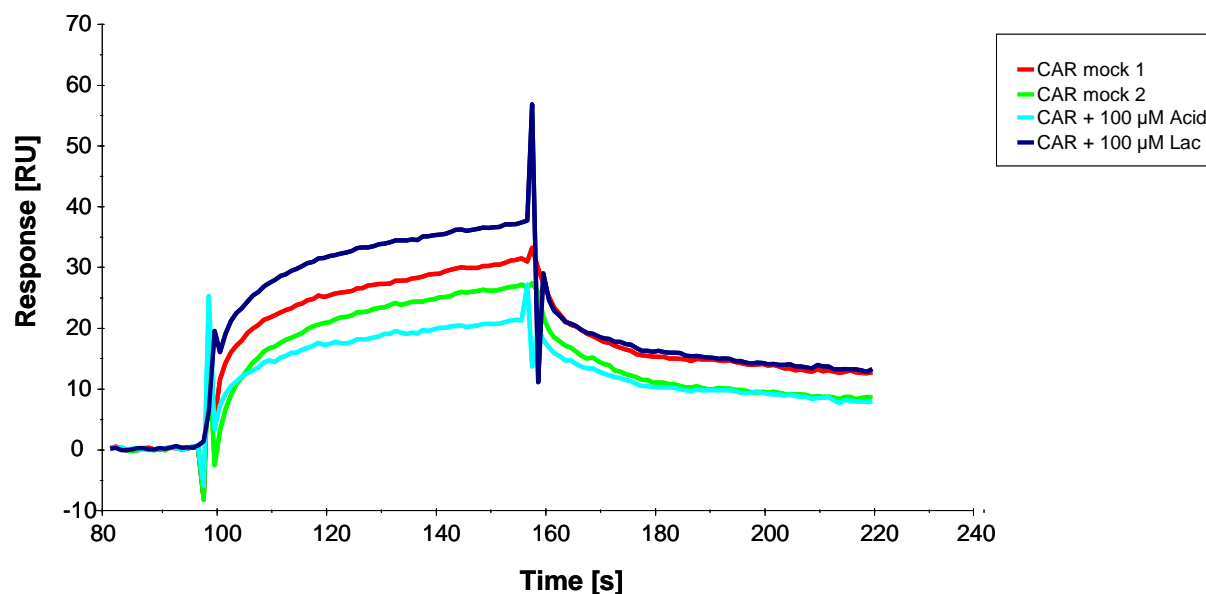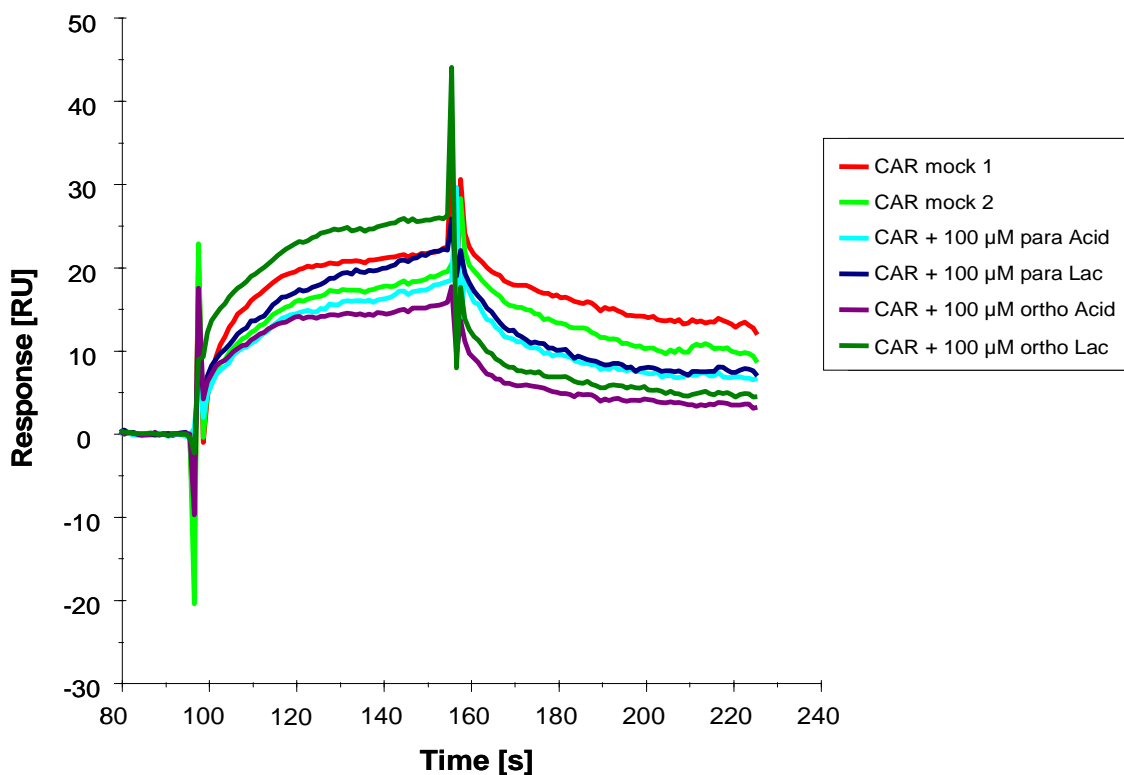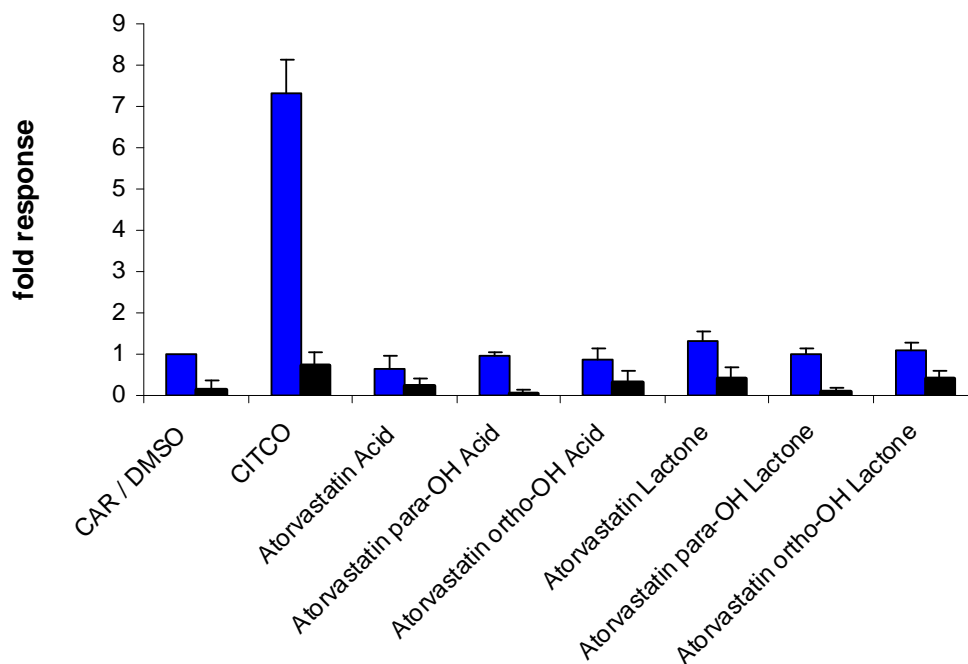
Figure 3.21 Atorvastatin-dependent binding between the immobilized co-activator SRC-1 and the nuclear receptor CAR. CITCO-dependent binding between SRC-1 and CAR was added to provide comparison between inducers and non-inducers. Blue bars depict the ligand-dependent interactions, black bars constitute the negative controls of injected drugs without CAR. The blue bar named CAR displays the binding between CAR and SRC-1 in the absence of any ligand. The association responses yielded from ligand-dependent interactions were depicted as x-fold responses of the ligand-free binding. Data represent the standard deviation of six (Atorvastatin acid and lactone), four (para- and ortho-OH-metabolites of Atorvastatin) and thirteen (DMSO) individual binding analyses.

3.6.1.4   The influence of drugs on the association of CAR and SRC-2

SRC-2 is like SRC-1 one co-activator out of several which have been shown to interact *in vitro* with CAR. Interestingly, there is no clear evidence which co-activator is favored by the receptor or whether CAR prefers one protein to the other over different conditions apart from tissue dependent expression patterns. In order to address this question, SRC-2 was also immobilized on a Biacore CM5 chip the same way as SRC-1 was. This way interaction between CAR and SRC-2 can be investigated in a drug-dependent manner. CAR which served as the analyte was diluted to a final concentration of 50 nM. For binding SRC-2 CAR needed a concentration of only 50 nM to yield an association response of about 5 RU in order to be able to detect further enhancement of association by addition of drugs.

Figure 3.22 shows the drug-free binding between CAR and SRC-2 depicted as red and green curves (CAR mock 1 and 2). The remaining curves in the sensorgram represent the drug-dependent interactions between the two proteins. CAR mock 1 and 2 clearly show that after stop of injection CAR hardly dissociated from the immobilized SRC-2. Compared to the binding of CAR to SRC-1 it is evident that SRC-2 bound more intense to the receptor since there was almost no dissociation detectable. Apart from Phenobarbital all drug-related samples led to an increase in response. The samples containing Fenofibrate and Clotrimazole yielded the same enhancement of response whereas CITCO resulted being one of the highest augmentations relative to the non-liganded protein interactions. On the other hand, the CITCO sample showed less tight binding of CAR to SRC-2 since there was some dissociation visible after injection stop of the analyte.
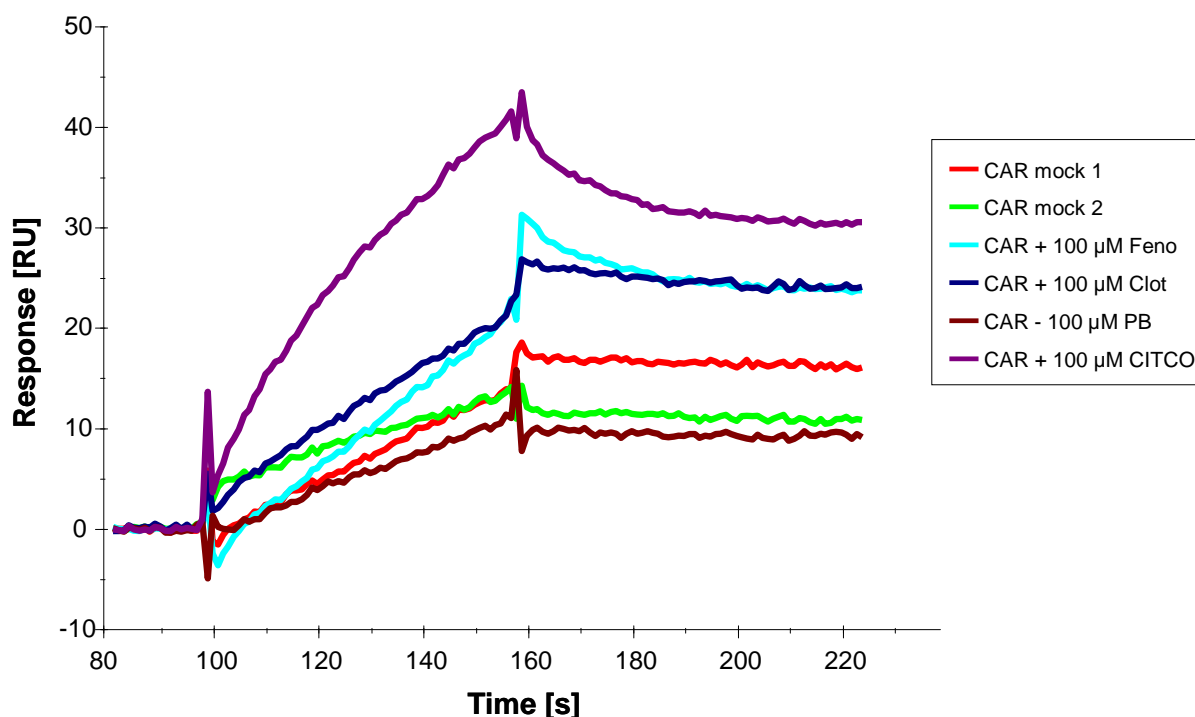
Figure 3.22 Sensorgram of the ligand-dependent binding between the immobilized co-activator SRC-2 and the nuclear receptor CAR. Before injection of the analyte over the co-activator surface, 0.05 µM CAR was pre-incubated with 100 µM of each drug respectively. Drugs used: PB: Phenobarbital, Feno: Fenofibrate, Clot: Clotrimazole und CITCO. CAR mock 1 and 2 represent the constitutive and ligand-independent receptor – co-activator binding.

Another set of drugs including Artemisinin, Arteether, Artemether, and Triphenylphosphate was tested (figure 3.23). Among all drugs tested, Arteether yielded the highest increase in

response considering the interaction between CAR and SRC-2 followed by Triphenylphosphate and Artemether which resulted in lower but similar values of enhanced association responses. Artemisinin demonstrated the lowest increase in this sensorgram with its association curve running only a little higher than CAR mock 1 and 2.
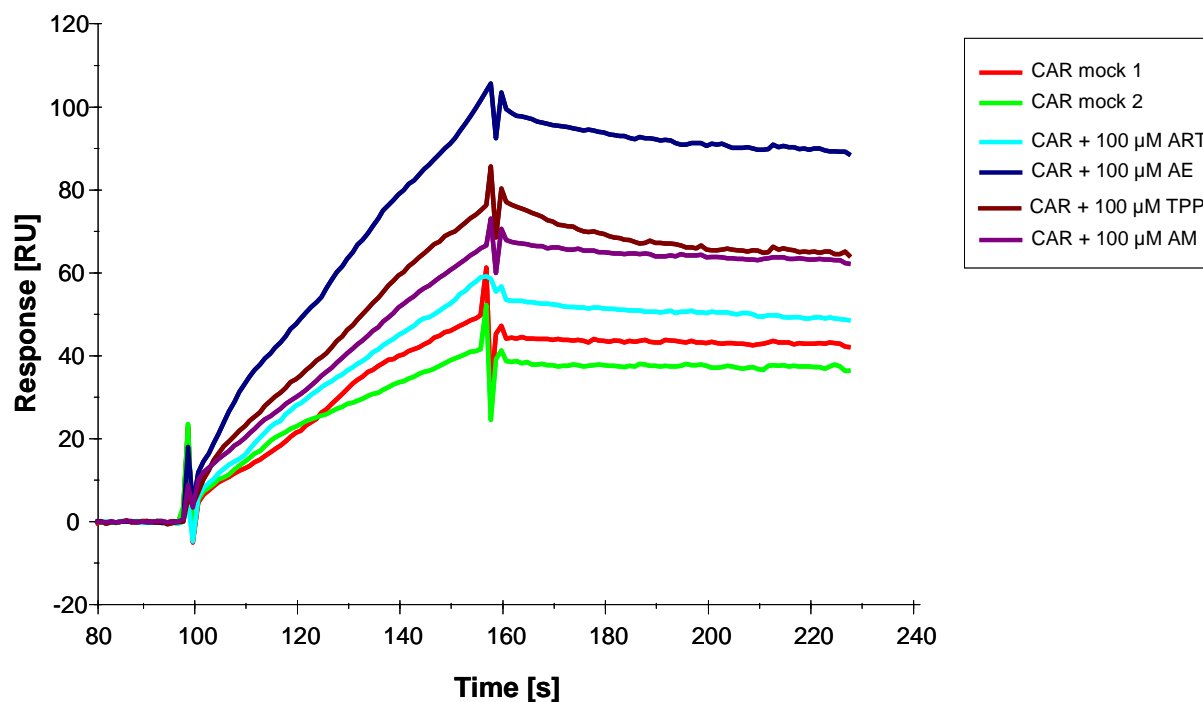
Figure 3.23 Sensorgram of the ligand-dependent binding between the immobilized co-activator SRC-2 and the nuclear receptor CAR. Before injection of the analyte over the co-activator surface, 0.05 µM CAR was preincubated with 100 µM of each drug respectively. Drugs used: TPP: Triphenylphosphate, ART: Artemisinin, AM: Artemether and AE: Arteether. CAR mock 1 and 2 represent the constitutive and ligand-independent receptor – co-activator binding.

Figure 3.24 displays the chart of association responses of the CAR – SRC-2 interactions depending on the drugs above mentioned. Phenobarbital, which induces but does not bind CAR, yielded an association response below the drug free interaction reaching a value of only 0.8x. CAR being incubated with Artemisinin achieved a 1.4x higher value and, thus, only a slight increase of association. Clotrimazole the inverse agonist of human CAR, as well as Fenofibrate resulted in a 1.6x higher response value. Artemether and Triphenylphosphate attaining 1.8x and 2.1x higher association responses respectively appeared to be medium association inducers. CAR incubated with CITCO and Arteether achieved 2.4x and 2.6x higher association responses respectively. Thus, these drugs demonstrated to induce the strongest association between CAR and SRC-2. Hence, liganded CAR binding its co-activator SRC-2 resulted in a hierarchy of association as follows:

AE > CITCO > TPP > AM > Feno / Clot > ART > PB

The hierarchy is based on the enhanced association responses of ligand-dependent CAR – SRC-2 interactions relative to ligand-free interactions designated as CAR mock 1 and 2. Since none of the drugs yielded association responses higher than 3x binding of the non-liganded proteins no strong association inducer could be verified between CAR and SRC-2.
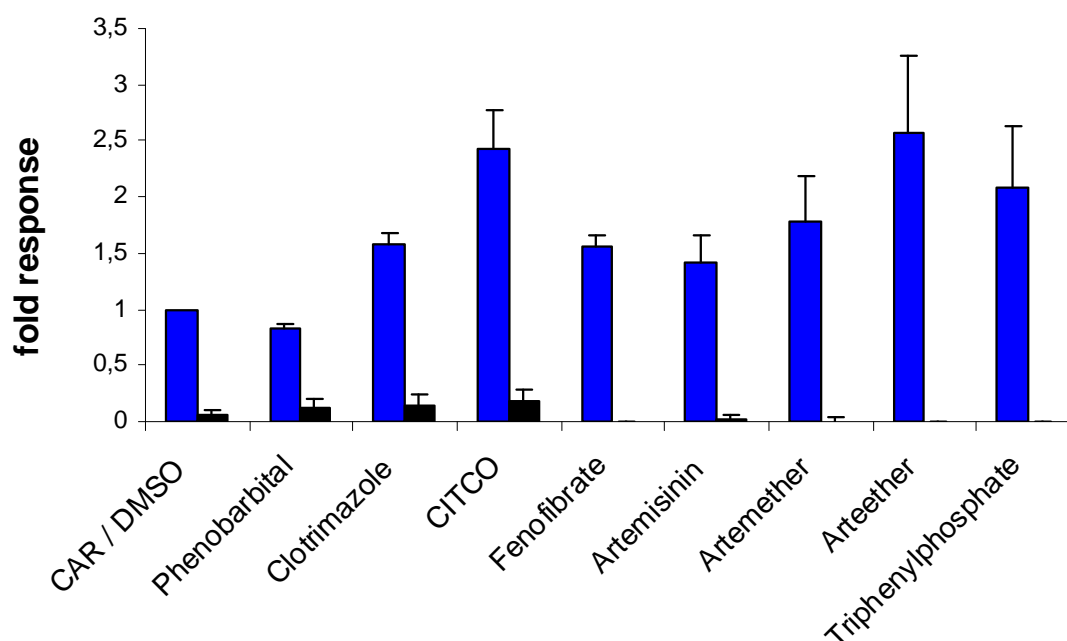
Figure 3.24 Ligand -binding between the immobilized co-activator SRC-2 and the nuclear receptor CAR. Blue bars depict the ligand-dependent interaction, black bars constitute the negative controls of injected drugs without CAR. The blue bar named CAR displays the binding between CAR and SRC-2 in the absence of any ligand. The association responses yielded from ligand-dependent interactions were depicted as x-fold responses of the ligand-free binding. Data represent the standard deviation of three (Phenobarbital and CITCO), seven (Fenofibrate), thirteen (DMSO + Clotrimazole) and four (remaining drugs) individual binding analyses.

Table 3.1 describes the binding between CAR and the respective co-activator under the influence of the above quoted drugs. CAR displayed the highest enhancement of association response caused by drugs when interacting with the co-activator SRC-1. The range covered 1.2 fold for Clotrimazole up to 7.3 fold association for CITCO. The CAR – SRC-2 interaction could not be influenced by drugs as much as the CAR – SRC-1 interaction. The highest

augmentation induced by small molecules was a 2.6x higher association response when co-incubated with Arteether. The lowest alteration was gained by co-incubation with Phenobarbital leading to only 0.8 fold binding.

Table 3.1 Drug-dependent enhancement of the constitutive binding between CAR and the co-activators SRC-1 and SRC-2.

Drugs added in a final concentration of 100 µM	x-fold binding of CAR and co-activator	
	SRC-1	SRC-2
CITCO*	7.3	2.4
Arteether	5.3	2.6
Artemether	3.2	1.8
Artemisinin	2.5	1.4
Triphenylphosphate	3.2	2.1
Fenofibrate	2.2	1.6
Phenobarbital	1.4	0.8
Clotrimazole	1.2	1.6

* CITCO was added in a final concentration of 10 µM

3.6.2 Interaction analyses describing kinetics of receptor - co-activator binding

Binding assays between CAR and its co-activators already yielded information on the association of the receptor with either SRC-1 or SRC-2 under the influence of certain drugs and putative ligands. These binding experiments led to a distinctive hierarchy of association for each protein pair that described in the majority of cases enhanced binding in a ligand-dependent manner. But association does not equal kinetics since the latter tells more about the nature of the binding between two proteins than association does. For example, binding of different proteins that demonstrate equal affinities does not have to reveal equal kinetic data. This means kinetic data reveals more detailed and crucial information than association or

affinity does. In this case, kinetic experiments ought to serve as another tool to investigate which of the co-activators might be favored by CAR.

Therefore, the nuclear receptor was immobilized at low densities on a regular Biacore CM5 chip. The co-activators SRC-1 and SRC-2 were injected over the receptor surface to investigate the protein binding. Each assay contained five different concentrations of analyte comprising 0.75, 2, 4, 6 and 8 µM of the respective co-activator. In order to cover a broad spectrum of sample concentrations, the co-activator was injected over the receptor with the highest concentration being ten times higher than the lowest. The goal of this experiment was to yield kinetic data describing the nature of kinetics achieved by CAR binding to either SRC-1 or SRC-2.

3.6.2.1   Kinetic investigation of the CAR – co-activator interaction

The first aim was to characterize the CAR – co-activator binding. For this purpose the interaction between the immobilized nuclear receptor CAR and either SRC-1 or SRC-2 was investigated without any influence from drugs. Therefore, the association as well as the dissociation was monitored for one minute. This assay allows a comparison between the two co-activators which could lead to further information on CAR's selectivity over its protein binding partners.

Figure 3.25 displays CAR binding the co-activator SRC-1. The different concentrations of SRC-1 ranging from 2 to 8 µM demonstrate the concentration-dependent interaction between the two proteins. The highest concentration of SRC-1 of 8 µM yielded the maximum response of almost 25 RU in this binding assay. In case of the highest concentration of SRC-1 injected the dissociation seems to happen in a rather slow way since after one minute there is still more than 50% of each concentration's maximum response bound to the receptor surface. All the other concentrations of SRC-1 did not seem to dissociate from the receptor at all since the amount of co-activator bound to CAR at the end of one minute of dissociation matched the amount at the highest point of association. In order to yield kinetic data from this assay the experimental curves were evaluated using the 1:1 Langmuir binding model with drifting baseline. The kinetic data obtained is displayed in table 3.2.

The residual plot serves as a tool to illustrate the discrepancy between the experimental curves and the global fit. Using this plot makes it easier to evaluate the match or mismatch between the experiment and the fit. A value of 2 is still being considered as instrument noise while

values up to 10 can be seen as a tolerable deviation of a good match. The sensorgram of figure 3.25 as well as the residual plot of figure 3.26 displays a slight mismatch especially in the beginning and the end of the association phase of the binding cycle. The lowest concentration of 2 µM of SRC-1 displayed the worst match between experimental and fit curve. All others demonstrated a good match with values of up to +4 and -5.

Figure 3.25 Immobilized nuclear receptor CAR binds the co-activator SRC-1 in a concentration-dependent manner. The interaction between CAR and SRC-1 is fitted to a 1:1 Langmuir binding model with drifting baseline. The black curves represent the global fit, the remaining lines represent the experimental curves. The kinetic constants obtained from three individual assays are reported in table 1.2. Spikes caused by slight mismatches in DMSO concentration were cut in order to display the association and dissociation properly. The kinetic constants obtained from three individual assays are reported in table 3.2.

Figure 3.26 Residual Plot of the concentration-dependent binding between CAR and SRC-1. The interaction between CAR and SRC-1 is fitted to a 1:1 Langmuir binding model with drifting baseline. The black zero line constitutes the global fit. The data of the experimental curves are represented as dots of the same color.

Figure 3.27 displays CAR binding the co-activator SRC-2. The different concentrations of SRC-2 ranging from 0.75µM to 8 µM demonstrate the concentration-dependent interaction between the two proteins as seen for the interaction with SRC-1. The highest concentration of SRC-2 of 8 µM reached the maximum response of 70 RU in this binding assay. The dissociation of SRC-2 from CAR happened rather fast since after one minute there was less than 50% of co-activator bound to the receptor. In order to yield kinetic data this assay was evaluated using the 1:1 Langmuir binding model with drifting baseline. The kinetic data obtained is displayed in table 3.2.

The residual plot demonstrated a good evaluation of the experimental and the fit curves, depicted as colored dots and the black zero line respectively (figure 3.28). The only distinctive deviations of the global fit from the binding curves were measured in the very beginning of both the association and the dissociation of this binding assay with values of up to -7 and +13.
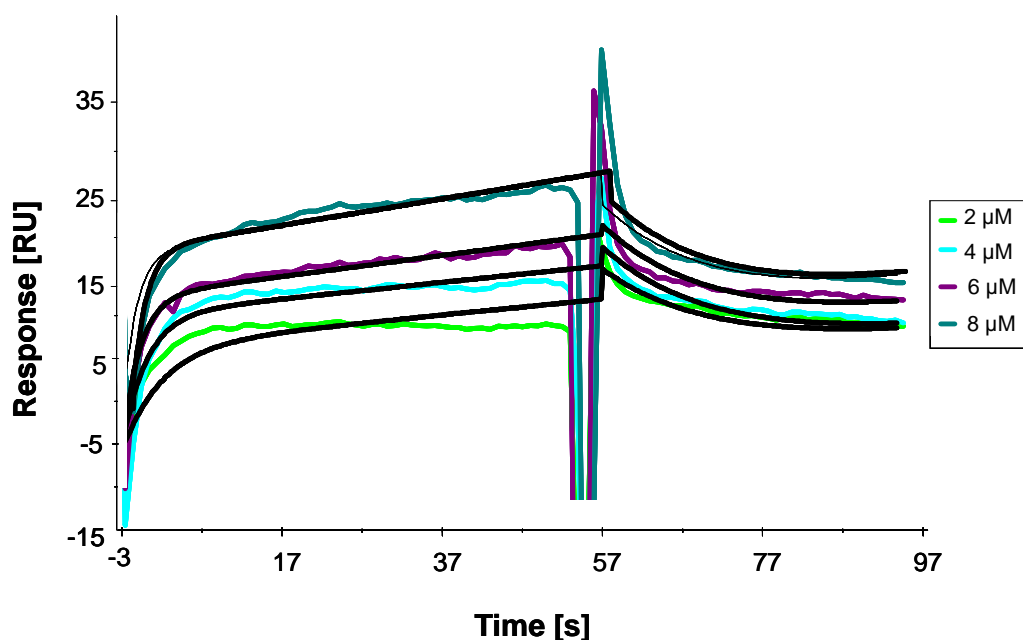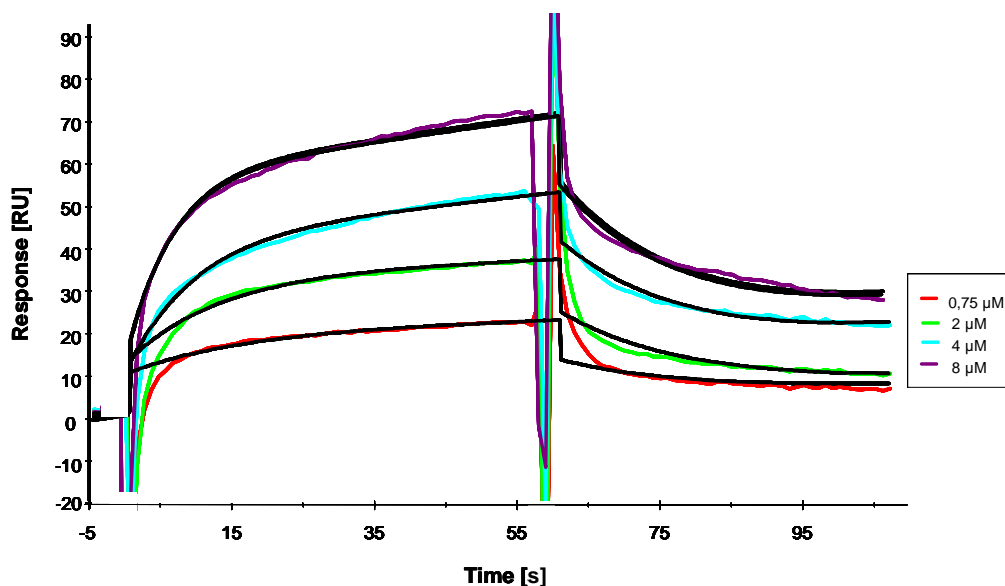
Figure 3.27 Immobilized nuclear receptor CAR binds the co-activator SRC-2 in a concentration-dependent manner. The interaction between CAR and SRC-2 is fitted to a 1:1 Langmuir binding model with drifting baseline. The black curves represent the global fit, the remaining lines represent the experimental curves. The kinetic constants obtained from three individual assays are reported in table 1.2. Spikes caused by slight mismatches in DMSO concentration were cut in order to display the association and dissociation properly. The kinetic constants obtained from three individual assays are reported in table 3.2.
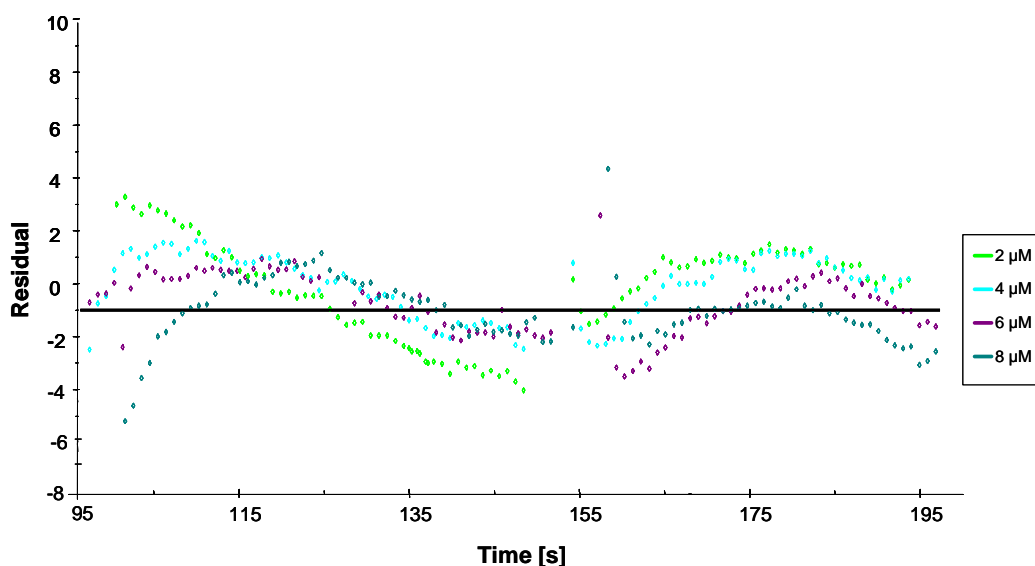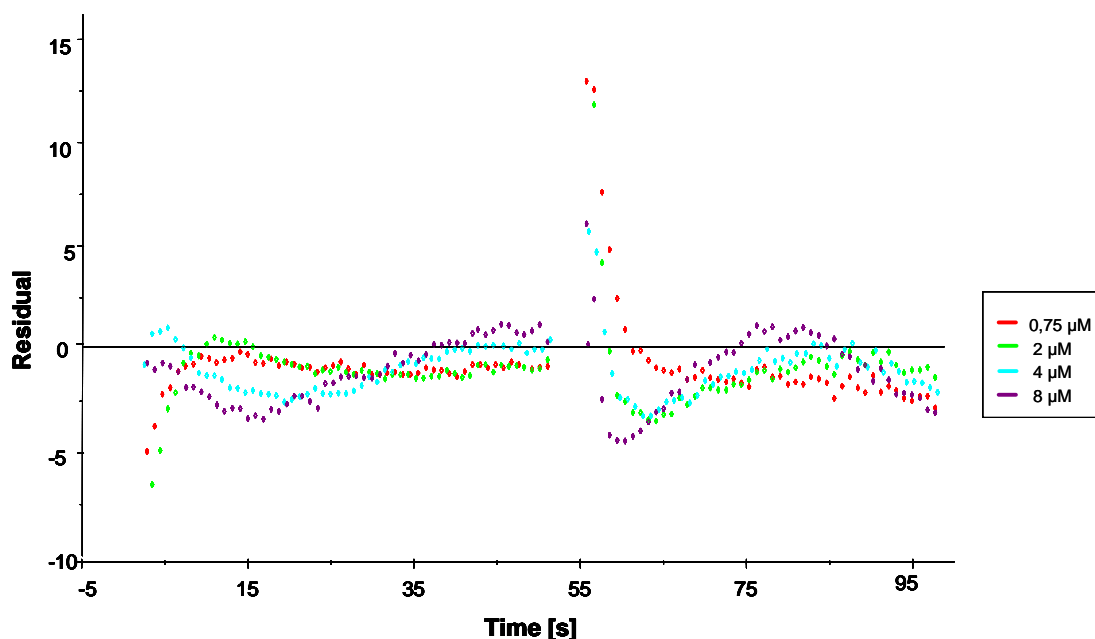

Figure 3.28 Residual Plot of the concentration-dependent binding between CAR and SRC-2. The interaction between CAR and SRC-2 is fitted to a 1:1 Langmuir binding model with drifting baseline. The black zero line constitutes the global fit. The data of the experimental curves are represented as dots of the same color.

The 1:1 Langmuir binding model with drifting baseline was used to calculate the K_D values of the binding assays. Table 3.2 displays the kinetic data from both assays and allows, therefore, a qualitative comparison between CAR binding either SRC-1 or SRC-2. Considering K_D as a parameter of binding affinity and tendency of dissociation, SRC-1 binding CAR yielded a K_D value of 5.77×10^{-7}. SRC-2, on the other hand, yielded a value of 6.98×10^{-6}. Additionally, the complex formation between CAR and SRC-1 happened faster. The dissociation, compared to the one of SRC-2, did occur slower. The maximum response reached by SRC-2 binding immobilized CAR was almost three times higher than the one reached by SRC-1.

Table 3.2 Kinetic constants describing the binding between the nuclear receptor CAR and the co-activators SRC-1 and SRC-2 respectively.*

	k_a [1/ Ms]	k_d [1 / s]	K_D [M]
SRC-1	$9.21 +/- 2.85 \times 10^4$	$5.31 +/- 1.49 \times 10^{-2}$	5.77×10^{-7}
SRC-2	$1.03 +/- 0.21 \times 10^4$	$7.19 +/- 1.44 \times 10^{-2}$	6.98×10^{-6}

* Experiments were evaluated using the 1:1 Langmuir binding fitting model with drifting baseline.

3.6.2.2 Kinetic investigation of the liganded CAR – SRC-1 interaction

So far, assays were performed to investigate the ligand-free binding between CAR and either SRC-1 or SRC-2 in order to find out whether there is a preference of the receptor over one of its co-activators. Ligand-induced association assays demonstrated a ligand-dependent binding behavior between CAR and its co-activators which could be decreased by the inverse agonist. The kinetic data yielded by the binding assays above-mentioned demonstrated the co-activator SRC-1 to be slightly preferred by CAR due its lower K_D value. Since association was distinctively influenced by drugs, assays were performed to find out whether kinetics between receptor and co-activator could be affected by drugs.

In this binding assay concentrations of SRC-1 ranged from 0.75 to 8 µM. Additionally 100 µM of drug or 10 µM of CITCO was added to each sample of the co-activator and then injected over the receptor surface.

Figures 3.29 to 3.35 display the sensorgrams of drug-induced binding of SRC-1 to immobilized CAR. The drugs used were CITCO, Clofibrate, Arteether, Artemisinin, Artemether, Triphenylphosphate, and Fenofibrate. All drug-induced binding assays demonstrated concentration-dependent binding similar to the non-induced assays. In contrast to non-induced binding between CAR and SRC-1, drug-related assays revealed a response

curve approaching the baseline much faster. The maximum response of SRC-1 binding non-induced CAR was about 25 RU. All drug-induced assays yielded a maximum response which was in most cases distinctively higher than the one reached by the pure protein interaction.

Figure 3.29 CITCO-induced binding of immobilized CAR to SRC-1. In order to obtain kinetic constants from the CITCO-induced interaction the experimental curves were fitted to the 1:1 Langmuir binding model. The black curves represent the global fit, the remaining colored lines represent the experimental curves. The co-analyte CITCO was added in a final concentration of 10 µM whereas SRC-1 was injected in concentrations ranging from 0.75 to 8 µM. The kinetic constants obtained from three individual assays are reported in table 3.3.
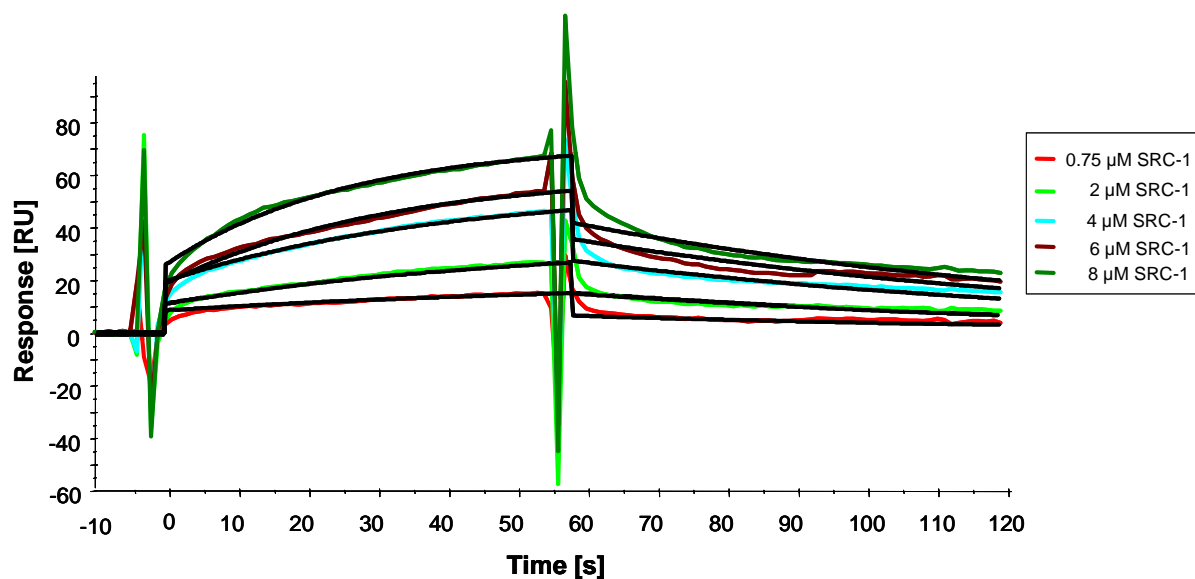
Figure 3.30 Clofibrate-induced binding of immobilized CAR to SRC-1. In order to obtain kinetic constants from the Clofibrate-induced interaction the experimental curves were fitted to the 1:1 Langmuir binding model. The black curves represent the global fit, the remaining colored lines represent the experimental curves. The co-analyte Clofibrate was added in a final concentration of 100 µM whereas SRC-1 was injected in concentrations ranging from 0.75 to 8 µM. The kinetic constants obtained from three individual assays are reported in table 3.3.
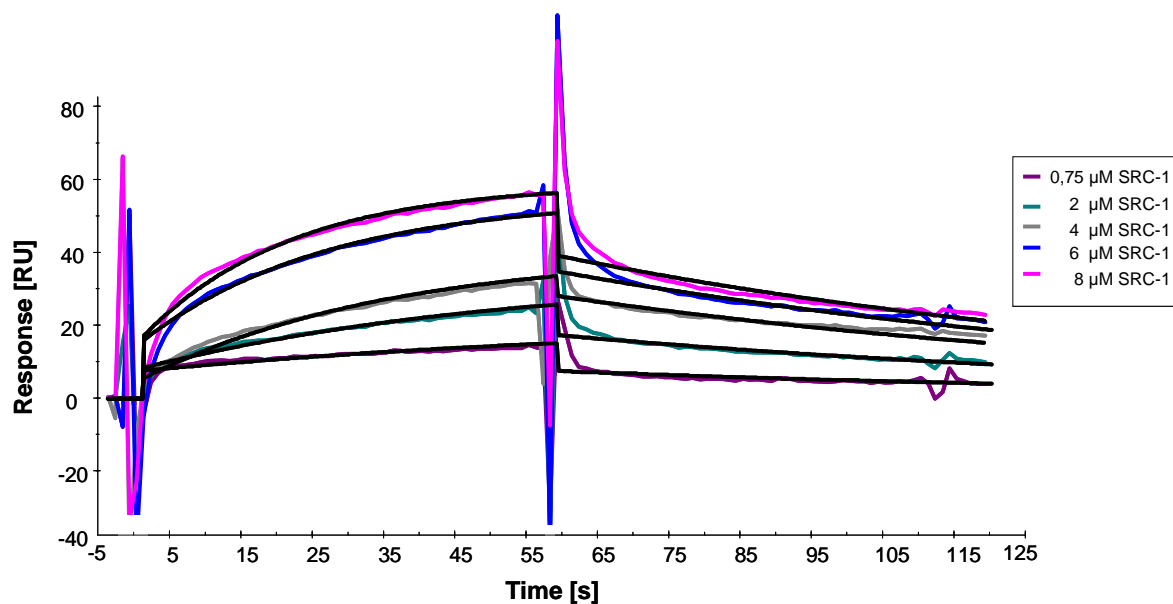
Figure 3.31 Arteether-induced binding of immobilized CAR to SRC-1. In order to obtain kinetic constants from the Arteether-induced interaction the experimental curves were fitted to the 1:1 Langmuir binding model. The black curves represent the global fit, the remaining colored lines represent the experimental curves. The co-analyte Arteether was added in a final concentration of 100 µM whereas SRC-1 was injected in concentrations ranging from 0.75 to 8 µM. The kinetic constants obtained from three individual assays are reported in table 3.3.
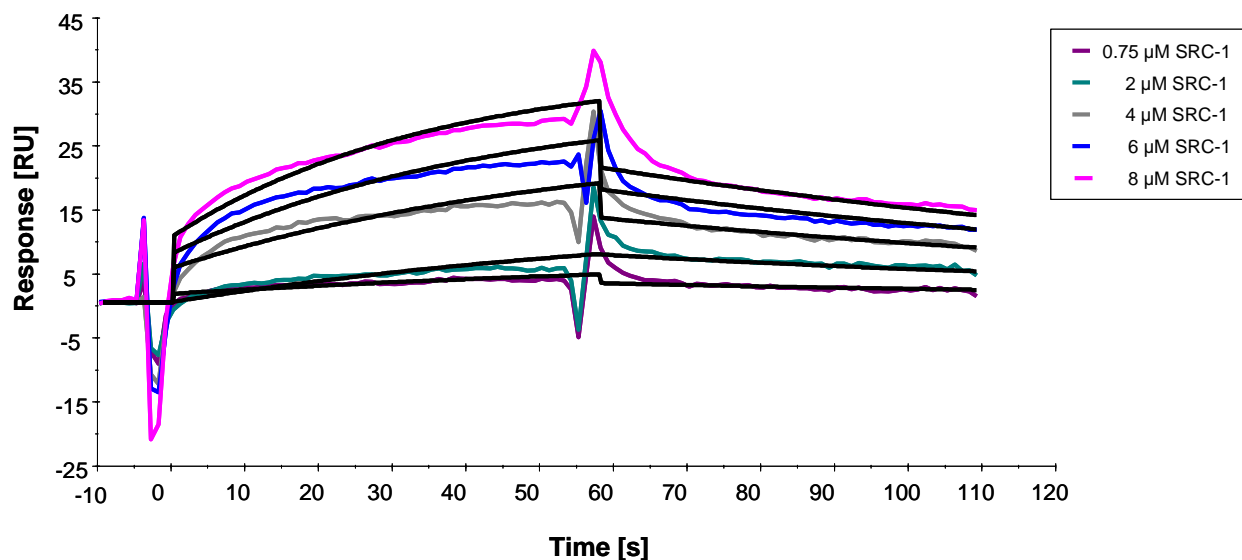
Figure 3.32 Artemisinin-induced binding of immobilized CAR to SRC-1. In order to obtain kinetic constants from the Artemisinin-induced interaction the experimental curves were fitted to the 1:1 Langmuir binding model. The black curves represent the global fit, the remaining colored lines represent the experimental curves. The co-analyte Artemisinin was added in a final concentration of 100 µM whereas SRC-1 was injected in concentrations ranging from 0.75 to 8 µM. The kinetic constants obtained from four assays are reported in table 3.3.
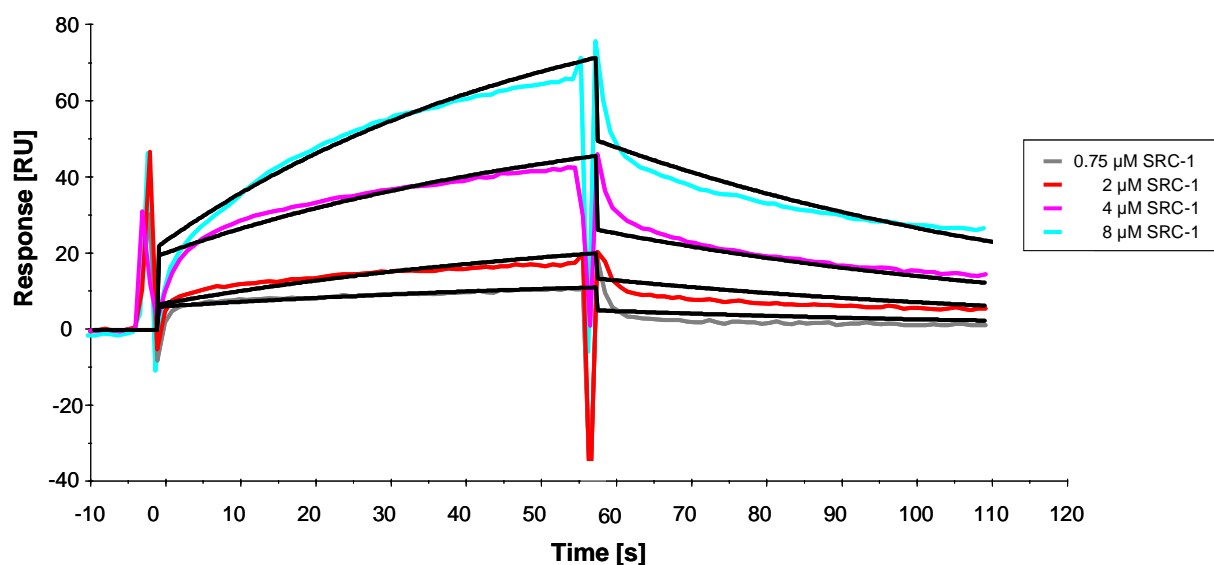
Figure 3.33 Artemether-induced binding of immobilized CAR to SRC-1. In order to obtain kinetic constants from the Artemether-induced interaction the experimental curves were fitted to the 1:1 Langmuir binding model. The black curves represent the global fit, the remaining colored lines represent the experimental curves. The co-analyte Artemether was added in a final concentration of 100 µM whereas SRC-1 was injected in concentrations ranging from 0.75 to 8 µM. The kinetic constants obtained from five individual assays are reported in table 3.3.
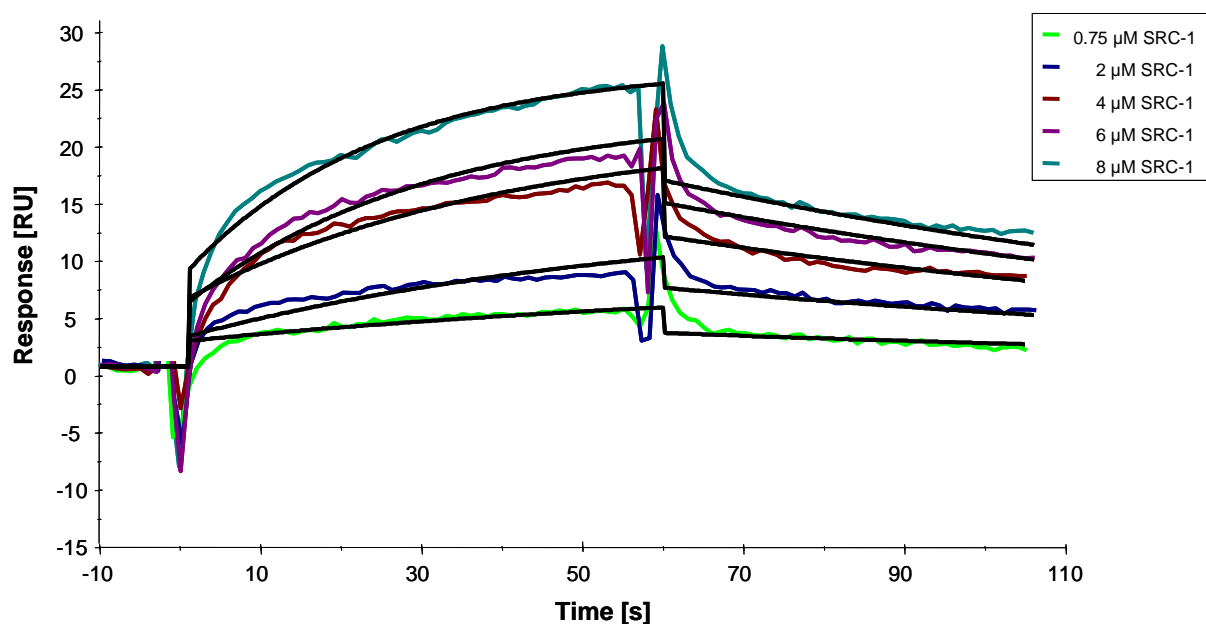
Figure 3.34 Triphenylphosphate-induced binding of immobilized CAR to SRC-1. In order to obtain kinetic constants from the Triphenylphhosphate-induced interaction the experimental curves were fitted to the 1:1 Langmuir binding model with drifting baseline. The black curves represent the global fit, the remaining colored lines represent the experimental curves. The co-analyte Triphenylphhosphate was added in a final concentration of 100 µM whereas SRC-1 was injected in concentrations ranging from 0.75 to 8 µM. The kinetic constants obtained from three individual assays are reported in table 3.3.
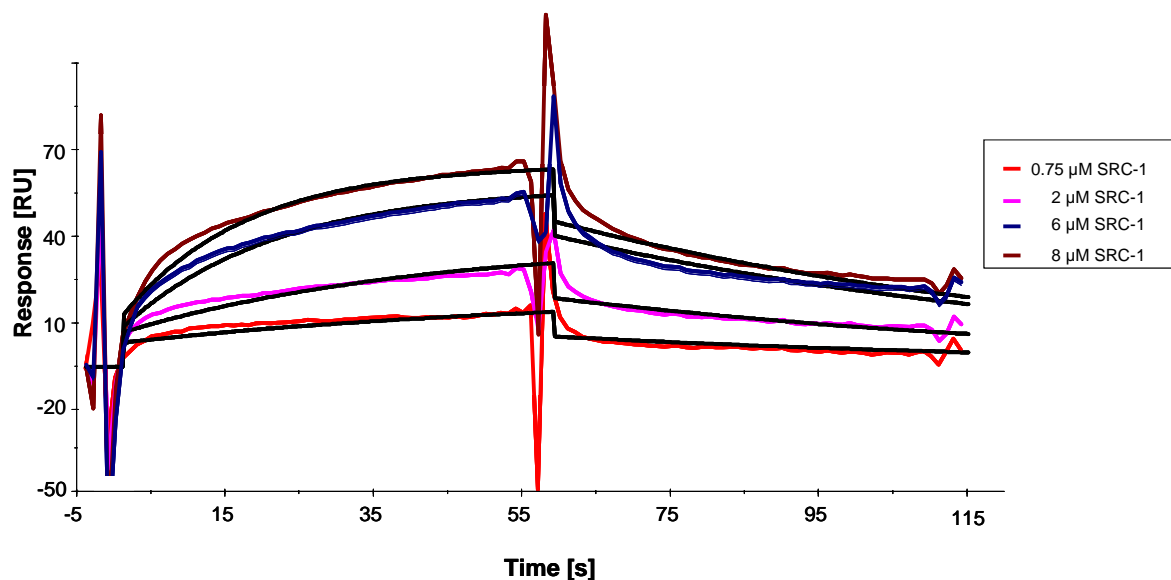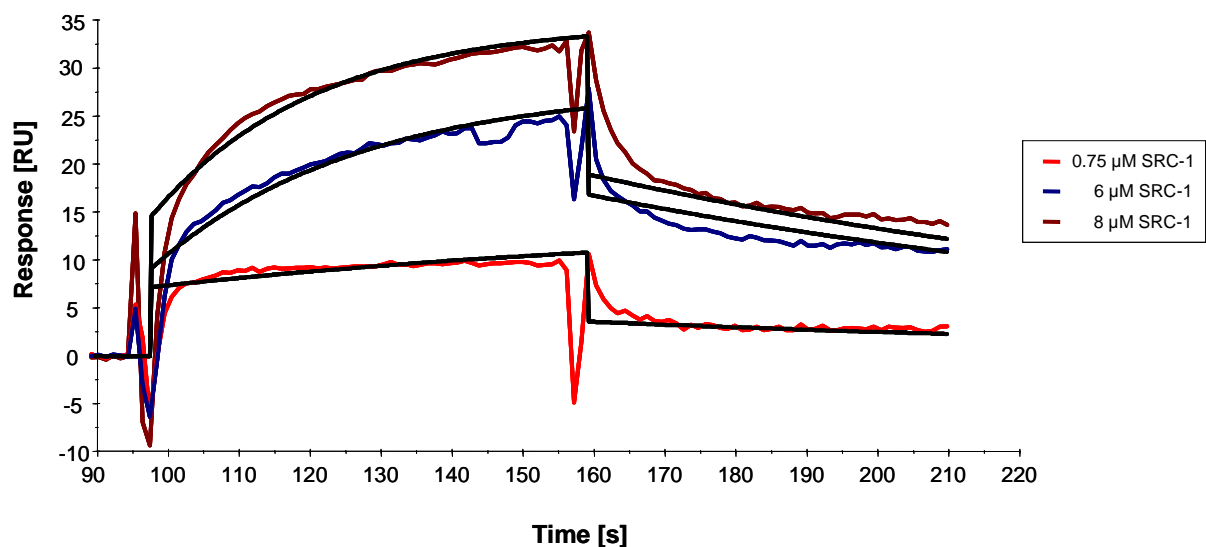

Figure 3.35 Fenofibrate-induced binding of immobilized CAR to SRC-1. In order to obtain kinetic constants from the Fenofibrate-induced interaction the experimental curves were fitted to the 1:1 Langmuir binding model with drifting baseline. The black curves represent the global fit, the remaining colored lines represent the experimental curves. The co-analyte Fenofibrate was added in a final concentration of 100 µM whereas SRC-1 was injected in concentrations ranging from 0.75 to 8 µM. The kinetic constants obtained from three individual assays are reported in table 3.3.

132

The kinetic constants which were yielded from the assays depicted in figures 3.29 to 3.35 were summarized in table 3.3. The lowest K_D value was shown for Artemisinin with 5 x 10^{-6} M. The highest was reported for CITCO with 2.41 x 10^{-6} M. All other values are in between the ones reported. Obviously, the K_D values of drug-induced binding of SRC-1 to CAR are rather similar. There was no enhancement of the SRC-1 – CAR affinity by drugs regarding equilibrium dissociation constants since the values mentioned above did not alter the K_D values of the pure protein interaction, neither for SRC-1 nor for SRC-2. On the other hand, the rate constants k_a and k_d displayed ligand-dependent differences. Drug-induced complex formation was performed the fastest in case of Artemether, Triphenylphosphate and Fenofibrate. Artemisinin displayed the slowest formation of complex. In case of dissociation of proteins CITCO, Clofibrate, Arteether and Artemisinin proved to cause the most stable complexes. Artemether seemed to be responsible for the weakest complex.

Table 3.3 Kinetic constants describing the ligand-dependent binding between the nuclear receptor CAR and the co-activator SRC-1.* In order to provide a useful comparison between ligand-dependent and ligand-independent receptor – co-activator interaction, kinetic data obtained from the drug-free interaction (table 3.2) were added in the last two rows.

Drug	k_a [1/ Ms]	k_d [1 / s]	K_D [M]
CITCO	4.49 +/- 1.30 x 10^3	1.08 +/- 0.24 x 10^{-2}	2.41 x 10^{-6}
Clofibrate	3.29 +/- 0.39 x 10^3	1.37 +/- 0.29 x 10^{-2}	4.16 x 10^{-6}
Arteether	3.89 +/- 0.89 x 10^3	1.01 +/- 0.09 x 10^{-2}	2.6 x 10^{-6}
Artemisinin	2.26 +/- 0.75 x 10^3	1.13 +/- 0.40 x 10^{-2}	5 x 10^{-6}
Artemether	1.27 +/- 0.18 x 10^4	6.22 +/- 0.12 x 10^{-2}	4.9 x 10^{-6}
Triphenylphosphate	1.18 +/- 0.38 x 10^4	4.36 +/- 0.35 x 10^{-2}	3.69 x 10^{-6}
Fenofibrate	1.19 +/- 0.07 x 10^4	4.4 +/- 0.44 x 10^{-2}	3.7 x 10^{-6}
Drug-free interaction			
CAR – SRC-1[1]	9.21 +/- 2.85 x 10^4	5.31 +/- 1.49 x 10^{-2}	5.77 x 10^{-7}
CAR – SRC-2[1]	1.03 +/- 0.21 x 10^4	7.19 +/- 1.44 x 10^{-2}	6.98 x 10^{-6}

* Experiments were evaluated using the 1:1 Langmuir binding fitting model. In case of Triphenylphosphate and Fenofibrate the 1:1 Langmuir binding fitting model with drifting baseline was used for evaluation.

[1] Experiments were evaluated using the 1:1 Langmuir binding fitting model with drifting baseline.

4 Discussion

The aim of this work was to investigate and characterize the nuclear receptor CAR. Therefore, interactions of CAR with diverse putative ligands, agonists, inverse agonists, non-ligand inducers of activation, and protein binding partners were measured using surface plasmon resonance. The interaction partners include small molecules like the prominent CAR ligand and agonist CITCO, diverse endogenous and exogenous compounds, pharmaceuticals like the Atorvastatin drugs as well as the co-activators SRC-1 and SRC-2. Both the nuclear receptor and the co-activators were expressed using a bacterial expression system and purified via IMAC in order to produce functional target proteins. Using Biacore CM5 chips CAR – SRC-1 and CAR – SRC-2 interactions with or without selective compounds were carried out to produce and evaluate both binding and kinetic data. The association- and kinetic-based data were supposed to characterize CAR regarding preference of co-activators, verification of drugs as agonist ligands, and putative regulation and / or activation mechanisms through ligand binding.

4.1 Expression and purification of the nuclear receptor CAR and the co-activators SRC-1 and SRC-2

4.1.1 The nuclear receptor CAR

The aim of expressing the ligand binding domain (LBD) of CAR was realized using *E. coli* BL21(DE3). Initially, protein expression of CAR was performed at 25°C and 140 rpm for 4 hours. Protein expression of CAR-LBD was successful (figure 3.1A). The induced culture displayed time-dependent increase in the course of four hours depicted by a protein band running between 20 and 29 kDa. The ligand binding domain of CAR has a molecular weight of 29.2 kDa. After sonication CAR was detected in the insoluble pellet fraction of the induced culture (figure 3.1B). Western blot confirmed the result of the Coomassie staining depicted in figure 3.6A and demonstrated that the lysate showed no distinctive overexpression of the target protein. The goal of expessing a soluble his-tagged target protein is the easy and fast

purification via IMAC from the lysate of *E. coli* cells. There was an additional protein band visible running between 17 and 26 kDa which probably consists of degraded CAR protein harboring an N-terminal peptide. The pellet fraction on the other hand, showed, apart from overexpression, a large amount of truncated CAR protein even smaller than 17 kDa. Putative truncated CAR protein not harboring the N-terminal part but other parts of the protein could not be detected by the Western blot due to the primary antibody used, which detects the 6x his-tag. Thus, solubly as well as insolubly expressed CAR protein demonstrated impaired protein expression. The overexpression of human proteins into inclusion bodies of *E. coli* is a common difficulty which has been reported frequently (Itakura *et al.*, 1977; Goeddel *et al.*, 1979b; Marston *et al.*, 1986). Aggregation may be caused by the oxidative folding of disulfide-bonds of recombinant proteins being affected by the reducing cytosol environment. The overexpression into inclusion bodies could not be altered by lower concentrations of IPTG (results not shown). Higher concentrations of IPTG only increased the amount of protein in the pellet fraction. The goal of overexpression of CAR protein was to yield soluble target protein which could be purified from the lysate of *E. coli* cells which could not be realized by expressing the receptor at 25°C and 140 rpm for 4 hours. However, it is possible to solubilize proteins in inclusion bodies with the help of high concentrated urea. High purity is a considerable benefit of solubilizing target proteins from inclusion bodies. Since there exists no simple and straightforward activity test for nuclear receptors to check their functional integrity, it is hard to determine the quantity of target protein being still functional after de- and renaturation of *E. coli* inclusion bodies. Thus, solubilizing CAR protein from inclusion bodies was not performed. However, there are alternatives like co-expressing CAR with partner proteins or chaperones and changing expression conditions (Li *et al.*, 1997). Li and colleagues have already proven that expression of the nuclear receptor retinoic acid receptor (RAR), expressed on its own, results in *E. coli* inclusion bodies. By co-expressing the heterodimerization partner RXR and RAR, they could prove that RAR could be shifted into the lysate due to RXR which, produced on its own, is already expressed solubly (Li *et al.*, 1997). The soluble production of both proteins was explained by the formation of a stable heterodimer. It was even proposed that RXR might serve as a molecular chaperone helping the RAR protein to fold properly and, thus, enhancing its activity. CAR was co-expressed with SRC-1 which is one of its co-activators (figure 3.2). If SRC-1 is expressed on its own, it is produced both in the lysate and in inclusion bodies of *E. coli* cells (figure 3.4A). Consistent with the findings of Li, CAR co-expressed with SRC-1 was indeed produced solubly even though part of the CAR protein was still in the pellet fraction (figure 3.2A and B). Probably

by binding SRC-1 CAR was kept soluble in the lysate of *E. coli* cells. But since separation of the co-expressed proteins by means of anion chromatography and elution via enhanced salt concentrations was not successful (results not shown), a second alternative of changing expression conditions was chosen to yield soluble CAR protein: optimization of expression conditions. These optimizations included lowering temperature from 25° to 16°C, variation of both expression duration from 4 hours to 20 hours and shaking velocity from 140 rpm to 120 rpm. These changes resulted partly in protein production in the lysate of *E. coli* cells (figure 3.3, arrows).

The solubly expressed and via IMAC purified CAR protein was then analyzed by Coomassie and silver staining. Since silver staining visualizes up to 0.1 ng protein per band, both stainings confirmed the high purity of the eluted target protein (figure 3.8A and B).

Protein expression in 100 ml LB media yielded between 0.1 and 0.2 mg/ml CAR protein. A high concentration of target protein was not necessarily important for Biacore interactions, but a high degree of purity in order to avoid non-specific binding was pivotal for measuring qualitative and informative SPR interactions.

4.1.2 The co-activators SRC-1 and SRC-2

The human co-activators SRC-1 and SRC-2 were expressed in *E. coli* BL21(DE3) in order to produce highly purified, soluble, and functional proteins.

The recombinant expression is demonstrated by a time-dependent expression of SRC-1 running between 18.4 and 25 kDa in the course of 4 hours (figure 3.4B, arrow). Unlike the SRC-1 protein which was co-expressed with CAR, this SRC-1 protein was attached to an N-terminal 10x histidine tag and has a molecular weight of 18 kDa. SRC-2, a protein of 24 kDa, was successfully expressed, too (figure 3.5A, arrow). Especially SRC-1 could be detected both in the lysate and the pellet fraction as demonstrated by SDS-PAGE and Western Blot (figure 3.4A and 3.7). However, compared to CAR, both co-activators could be expressed more easily in the soluble fraction (figures 3.4A and 3.5B). Apart from the respective co-activator bands, an additional slight band was visible which could not be detected by Western Blot of SRC-1 (figure 3.9A and B; figure 3.7). Thus, the protein band running lower than 25 kDa and approximately at 35 kDa for SRC-1 and SRC-2 respectively, probably consists of *E. coli* BL21(DE3) housekeeping proteins. Protein expression in 100 ml LB media yielded

between 0.2 and 0.3 mg/ml SRC-1 and 0.1 and 0.2 mg/ml SRC-2. Yet, both co-activators were expressed and purified to a high degree in order to be analyzed via SPR technology.

4.2 Surface plasmon resonance

There are diverse analytical methods through which protein-protein interactions can be detected and measured both quantitatively and qualitatively. Western Blots, ELISAs and Immunoblots are only few examples of quantitative techniques to be considered. The Biacore 3000 system which is able to perform both quantitative and qualitative protein – protein as well as protein – drug interactions is a rather new technique which has gained growing popularity in the last decade. It is based on surface plasmon resonance (SPR) and enables interactions to be measured in real-time without proteins to be linked to tags like histidine residues or bulky fluorescence-based labels which might influence the structural integrity and, thus, the activity of the protein.

The aim of the Biacore experiments was to investigate and characterize complex formation of the nuclear receptor CAR and the co-activators SRC-1 and SRC-2 in the absence and presence of drugs. The information yielded might allow conclusions on kinetics of binding, the degree of modulation by drugs, verification of drugs as agonist ligands, and preference of co-activators.

4.2.1 The influence of drugs on the association of CAR with its co-activators SRC-1 and SRC-2

Although CAR recruits ligand-independently co-activators and, therefore, does not need agonist binding to be active, it has been known that its activity can be further enhanced by interactions with agonists (Moore *et al*., 2000; Maglich *et al*., 2003; Burk *et al*., 2005). Since CAR is responsible for the regulation of genes encoding enzymes and proteins involved in the metabolism of drugs during detoxification, the aim of this work was to investigate if and to what extent CAR can be manipulated and regulated by drug binding by *in vitro* measurements. These drugs were chosen because they were identified as agonists in the course of drug screenings at the IKP.

Firstly, the influence of potent ligands on the association of CAR with SRC-1 was analyzed using SPR. There was a distinctive drug-dependent hierarchy in association responses of the SRC-1 – CAR complex evident. All drugs and substances could be clearly categorized into no or low, medium or strong inducers of interaction, thus agonists (figure 3.13). The strongest increase in interaction was achieved by CITCO which was expected since the imidazole derivative was found to both directly bind and activate the nuclear receptor leading to nuclear translocation and, thus, further activation of CAR (Maglich *et al*., 2003). In contrast to CITCO, PB and Clotrimazole did not significantly increase the interaction between CAR and SRC-1. Unlike CITCO, Phenobarbital does not directly bind CAR but activates it in an indirect manner including intracellular signaling cascades and, thus, serves as the negative control. Being the inverse agonist of human CAR which can force co-activator or agonist release upon direct binding, Clotrimazole, on the other hand, was supposed to weaken the binding of the receptor to the co-activator (Maglich *et al*., 2003 and Moore *et al*., 2000). By means of SPR Clotrimazole was evidently not able to decrease the receptor – co-activator interaction (figure 3.13). The second most potent inducers of association were Clofibrate and Arteether. Clofibrate and Fenofibrate have been proven before to be CAR activators and putative agonists by mediating nuclear translocation in mouse liver (Guo *et al*., 2007). Yet, direct ligand binding activity could not be proven for Clofibrate. Direct ligand binding of both fibrates was successfully demonstrated in the Biacore experiments. Interestingly, the amount of induction of binding of the respective fibrates varied significantly (figure 3.13). Clofibrate was the second potent ligand of CAR as measured by interaction with SRC-1. Fenofibrate, however, belonged to the weakest ligands concerning both CAR – SRC-1 and CAR – SRC-2 interactions (figure 3.13 and 3.24). Bisphenol A which was already shown to be an agonist of CAR3, a splice variant of CAR, only led to a weak association similar to interactions including PB and Clotrimazole (figure 3.13) (Dring *et al*., 2010). Thus, Bisphenol A could not be verified as potent CAR agonist by SPR assays consistent with the findings of Dring. Fenofibrate, Triphenylphosphate, Artemisinin, and Artemether are all substances which led to medium augmentation compared to the whole set of drugs used. Triphenylphosphate was run through molecular dynamics (MD) simulations and docked in the LBP of CAR to test it as a putative agonist of the receptor (figure 3.13) (Jyrkkärinne *et al*., 2005). Several MD simulations resulted in TPP always forming a hydrogen bond to His[203] of CAR LBP. Additionally, TPP demonstrated species-specific behavior since it activated human CAR but resulted in contradictory behavior in mouse CAR (Honkakoski *et al*., 2004). Thus, TPP has been shown previously to be a putative agonist of CAR. SPR based binding experiments have

indeed proven that TPP acted as a direct ligand and agonist of CAR (figure 3.13). Artemisinin drugs are known to significantly activate human PXR and also to a lower degree human and mouse CAR. By doing that the expression of their respective target genes *CYP3A4* and *CYP2B6* as well as *MDR1* is induced in hepatocytes (Burk *et al.*, 2005). Direct agonist binding of CAR as well as PXR was suggested by Artemisinin-dependent increase of the nuclear receptors interacting with their respective co-regulators in mammalian two hybrid assays (Burk *et al.*, 2005). Biacore experiments prove direct interactions of the Artemisinin drugs with the nuclear receptor CAR *in vitro*, thereby confirming them to be agonist ligands (figure 3.13). More importantly, Arteether proved to be the most efficient inducer for interactions with SRC-2 and the second best for SRC-1 resulting in an association hierarchy of Artemisinin drugs of Arteether > Artemether > Artemisinin for both co-activators (figure 3.24 and 3.13).

Evidently, ligand-induced increase in CAR – co-activator binding was always higher when binding SRC-1 compared to SRC-2 (table 3.1). In mammalian two hybrid assays interactions of CAR with different co-activators were measured with or without the potent agonist CITCO (Arnold *et al.*, 2004). CITCO-enhanced as well as CITCO-free co-activator interactions revealed that the highest interactions were measured with co-activator DRIP 205 (vitamin D-interacting protein 205), followed by SRC-1, SRC-2 and SRC-3 (Arnold *et al.*, 2004). Interestingly, interactions with DRIP 205 more than doubled activation compared to SRC-1, the most potent of the p160 co-activators. Within the group of p160 proteins, SRC-1 displayed more than doubled activation compared to SRC-2. Considering the most potent agonists CITCO, Arteether and Artemether, association responses measured were at least two-fold higher for SRC-1 compared to SRC-2 (table 3.1). The findings of the mammalian two hybrid assays matched and confirmed the SPR findings, yet the Biacore results were yielded using a wide variety of different drugs and were not limited to CITCO alone.

The endogenous metabolites Androstenol (5α-androst-16-en-3α-ol) and Androstanol (5α-androst-3α-ol) were chosen to investigate their influence on the constitutive association of CAR and SRC-1 (Moore *et al.*, 2000).

The androstane-based interactions were similar to the PB-based interaction (figure 3.12 and 3.14). Both androstanes derivatives are known to bind both human and murine CAR but act as selective potent mouse but weak human CAR inverse agonists (Moore *et al.*, 2000). Using SPR technology, the androstanes exhibited no influence on the constitutive binding between CAR and SRC-1. Inverse agonist activity, as demonstrated for Clotrimazole in figure 3.18, could not be proven for the androstanes (results not shown).

Regarding the association of CAR and SRC-2, the same set of drugs apart from Bisphenol A and Clofibrate were used. Compared to complex formation with SRC-1, SRC-2 and CAR yielded association responses which were not divergent but similar and low. Whereas SRC-1 – CAR binding yielded an increase in association of 1.2 to 7.3 fold of the constitutive binding, SRC-2 – CAR yielded values of 0.8 to 2.6 only (figure 3.24). Phenobarbital achieved low association as it was expected for the non-binder and demonstrated for SRC-1, too. Artemisinin, Artemether, Triphenylphosphate, and Fenofibrate proved to be medium inducers of binding compared to all drugs tested. CITCO and Arteether led the ranking of drugs causing the highest increase in association.

It is striking that complex formation of liganded CAR with either SRC-1 or SRC-2 varies to a great deal. Being complexed to SRC-1, CAR displayed a high variety of different association responses which means dependent on the drug of interest, association of the receptor – co-activator complex can be regulated and modulated easily. Especially CITCO, Arteether, and Clofibrate showed great capability to actively modulate CAR constitutive activity through increasing binding to SRC-1. Complex formation of CAR and SRC-2 however, could be slightly altered and did not allow an equally clear discrimination of non-, medium, and strong ligands. As a result of this it seems as if modulation of CAR activity through drugs and substances generally depends on the choice of the p160 co-activator. There are evident differences especially in the intensity of association. The strongest inducers in increase for both co-activators did not demonstrate equal intensity. Regarding SRC-1 it was CITCO which induced the clearly highest increase with a fold response of 7.3 (table 3.1). Arteether and Clofibrate followed displaying a common value of 5.3 fold response in increase. Concerning SRC-2 it was Arteether that led to the highest increase of 2.6 which was closely followed by CITCO with 2.4 and TPP with 2.1 fold response in augmentation. After all the most efficient modulation of CAR activity was carried out by CITCO for binding SRC-1 and by Arteether for binding SRC-2. Due to technical reasons incubation of CAR to Clofibrate and Bisphenol A in order to bind SRC-2 could not be examined. Clofibrate led to the second highest increase in response for SRC-1. Thus, it would have been interesting to see the effect of Clofibrate on the receptor's behavior towards SRC-2. A similar outcome might be assumed due to the fact that most drugs behaved similarly concerning relative association intensities regardless of the co-activator.

CAR – SRC-1 binding was not significantly altered by incubation with the inverse agonist Clotrimazole. However, in case of SRC-2 Clotrimazole led to the same or a similar association value as Fenofibrate, Artemisinin, and Artemether which, on the other hand, did

enhance the association of CAR and SRC-1. These findings emphasize how low the influence of Fenofibrate and the Artemisinins is on the binding of SRC-2 and CAR.

Yet, there are similarities of both co-regulators in binding to CAR, too. CITCO and Arteether led to the highest increase in association for both co-activators. PB did not show enhanced association regardless of the co-activator. Fenofibrate, Artemisinin, and Artemether led to medium augmentation of association.

In order to accomplish significant ligand-induced differences in association the constitutive binding between CAR and the respective co-activator should at least reach 5 to 10 response units [RU]. CAR binding to immobilized SRC-1 had a concentration of 0.21 µM in order to fulfill this precondition. However, CAR needed a concentration of only 0.05 µM to reach similar responses when associating with SRC-2. CAR injected in a concentration of 0.21 µM reached a much higher association curve on the SRC-2 surface compared to the SRC-1 surface. Additionally, dissociation of CAR from the immobilized co-activators occurred much slower for SRC-2. Unlike CAR - SRC-1 complexes, CAR - SRC-2 complexes were particularly stable which was depicted by a constant response signal during dissociation (figure 3.22 and 3.23). The stability of the CAR – SRC-2 complexes was evident both in the absence or presence of ligands. Thus, CAR obviously binds more efficiently immobilized SRC-2 than SRC-1 in the absence of ligands. It is unclear whether this might be due to enhanced affinity of the receptor to SRC-2 or enhanced stability of SRC-2 compared to SRC-1 after immobilization of the co-activators on CM5 chips. After immobilization for ligand-induced binding assays, more SRC-2 than SRC-1 molecules might have maintained the right conformation, and, thus functional integrity. Hence, in the absence of ligands, CAR seems to bind SRC-2 more efficiently than SRC-1. However, if CAR was pre-incubated with ligands, it was SRC-1 to demonstrate a distinctive and high increase in association, and not SRC-2. The interaction of CAR to SRC-1 could be strengthened by ligands whereas the interaction of CAR and SRC-2 could not be intensified to the same degree since it might have already reached almost the maximum in the absence of ligands. Obviously CAR injected over the respective co-activator surface displayed different enhanced activation modi dependent on the co-activator and on the absence or presence of ligands.

Modulation of CAR activity towards binding co-regulators by drugs, xenobiotics and endogenous compounds has already been proven for more than a decade (Moore *et al*., 2000; Maglich *et al*., 2003; Burk *et al*., 2005). CAR demonstrated increased binding to SRC-1 when co-incubated with CITCO and decreased binding when co-incubated with Clotrimazole. CAR

behaved the same way when complexed in a heterodimer with RXR and bound to DNA (Lempiäinen *et al*., 2005). These findings suggest that modulation of CAR activity through drugs or other xenobiotics is not altered by the presence of its heterodimerization partner RXR. Thus, drug-based modulation of the receptor inside the nucleus via its heterodimerization partner RXR does not seem to be of importance and, furthermore, stresses the significance of ligand-induced alteration of receptor-co-regulator binding. Since SRC-2 behaved similar to RXR, SRC-1 seems to be one of the targets to be capable of being modulated by drugs.

Often ligand-dependent increase in association is regarded as enhanced affinity of the receptor to its binding partner. Yet, there are nuclear receptors known to homodimerize like the estrogen receptor or the xenosensor PXR (Kumar and Chambon, 1988; Noble *et al*., 2006). Indeed, the increase has to be proven as actual change in binding affinity by means of kinetic interaction analysis to rule out the possibility of a ligand-based dimerization of the receptor, especially when the receptor is used as the analyte. In the kinetic-based SPR assays the immobilized co-activator served as the ligand and CAR as the analyte. Homodimerization of the receptor would therefore lead to doubled association responses (equation (2)).

$$(2) \qquad R_{max} \quad = \quad \frac{M \text{ (analyte)}}{M \text{ (ligand)}} \quad x \quad R_{L} \quad x \quad \text{stoichiometric ratio}$$

R_{max}:   maximum response

R_{L}:   level of immobilization (amount of immobilized protein)

M: molecular weight

But so far, no evidence has been found which prove CAR to homodimerize. Even if CAR indeed homodimerized, the variety of ligand-induced intensities in association would therefore account for the respective drug or ligand to cause self-assembly of the receptor to different degrees. CAR was co-incubated with drugs for at least half an hour and then injected over the immobilized co-activator surface yielding different and high association responses in conjunction with SRC-1 but rather similar and low ones with SRC-2. These findings indicate that ligand-induced homodimerization probably did not occur.

Liganded CAR displayed high divergence in association with SRC-1 but relatively low with SRC-2 which demonstrated a drug-induced interaction hierarchy for SRC-1 of CITCO >

Arteether = Clofibrate and for SRC-2 of Arteether > CITCO > Triphenylphosphate regarding the three most potent agonists. Yet, kinetic data only can reveal whether ligand-induced increased association responses were caused by strengthened affinity, enhanced recognition of the co-activator or conformational stabilization of CAR.

4.2.1.1 Inhibition of ligand-dependent increase in binding by the inverse agonist Clotrimazole

All ligand-depended interactions which originally increased binding between CAR and SRC-1, were reduced significantly by co-incubation with Clotrimazole (figure 3.18).

Interactions in the binding assays with the strongest inducers of association CITCO, Arteether, and Clofibrate were reduced the most. Increased binding caused by Artemisinin, Artemether, and Triphenylphosphate was also significantly diminished. Fenofibrate demonstrated one of the lowest decreases since the original increase of association was one of the lowest after all. Thus, inhibition by Clotrimazole abolished the ligand-induced hierarchy of increase in association of CAR and SRC-1 originally caused in the absence of the inverse agonist. These findings demonstrate and emphasize the biological effects of Clotrimazole which is generally used as pharmaceutical substance to fight fungi-related diseases (Plempel *et al.*, 1969). In the Biacore-based experiments Clotrimazole and the respective drug were added to CAR at the same time. Therefore, Clotrimazole seemed to have a higher affinity to CAR than all other ligands used since binding to SRC-1 was diminished significantly compared to Cotrimazole-free ligand-induced bindings (figure 3.18). As a result, binding of Clotrimazole to CAR might cause conformational changes in the binding pocket of the receptor which only slightly promote or even hamper additional binding by other drugs or co-activators through sustaining the receptor in an inactive conformation. But so far, simultaneous binding of multiple ligands to CAR has not been reported yet. Thus, the inverse agonist might only block the binding site for other drugs to bind to due to its alleged higher affinity. Direct binding assays between CAR and Clotrimazole and CAR and the respective agonist ligands would allow a direct comparison of the different affinities.

However, Clotrimazole is supposed to force release of both drugs and co-activators from the receptor (Lempiäinen *et al.*, 2005; Moore *et al.*, 2000). Yet, Clotrimazole was clearly shown not to diminish the constitutive binding between CAR and SRC-1 (table 3.1). Inconsistent with the findings of the Lempiäinen group, the co-activator used in the Biacore experiments was SRC-1 and not SRC-2. Yet, Clotrimazole had no repressing effect on the association of the receptor with SRC-2 in SPR assays, too, indicating that the absence of a repressive effect

did not depend on the co-activators (table 3.1). Thus, inverse agonist activity of Clotrimazole could only be demonstrated for ligand-induced CAR - SRC-1 as well as CAR - SRC-2 binding by means of SPR experiments.

It is a fact that Clotrimazole influences the activity of CAR. Accordingly all pathways that include both ligand-induced and ligand-independent activation of CAR should be blocked, hampered or at least minimized to a great amount *in vivo* after exposure to high concentrations of Clotrimazole. The simultaneous up take of Clotrimazole and drugs involving CAR-regulated detoxification might lead to side effects including cross reactivity. Ligand-induced activation of CAR by CITCO, Arteether, and Clofibrate demonstrated to be affected the most. Arteether and Clofibrate, unlike CITCO, are used as pharmaceuticals to fight Malaria and to reduce low (LDL) and very low density lipoproteins (VLDL) respectively (White, 2004). Thus, these agonist ligands demonstrate physiological and pharmaceutical relevance. It was already shown for the nuclear receptor PXR that Rifampicin-mediated induction of *CYP3A4* was inhibited by Clotrimazole (Trubetskoy *et al.*, 2005).

4.2.1.2 The influence of Atorvastatin and its metabolites on the association of CAR and SRC-1

Cell-based reporter assays using FLC7 cells identified Atorvastatin among other HMG-CoA reductase inhibitors as a potent, dose-dependent inducer of human CAR activity which could be distinctively diminished by adding 5α-androst-3α-ol (Kobayashi *et al.*, 2005). The same study revealed the inhibitors to activate human PXR, induce *CYP2B6* in primary human hepatocyte cultures, and 5α-androst-3α-ol to suppress human CAR activity. Interactions of CAR with its co-activator SRC-1 did not show any significant increase or decrease when co-incubated with different Atorvastatin metabolites (figure 3.21). Thus, SPR-based assays could neither verify Atorvastatin lactone, nor acid, nor their respective hydroxyl-metabolites as agonist ligands of CAR. Yet, among all other statins Atorvastatin belonged to the weakest inducers yielding only two fold induction at the most (Kobayashi *et al.*, 2005). Biacore-based experiments clearly proved that the Atorvastatin drugs did not bind the receptor. On the other hand they could still activate CAR in a PB-similar manner (Kawamoto *et al.*, 1999). However, recent work confirmed and revealed that statins including Atorvastatin induced the expression of *CYP2B6*, the main target gene of CAR, as well as *CYP3A4*, *CYP2C9* and other CYPs similar to previous findings (Feidt *et al.*, 2010; Monostory *et al.*, 2009). The Atorvasatin-regulated pathway may include indirect activation via a signal cascade causing dephosphorylation events which end up in the receptor being dephosphorylated in a

significant position like Ser[202] which was proven to be pivotal for CAR nuclear translocation after indirect activation by PB (Yoshinari *et al*., 2003; Hosseinpour *et al*., 2006).

4.2.2 Kinetic characterization of the receptor – co-activator complex

4.2.2.1 Characterization of CAR complex formation with SRC-1 and SRC-2

Ligand-induced binding assays revealed a distinctive hierarchy of increased complex formation of CAR and the co-activators SRC-1 and SRC-2 respectively. But increased association does not equal distinctive changes in kinetics of ligand-induced binding. Thus, kinetic binding experiments of CAR and the respective p160 co-activator were performed in order to yield more data and, thus, information on the nature of receptor - co-activator binding in the presence and absence of ligands.

Beyond from kinetic evaluation of the experimental SPR binding assays, visual characterization of complex formation also revealed significant findings. The 1:1 Langmuir binding model fitted the experimental curves of the interactions between CAR and SRC-1 good since there were only minor deviations (figure 3.25). This observation was confirmed by the residual plot serving as another tool to depict deviations between experimental and model curves (figure 3.26). Values below 2 RU are considered technical background noise and are, therefore, not taken into account.

The kinetic data displayed that the CAR - SRC-1 complex associated nine times faster than the CAR - SRC-2 complex (table 3.2). However, dissociation from the receptor was low and quite similar in speed for both co-activators indicating that stability of the complex was equal and did not dependent on the co-activator. But regarding the equilibrium dissociation constants the CAR - SRC-1 complex demonstrated a twelve times higher affinity than the CAR - SRC-2 complex caused by a distinctively higher association rate. Values for equilibrium dissociation, association rate and dissociation rate constants typically range from $1x10^{-5}$ – $1x10^{-12}$ M, $1x10^{3}$ – $1x10^{7}$ 1/ Ms and $1x10^{-1}$ – $5x10^{-6}$ 1 / s respectively. The K_D values of CAR interacting with both SRC-1 and SRC-2 respectively demonstrated a rather weak binding of both complexes but especially for SRC-2. The association rate constants characterize the SRC-1 – CAR complex as rather medium in speed of association whereas the complex with SRC-2 only slowly formed. Yet, both co-activators demonstrated a relatively high decay of complexes. The affinity of binding and, thus, the stability of the receptor – co-activator complex was apparently higher for SRC-1 than for SRC-2 especially due to a faster

association making SRC-1 the preferred co-activator for CAR in the absence of ligands. But regarding selectivity of co-activators physiological factors like expression levels and tissue-specific expression profiles have to be taken into account, too.

Due to different binding behavior of non-liganded CAR to the immobilized co-activators, it was unclear whether CAR really displayed higher affinity towards SRC-2 or not (chapter 4.2.1). In the kinetic assays CAR was immobilized and the co-activators were injected over the receptor surface. The injection of the same concentration of co-activator caused a higher response for SRC-2 compared to SRC-1. SRC-2 has a higher molecular weight and the immobilization level of CAR on the chip used for CAR – SRC-2 interactions was distinctively higher so that more complexes of CAR and SRC-2 could be formed causing a higher response signal. Thus, the relevant and initial information in the kinetic binding assays is not delivered by absolute response values but by the kinetic data. These data strongly indicate an equal stability of both receptor – co-activator complexes but a distinctively faster association of CAR and SRC-1 as described before. Therefore, more SRC-2 than SRC-1 molecules must have kept their structural integrity after immobilization.

Both ERα and ERβ binding co-activators of the p160 family by means of SPR displayed higher affinity values with SRC-1 in comparison to SRC-2 (Cheskis *et al*., 2003; table 4.1). Thus, both receptors preferred SRC-1 over SRC-2 and regarding ERβ, SRC-1 was the most preferred co-activator of all. Consistent with these results CAR displayed lower equilibrium dissociation constants when binding SRC-1 and, thus, displayed a higher affinity to SRC-1 preferring it to SRC-2 (table 4.1). Yet, CAR demonstrated a significantly higher preference over SRC-1 regarding the discrepancy in affinity values of the estrogen receptors. On the other hand, interactions between CAR and its co-activators demonstrated to be weaker than those of both estrogen receptors with every single steroid receptor co-activator concerning the equilibrium dissociation constants, though comparison was hardly possible due to different binding models (Cheskis *et al*., 2003). It was postulated that the interactions were subject to a bipartite binding. Hence, evaluation of ER – SRC-1 interactions was performed using the two-state binding model which yielded two different rate constants for both the association and the dissociation describing a first unstable and transitional complex being followed by a more slowly and stable complex (Cheskis *et al*., 2003). For CAR interacting with its co-activators in the absence of ligands no better fitting was achieved by using the two-state model instead of the Langmuir 1:1 binding model proposing CAR was not subject to a bipartite binding model. Yet, it is obvious that the nuclear receptor ER demonstrates a much

higher affinity to the few ligands it binds whereas CAR interacts with more ligands which it binds with lower affinity. When compared to farnesoid X receptor (FXR) CAR displayed higher binding affinities with both co-activators (Fujino *et al.*, 2003; table 4.1). SRC-2 displayed an almost twice as fast and SRC-1 an even sixteen times as fast association than SRC-1 with FXR (table 4.1). Even the dissociation happened much faster for FXR than for CAR which proved the CAR – SRC-1 / SRC-2 complexes to be more stable. As a result, strength of binding does not necessarily depend on the p160 co-activators only but also on the receptor they bind.

Table 4.1 Kinetic constants describing the binding between the p160 co-activators SRC-1, SRC-2, and SRC-3 and diverse nuclear receptors.

Nuclear receptor – co-activator	k_a [1/Ms]	k_d [1/s]	K_D [M]
CAR - SRC-1	$9.21 +/- 2.85 \times 10^4$	$5.31 +/- 1.49 \times 10^{-2}$	5.77×10^{-7}
CAR - SRC-2	$1.03 +/- 0.21 \times 10^4$	$7.19 +/- 1.44 \times 10^{-2}$	6.98×10^{-6}
ERα - SRC-1[a]	-	-	1.28×10^{-8}
ERα - SRC-2 [a]	-	-	1.56×10^{-8}
ERα - SRC-3 [a]	-	-	4.55×10^{-9}
ERβ - SRC-1 [a]	-	-	2.78×10^{-8}
ERβ - SRC-2 [a]	-	-	3.25×10^{-8}
ERβ - SRC-3 [a]	-	-	4.44×10^{-8}
FXR - SRC-1 [b]	0.58×10^4	2.10×10^{-1}	3.62×10^{-5}

[a]: Cheskis *et al.*, 2003
[b]: Fujino *et al.*, 2003

4.2.2.2 Kinetic characterization of CAR complex formation with SRC-1 under the influence of drugs

Since affinity measurements of liganded CAR binding its co-activators revealed distinctive enhancement of association, kinetic binding assays were performed to figure out the impact of a ligand on CAR regarding the kinetics of complex formation. Surprisingly, no enhanced affinity between CAR and SRC-1 could be measured for any of the added ligands (table 3.3). Contrariwise, equilibrium dissociation constants displayed weaker affinities when interactions took place with CAR bound to a ligand. Evidently, binding curves of liganded CAR interacting with SRC-1 ran distinctively higher than the ones of the non-liganded CAR – SRC-1 complex even though concentrations of the injected analyte SRC-1 ranging from 2 to 8 µM had not changed in both liganded and non-liganded assay set-ups (figures 3.25 and 3.29 – 3.35). Thus, more complexes of CAR and SRC-1 must have formed in the presence of

ligands. Considering k_a and k_d is recommended, since they are able to characterize complex formation more detailed than regarding K_D only. Complex formation occurred slowly for all drug-dependent protein assays (table 3.3). Interactions with Artemeether, Triphenylphosphate and Fenofibrate were about seven to eight times smaller whereas the rest of the drugs yielded 20 to 40 times smaller k_a values. This means that no drug was able to accelerate recognition of SRC-1, so that complexes would be formed more rapidly. In contast, complex formation was clearly hindered in respect to the speed of binding liganded CAR.

For properly evaluating kinetics, k_d might be preferred since it, in contrast to k_a, is a concentration-independent kinetic constant and does not account for proteins on both the immobilized surface and in the analyte solution which are not functional and active and may, therefore, affect kinetic values. Selective drugs decelerated association tremendously but demonstrated enhanced stability, and, thus affinity of the receptor – co-activator complex. CITCO, Clofibrate, Arteether and Artemisinin led to distinctively slower association rates which might be explained by a two-step association with an initial faster and a following slower association phase. In any case, these drugs led to a slower dissociation, and, thus to a more stable receptor – co-activator complex. Artemether, Triphenylphosphate and Fenofibrate did not show enhanced stability and an association rate constant which was also slower but matched the constitutive binding of the CAR – SRC-1 complex (table 3.3).

Although, all ligand-induced kinetic assays displayed no enhanced equilibrium dissociation constants, rate constants revealed a two class system of ligands and their impact on the CAR – SRC-1 complex. Artemether, Triphenylphosphate, and Fenofibrate displayed dissociation rate constants that matched the constitutive binding of CAR and SRC-1. Thus, the enhanced association was caused by a higher number of receptors binding co-activators and not due to an enhanced affinity of the single receptor itself to the co-activator (figure 3.22 and 3.23). So, the effect of the respective ligands might be an enhanced conformational stabilization of more receptor molecules to further facilitate binding of more co-activator molecules. Since these drugs evidently had no effect on the kinetics of the protein complex the higher association responses must be explained as more complexes bound. The second class of ligands including CITCO, Clofibrate, Arteether and Artemisinin appeared to lead to conformational changes that include both more CAR molecules to bind SRC-1 and the single receptor to bind more stably the co-activator. The dissociation rate constants proved the CAR – SRC-1 complex to decay more slowly when the receptor is ligand-bound. Correspondingly, Clotrimazole-based ligand-dependent increase in association was hindered most efficiently for the ligands of the second class (figure 3.18).

Dimerization of CAR as a possible explanation for the enhanced association responses may be ruled out since doubling the molecular weight of the receptor would only halve but not increase the maximum response since CAR was immobilized on the chip surface and SRC-1 was used as the analyte (equation (2); see chapter 4.2.1).

So, both liganded as well as non-liganded CAR prefers SRC-1 over SRC-2 consistent with the results obtained with ER (Cheskis *et al*., 2003).

4.3 Conclusion

In the presented thesis work the nuclear receptor CAR and the co-activators SRC-1 and SRC-2 were successfully expressed and purified to a large extent from *E. coli* cell lysate.

This thesis work revealed co-activator- and ligand-dependent differences in complex formation of CAR investigated by means of SPR. Ligand-induced binding assays of CAR and SRC-1 allowed a clear discrimination of drugs between non- or low, weak, and strong binders of the receptor and revealed CITCO > Arteether = Clofibrate as the top three agonists with regard to co-activator binding. The CAR – SRC-2 complex formation was not strongly affected by ligands and, therefore, clear discrimination of drugs was not possible. Arteether > CITCO > Triphenylphosphate demonstrated to be the three most competent inducers. Thus, CAR – SRC-1 interaction appears to be more susceptible to manipulation by the selected drugs, especially by the top agonists. Unlike CITCO, Clofibrate belongs to the group of lipid lowering agents whereas Arteether is used against severe *Plasmodium falciparum* malaria (White, 2004). Thus, the simultaneous administration of the agonist ligands and Clotrimazole *in vivo* might lead to decreased activity of the xenosensor CAR.

Kinetic binding assays revealed that the constitutive binding of CAR with SRC-1 occurred much faster than with SRC-2 whereas the stability of both receptor - co-activator complexes was low and displayed no differences. These findings strongly indicate that SRC-1 is the prime co-activator of interest for CAR which is verified by mammalian two hybrid assays revealing it to be the most potent of the p160 co-activators and by ligand-induced binding assays with CAR and the respective co-activator (Arnold *et al*., 2004). Consistent with these findings, SPR based interactions of ERα (Estrogen Receptor α) and ERβ with the p160 co-activators revealed SRC-1 to be the preferred over SRC-2 for both receptors (Cheskis *et al*., 2003). Additionally, the co-activator SRC-1, unlike SRC-2, revealed to be a potent tool of

identification and characterization of further putative agonists which can increase the constitutive binding using SPR techniques. As demonstrated in this work, SPR binding assays enable a fast and easy identification of drugs as ligand or indirect non-ligand activators unlike cell-based reporter assays. Furthermore, since Biacore assays are *in vitro* systems, interactions are not influenced by drug-based cytotoxic effects.

Mammalian two hybrid assays also showed that DRIP 205 revealed to be a more potent co-regulator than all of the p160 co-activators both in the presence and absence of CITCO (Arnold *et al*., 2004). Therefore, further SPR binding and kinetic assays ought to include DRIP 205 as non-p160 co-activator of CAR as a perfect alternative tool to characterize CAR . Additionally, identification of further putative agonists which could influence the activity of the nuclear receptor CAR might be identified and characterized. Ligand-induced kinetic binding assays revealed two classes of CAR ligands. The first class of ligands led to the formation of more complexes whereas the second class of ligands also enhanced the stability of the CAR – SRC-1 complex. This finding emphasizes the importance of kinetic assays. It is crucial that enhanced complex formation measured in SPR binding assays is confirmed by kinetic assays in order to characterize the actual influence of a ligand on the receptor. Thus, both binding and kinetic assays need to be performed to identify putative agonist ligands with a high impact on the kinetics of CAR – co-activator complexes since only these ligands might have an actual impact on the dynamics of CAR. Additionally, direct protein – drug binding assays of immobilized CAR with the top agonists respectively could characterize receptor – agonist interactions in a co-activator-independent manner. These experiments might reveal crucial information on kinetics regarding the receptor – agonist complex and would allow characterization and maybe prediction of medical side effects.

SPR binding assays revealed that the HMG-CoA reductase inhibitor Atorvastatin and its metabolites are not ligands of CAR. Since Atorvastatin among other statins induces gene expression of *CYP2B6*, the main target gene of CAR, *CYP3A4*, and *CYP2C9,* the receptor probably acts as an indirect activator in a PB-similar way (Kawamoto *et al*., 1999; Feidt *et al*., 2010; Monostory *et al*., 2009). Yet, other HMG-CoA reductase inhibitors may directly bind and activate CAR.

Unlike Atorvastatin, SPR binding assays could identify compounds, already known as CAR activators and inducers of nuclear translocation, as agonists. These drugs include Clofibrate and Fenofibrate and, therefore, indicate a direct activation of CAR *in vivo* by these agonists (Guo *et al*., 2007). The presented thesis work could only partly confirm Clotrimazole as inverse agonist of CAR since it led to the release of ligand-induced binding of SRC-1 but did

not lead to co-activator release in the absence of ligands. Phenobarbital and CITCO were also confirmed to be non-ligand and ligand and, thus, an indirect activator and agonist respectively. Hence, SPR techniques are perfectly suitable for identification and characterization of further agonist ligands and confirming activators to be direct agonists.

Literature

Anzick, S. L., J. Kononen, et al. (1997). "AIB1, a Steroid Receptor Coactivator Amplified in Breast and Ovarian Cancer." Science 277(5328): 965-968.

Arnold, K., M. Eichelbaum, et al. (2004). "Alternative splicing affects the function and tissue-specific expression of the human constitutive androstane receptor." Nuclear Receptor 2(1): 1.

Auerbach, S. S., R. Ramsden, et al. (2003). "Alternatively spliced isoforms of the human constitutive androstane receptor." Nucleic Acids Res 31: 3194 - 3207.

Baes, M., T. Gulick, et al. (1994). "A new orphan member of the nuclear hormone receptor superfamily that interacts with a subset of retinoic acid response elements." Mol Cell Biol 14: 1544 - 1552.

Beilke, L. D., L. M. Aleksunes, et al. (2009). "Constitutive Androstane Receptor-Mediated Changes in Bile Acid Composition Contributes to Hepatoprotection from Lithocholic Acid-Induced Liver Injury in Mice." Drug Metabolism and Disposition 37(5): 1035-1045.

Bertilsson, G. r., J. Heidrich, et al. (1998). "Identification of a human nuclear receptor defines a new signaling pathway for CYP3A induction." Proceedings of the National Academy of Sciences of the United States of America 95(21): 12208-12213.

Biacore Getting Started 28-9384-71 Edition AC.

Biacore Sensor Surface Handbook, version AA.

BIAtechnology Handbook.

Black, D. M., R. G. Bakker-Arkema, et al. (1998). "An Overview of the Clinical Safety Profile of Atorvastatin (Lipitor), a New HMG-CoA Reductase Inhibitor." Arch Intern Med 158(6): 577-584.

Bohan, A. and J. L. Boyer (2002). "Mechanisms of hepatic transport of drugs: implications for cholestatic drug reactions." Semin Liver Dis 22: 123–136.

Burk, O., K. A. Arnold, et al. (2005). "Antimalarial Artemisinin Drugs Induce Cytochrome P450 and MDR1 Expression by Activation of Xenosensors Pregnane X Receptor and Constitutive Androstane Receptor." Molecular Pharmacology 67(6): 1954-1965.

Burk, O., H. Tegude, et al. (2002). "Molecular mechanisms of polymorphic CYP3A7 expression in adult human liver and intestine." J Biol Chem 277: 24280 - 24288.

Cheskis, B. J., N. J. McKenna, et al. (2003). "Hierarchical Affinities and a Bipartite Interaction Model for Estrogen Receptor Isoforms and Full-length Steroid Receptor

Coactivator (SRC/p160) Family Members." Journal of Biological Chemistry 278(15): 13271-13277.

Choi, H. S., M. Chung, et al. (1997). "Differential transactivation by two isoforms of the orphan nuclear hormone receptor CAR." J Biol Chem 272: 23565 - 23571.

Chong, P. H. and J. D. Seeger (1997). "Atorvastatin calcium: an addition to HMG-CoA reductase inhibitors." Pharmacotherapy 17: 1157–1177.

Conney, A. H. (1982). "Induction of Microsomal Enzymes by Foreign Chemicals and Carcinogenesis by Polycyclic Aromatic Hydrocarbons: G. H. A. Clowes Memorial Lecture." Cancer Research 42(12): 4875-4917.

Cooper MA (2003). "Label-free screening of bio-molecular interactions." Anal Bioanal Chem 377: 834-842.

De la Serna, G. and C. Cadarso (1999). "Fenofibrate decreases plasma fibrinogen, improves lipid profile, and reduces uricemia." Clin Pharmacol Ther 66(2): 166-172.

Ding, X. F., C. M. Anderson, et al. (1998). "Nuclear Receptor-Binding Sites of Coactivators Glucocorticoid Receptor Interacting Protein 1 (GRIP1) and Steroid Receptor Coactivator 1 (SRC-1): Multiple Motifs with Different Binding Specificities." Mol Endocrinol 12(2): 302-313.

Dring, A. M., L. E. Anderson, et al. (2010). "Rational quantitative structure-activity relationship (RQSAR) screen for PXR and CAR isoform-specific nuclear receptor ligands." Chemico-Biological Interactions 188(3): 512-525.

Dussault, I., M. Lin, et al. (2002). "A Structural Model of the Constitutive Androstane Receptor Defines Novel Interactions That Mediate Ligand-Independent Activity." Mol. Cell. Biol. 22(15): 5270-5280.

Eichelbaum, M. and O. Burk (2001). "CYP3A genetics in drug metabolism." Nat Med 7(3): 285-287.

Ekgasit S, Thammacharoen C, Knoll W (2004) "*Surface* plasmon resonance spectroscopy based on evanescent field treatment." Anal Chem 76: 561-568.

Enmark, E. and J. A. Gustafsson (1996). "Orphan nuclear receptors--the first eight years." Mol Endocrinol 10(11): 1293-1307.

Escriva, H., F. Delaunay, et al. (2000). "Ligand binding and nuclear receptor evolution." BioEssays 22(8): 717-727.

Evans, W. E. and M. V. Relling (1999). "Pharmacogenomics: Translating Functional Genomics into Rational Therapeutics." Science 286(5439): 487-491.

Fägerstam LG, Frostell-Karlsson A, Karlsson R, Persson B, Rönnberg I (1992) "Biospecific interaction analysis using surface plasmon resonance detection applied to kinetic, binding site and concentration analysis." J Chromatogr 597: 397-410.

Feidt, D. M., K. Klein, et al. (2010). "Profiling Induction of Cytochrome P450 Enzyme Activity by Statins Using a New Liquid Chromatography-Tandem Mass Spectrometry Cocktail Assay in Human Hepatocytes." Drug Metabolism and Disposition 38(9): 1589-1597.

Forman, B. M., I. Tzameli, et al. (1998). "Androstane metabolites bind to and deactivate the nuclear receptor CAR-beta." Nature 395: 612 - 615.

Frank, C., F. Molnár, et al. (2004). "Agonist-dependent and Agonist-independent Transactivations of the Human Constitutive Androstane Receptor Are Modulated by Specific Amino Acid Pairs." Journal of Biological Chemistry 279(32): 33558-33566.

Fujino, T., Y. Sato, et al. (2003). "In vitro farnesoid X receptor ligand sensor assay using surface plasmon resonance and based on ligand-induced coactivator association." The Journal of Steroid Biochemistry and Molecular Biology 87(4-5): 247-252.

Garfinkel, D. (1958). "Studies on pig liver microsomes. I. Enzymic and pigment composition of different microsomal fractions." Archives of Biochemistry and Biophysics 77(2): 493-509.

Gehin, M., M. Mark, et al. (2002). "The Function of TIF2/GRIP1 in Mouse Reproduction Is Distinct from Those of SRC-1 and p/CIP." Mol. Cell. Biol. 22(16): 5923-5937.

Germain, P., J. Iyer, et al. (2002). "Co-regulator recruitment and the mechanism of retinoic acid receptor synergy." Nature 415: 187 - 192.

Germain, P., B. Staels, et al. (2006). "Overview of Nomenclature of Nuclear Receptors." Pharmacological Reviews 58(4): 685-704.

Goeddel, D. V., D. G. Kleid, et al. (1979). "Expression in Escherichia coli of chemically synthesized genes for human insulin." Proceedings of the National Academy of Sciences of the United States of America 76(1): 106-110.

Goldstein, J. A. and M. B. Faletto (1993). "Advances in mechanisms of activation and deactivation of environmental chemicals." Environ.Health Perspect. 100: 169-176.

Goodwin, B., E. Hodgson, et al. (2002). "Transcriptional regulation of the human CYP3A4 gene by the constitutive androstane receptor." Mol Pharmacol 62: 359 - 365.

Guo, D., J. Sarkar, et al. (2007). "Induction of Nuclear Translocation of Constitutive Androstane Receptor by Peroxisome Proliferator-activated Receptor α Synthetic Ligands in Mouse Liver." Journal of Biological Chemistry 282 (50): 36766-36776.

Christoph Handschin and Urs A. Meyer (2003). "Induction of Drug Metabolism: The Role of Nuclear Receptors." Pharmacological Reviews 55: 649-673.

Homola J, Yee SS, Gauglitz G (1999) "Surface plasmon resonance sensors: review." Sensors and Actuators B-Chemical 54: 3-15.

Honkakoski, P. and M. Negishi (2000). "Regulation of cytochrome P450 (CYP) genes by nuclear receptors." Biochem. J. 347(2): 321-337.

Honkakoski, P., J. J. Palvimo, et al. (2004). "Effects of triaryl phosphates on mouse and human nuclear receptors." Biochemical Pharmacology 67(1): 97-106.

Honkakoski, P., I. Zelko, et al. (1998). "The nuclear orphan receptor CAR-retinoid X receptor heterodimer activates the phenobarbital-responsive enhancer module of the CYP2B gene." Mol Cell Biol 18: 5652 - 5658.

Hosseinpour, F., R. Moore, et al. (2006). "Serine 202 Regulates the Nuclear Translocation of Constitutive Active/Androstane Receptor." Molecular Pharmacology 69(4): 1095-1102.

Huang, Z. J., I. Edery, et al. (1993). "PAS is a dimerization domain common to Drosophila Period and several transcription factors." Nature 364(6434): 259-262.

Itakura, K., T. Hirose, et al. (1977). "Expression in Escherichia coli of a chemically synthesized gene for the hormone somatostatin." Science 198(4321): 1056-1063.

Jacobsen, W., B. Kuhn, et al. (2000). "Lactonization Is the Critical First Step in the Disposition of the 3-Hydroxy-3-Methylglutaryl-Coa Reductase Inhibitor Atorvastatin." Drug Metabolism and Disposition 28(11): 1369-1378.

Jia, Y., G. L. Guo, et al. (2005). "Transcription coactivator peroxisome proliferator-activated receptor-binding protein/mediator 1 deficiency abrogates acetaminophen hepatotoxicity." Proceedings of the National Academy of Sciences of the United States of America 102(35): 12531-12536.

Juliano, R. L. and V. Ling (1976). "A surface glycoprotein modulating drug permeability in Chinese hamster ovary cell mutants." Biochimica et Biophysica Acta (BBA) - Biomembranes 455(1): 152-162.

Jyrkkärinne, J., B. r. Windshügel, et al. (2005). "Amino Acids Important for Ligand Specificity of the Human Constitutive Androstane Receptor." Journal of Biological Chemistry 280(7): 5960-5971.

Kakizaki, S., S. Karami, et al. (2002). "Retinoic acids repress constitutive active receptor-mediated induction by 1,4-bis[2-(3,5-dichloropyridyloxy)]benzene of the CYP2B10 gene in mouse primary hepatocytes." Drug Metab Dispos 30: 208 - 211.

Kast, H. R., B. Goodwin, et al. (2002). "Regulation of Multidrug Resistance-associated Protein 2 (ABCC2) by the Nuclear Receptors Pregnane X Receptor, Farnesoid X-activated Receptor, and Constitutive Androstane Receptor." Journal of Biological Chemistry 277(4): 2908-2915.

Kawamoto, T., T. Sueyoshi, et al. (1999). "Phenobarbital-responsive nuclear translocation of the receptor CAR in induction of the CYP2B gene." Mol Cell Biol 19: 6318 - 6322.

Klayman, D. L. (1985). "Qinghaosu (artemisinin): an antimalarial drug from China." Science 228(4703): 1049-1055.

Klingenberg, M. (1958). "Pigments of rat liver microsomes." Archives of Biochemistry and Biophysics 75(2): 376-386.

Kobayashi, K., T. Sueyoshi, et al. (2003). "Cytoplasmic accumulation of the nuclear receptor CAR by a tetratricopeptide repeat protein in HepG2 cells." Mol Pharmacol 64: 1069 - 1075.

Kobayashi, K., Y. Yamanaka, et al. (2005). "IDENTIFICATION OF HMG-CoA REDUCTASE INHIBITORS AS ACTIVATORS FOR HUMAN, MOUSE AND RAT CONSTITUTIVE ANDROSTANE RECEPTOR." Drug Metabolism and Disposition 33(7): 924-929.

Kocarek, T. A., M. S. Dahn, et al. (2002). "Regulation of CYP2B6 and CYP3A Expression by Hydroxymethylglutaryl Coenzyme A Inhibitors in Primary Cultured Human Hepatocytes." Drug Metabolism and Disposition 30(12): 1400-1405.

Kocarek, T. A. and A. B. Reddy (1996). "Regulation of cytochrome P450 expression by inhibitors of hydroxymethylglutaryl-coenzyme A reductase in primary cultured rat hepatocytes and in rat liver." Drug Metabolism and Disposition 24(11): 1197-1204.

Kocarek, T. A., E. G. Schuetz, et al. (1993). "Regulation of Phenobarbital-Inducible Cytochrome-P450 2B1/2 mRNA by Lovastatin and Oxysterols in Primary Cultures of Adult Rat Hepatocytes." Toxicology and Applied Pharmacology 120(2): 298-307.

Kretschmann E, Raether H (1968) "Radiative decay of non radiative surface plasmons excited by light" Z. Naturforsch 23a: 2135-2136.

Kumar, V. and P. Chambon (1988). "The estrogen receptor binds tightly to its responsive element as a ligand-induced homodimer." Cell 55(1): 145-156.

Lamba, V., J. Lamba, et al. (2003). "Hepatic CYP2B6 Expression: Gender and Ethnic Differences and Relationship to CYP2B6 Genotype and CAR (Constitutive Androstane Receptor) Expression." Journal of Pharmacology and Experimental Therapeutics 307(3): 906-922.

Lehmann, J. M., D. D. McKee, et al. (1998). "The human orphan nuclear receptor PXR is activated by compounds that regulate CYP3A4 gene expression and cause drug interactions." The Journal of Clinical Investigation 102(5): 1016-1023.

Lempiäinen, H., F. Molnar, et al. (2005). "Antagonist- and Inverse Agonist-Driven Interactions of the Vitamin D Receptor and the Constitutive Androstane Receptor with Corepressor Protein." Mol Endocrinol 19(9): 2258-2272.

Leo, C. and J. D. Chen (2000). "The SRC family of nuclear receptor coactivators." Gene 245(1): 1-11.

Li, C., J. W. R. Schwabe, et al. (1997). "Coexpression of nuclear receptor partners increases their solubility and biological activities." Proceedings of the National Academy of Sciences of the United States of America 94(6): 2278-2283.

Maglich, J. M., D. J. Parks, et al. (2003). "Identification of a novel human constitutive androstane receptor (CAR) agonist and its use in the identification of CAR target genes." J Biol Chem 278: 17277 - 17283.

Mäkinen, J., M. Reinisalo, et al. (2003). Dual action of oestrogens on the mouse constitutive androstane receptor.

Mangelsdorf, D. J. and R. M. Evans (1995). "The RXR heterodimers and orphan receptors." Cell 83: 841 - 8850.

Marais, A. D., J. C. Firth, et al. (1997). "Atorvastatin: An Effective Lipid-Modifying Agent in Familial Hypercholesterolemia." Arterioscler Thromb Vasc Biol 17(8): 1527-1531.

Marston, F. A. O. (1986). "The purification of eukaryotic polypeptides synthesized in Escherichia coli." TheBiochemical Journal 240(1): 1-12.

Min, G., J. K. Kemper, et al. (2002). "Glucocorticoid receptor-interacting protein 1 mediates ligand-independent nuclear translocation and activation of constitutive androstane receptor in vivo." J Biol Chem 277: 26356 - 26363.

Monostory, K., J.-M. Pascussi, et al. (2009). "Drug Interaction Potential of 2-((3,4-Dichlorophenethyl)(propyl)amino)-1-(pyridin-3-yl)ethanol (LK-935), the Novel Nonstatin-Type Cholesterol-Lowering Agent." Drug Metabolism and Disposition 37(2): 375-385.

Moore, L. B., D. J. Parks, et al. (2000). "Orphan Nuclear Receptors Constitutive Androstane Receptor and Pregnane X Receptor Share Xenobiotic and Steroid Ligands." Journal of Biological Chemistry 275(20): 15122-15127.

Muangmoonchai, R., D. Smirlis, et al. (2001). "Xenobiotic induction of cytochrome P450 2B1 (CYP2B1) is mediated by the orphan nuclear receptor constitutive androstane receptor (CAR) and requires steroid co-activator 1 (SRC-1) and the transcription factor Sp1." Biochem. J. 355(1): 71-78.

Müller, M. (2000). "Transcriptional control of hepatocanalicular transporter gene expression." Semin Liver Dis(20): 323–337.

Mullis, K., F. Faloona, et al. (1986). "Specific enzymatic amplification of DNA in vitro: the polymerase chain reaction " Cold Spring Harb Symp Quant Biol 51(1): 263-273.

Nawrocki, J. W., S. R. Weiss, et al. (1995). "Reduction of LDL Cholesterol by 25% to 60% in Patients With Primary Hypercholesterolemia by Atorvastatin, a New HMG-CoA Reductase Inhibitor." Arterioscler Thromb Vasc Biol 15(5): 678-682.

Nebert, D. W. and D. W. Russell (2002). "Clinical importance of the cytochromes P450." The Lancet 360(9340): 1155-1162.

Nelson, D. R., L. Koymans, et al. (1996). "P450 superfamily: update on new sequences, gene mapping, accession numbers and nomenclature." Pharmacogenetics 6: 1 - 42.

Noble, S. M., V. E. Carnahan, et al. (2006). "Human PXR Forms a Tryptophan Zipper-Mediated Homodimer" Biochemistry 45(28): 8579-8589.

Onate, S. A., V. Boonyaratanakornkit, et al. (1998). "The Steroid Receptor Coactivator-1 Contains Multiple Receptor Interacting and Activation Domains That Cooperatively Enhance

the Activation Function 1 (AF1) and AF2 Domains of Steroid Receptors." Journal of Biological Chemistry 273(20): 12101-12108.

Onate, S. A., S. Y. Tsai, et al. (1995). "Sequence and Characterization of a Coactivator for the Steroid Hormone Receptor Superfamily." Science 270(5240): 1354-1357.

Otto, A. (1969). "Excitation by light of ω+ and ω− surface plasma waves in thin metal layers." Zeitschrift für Physik A Hadrons and Nuclei 219(3): 227-233.

Park, J.-E. (2008). "Contribution of cytochrome P450 3A4 and 3A5 to the metabolism of atorvastatin." Xenobiotica 38: 1240-1251.

Plempel, M., K. Bartmann, et al. (1969). "Experimentelle Befunde über ein neues, oral wirksames Antimykotikum mit breitem Wirkungsspektrum." Deutsche Medizinische Wochenschrift 26(94): 1356-1364.

Qatanani, M. and D. D. Moore (2005). "CAR, The Continuously Advancing Receptor, in Drug Metabolism and Disease." Current Drug Metabolism 6: 329-339.

Raether H (1988) "Surface plasmons on smooth and rough surfaces and on gratings." Springer Tracts in Modern Physics. Höhler G. Springer-Verlag, Berlin; Volume 111.

Sambrook, J., J. Fritsch, et al. (1989). "Molecular Cloning - a laboratory manual, 2nd ed." Cold Spring Harbor Laboratory Press: New York.

Shan, L., J. Vincent, et al. (2004). "Structure of the murine constitutive androstane receptor complexed to androstenol: a molecular basis for inverse agonism." Molecular Cell 16: 907 - 917.

Shimada, T., H. Yamazaki, et al. (1994). "Interindividual variations in human liver cytochrome P-450 enzymes involved in the oxidation of drugs, carcinogens and toxic chemicals: studies with liver microsomes of 30 Japanese and 30 Caucasians." Journal of Pharmacology and Experimental Therapeutics 270(1): 414-423.

Sommariva, D., D. Bonfiglioli, et al. (1984). "Long-term effects of fenofibrate on serum lipids and on lipoprotein cholesterol in type II hyperlipoproteinemic patients." Pharmacological Research Communications 16(8): 809-820.

Spencer, T. E., G. Jenster, et al. (1997). "Steroid receptor coactivator-1 is a histone acetyltransferase." Nature 389(6647): 194-198.

Stieger, P. and P. J. Meyer (1998). "Bile acid and xenobiotic transporters in liver." Current Opinion in Cell Biology 10: 462-467.

Sueyoshi, T., T. Kawamoto, et al. (1999). "The Repressed Nuclear Receptor CAR Responds to Phenobarbital in Activating the Human CYP2B6 Gene." J Biol Chem 274: 6043 - 6046.

Sugatani, J., H. Kojima, et al. (2001). "The phenobarbital response enhancer module in the human bilirubin UDP-gulcuronosyltransferase UGT1A1 gene and regulation by nuclear receptor CAR." Hepatology 33: 1232 - 1238.

Suino, K., L. Peng, et al. (2004). "The Nuclear Xenobiotic Receptor CAR: Structural Determinants of Constitutive Activation and Heterodimerization." Molecular cell 16(6): 893-905.

Svensson, U. S. H., M. Ashton, et al. (1998). "Artemisinin induces omeprazole metabolism in human beings[ast]." Clin Pharmacol Ther 64(2): 160-167.

Yoaev E. Timsit and Masahiko Negishi (2007). "CAR and PXR: The xenobiotic-sensing receptors." Steroids 72 (2007): 231-246.

Trubetskoy, O., B. Marks, et al. (2005). "A Simultaneous Assessment of CYP3A4 Metabolism and Induction in the DPX-2 Cell Line." The AAPS Journal 7(1): E6-E13.

Turbadar, T. (1959). "Complete Absorption of Light by Thin Metal Films." Proceedings of the Physical Society 73(1): 40.

Tzameli, I., P. Pissios, et al. (2000). "The xenobiotic compound 1,4-Bis[2-(3,5-Dichloropyridyloxy)]Benzene is an agonist ligand for the nuclear receptor CAR." Mol. Cell. Biol. 20: 2951 - 2958.

Ueda, H. R., W. Chen, et al. (2002). "A transcription factor response element for gene expression during circadian night." Nature 418: 534 - 539.

Vincent, J., L. Shan, et al. (2005). "Crystallographic analysis of murine constitutive androstane receptor ligand-binding domain complexed with 5[alpha]-androst-16-en-3[alpha]-ol." Acta Crystallographica Section F 61(1): 156-159.

Voegel, J. J., M. J. S. Heine, et al. (1998). "The coactivator TIF2 contains three nuclear receptor-binding motifs and mediates transactivation through CBP binding-dependent and -independent pathways." EMBO J 17(2): 507-519.

Voegel, J. J., M. J. S. Heine, et al. (1996). "TIF2, a 160 kDa transcriptional mediator for the ligand-dependent activation function AF-2 of nuclear receptors." The EMBO Journal 15(14): 3667-3675.

Wang, H., S. Faucette, et al. (2003). "A novel distal enhancer module regulated by pregnane X receptor/constitutive androstane receptor is essential for the maximal induction of CYP2B6 gene expression." J Biol Chem 278: 14146 - 14152.

Wang, Z., D. W. Rose, et al. (2000). "Regulation of somatic growth by the p160 coactivator p/CIP." Proceedings of the National Academy of Sciences of the United States of America 97(25): 13549-13554.

Waxman, D. J. and L. Azaroff (1992). "Phenobarbital induction of cytochrome P-450 gene expression." Biochem. J. 281(3): 577-0.

Wei, P., J. Zhang, et al. (2002). "Specific and Overlapping Functions of the Nuclear Hormone Receptors CAR and PXR in Xenobiotic Response." The Pharmacogenomics Journal 2: 117 - 126.

White, N. J. (2004). "Antimalarial drug resistance." The Journal of Clinical Investigation 113(8): 1084-1092.

Wu, R.-C., Smith C. L. and O'Malley B. W. (1993). "Transcriptional Regulation by Steroid Receptor Coactivator Phosphorylation". Endocrine Reviews 26 (3): 393-399

Xia, J. and B. Kemper (2005). "Structural Determinants of Constitutive Androstane Receptor Required for Its Glucocorticoid Receptor Interacting Protein-1-mediated Nuclear Accumulation." Journal of Biological Chemistry 280(8): 7285-7293.

Xie, W., J. L. Barwick, et al. (2000). "Reciprocal activation of Xenobiotic response genes by nuclear receptors SXR/PXR and CAR." Genes & Development 14(23): 3014-3023.

Xu, J. and Q. Li (2003). "Review of the in Vivo Functions of the p160 Steroid Receptor Coactivator Family." Mol Endocrinol 17(9): 1681-1692.

Xu, J., L. Liao, et al. (2000). The steroid receptor coactivator SRC-3 (p/CIP/RAC3/AIB1/ACTR/TRAM-1) is required for normal growth, puberty, female reproductive function, and mammary gland development, National Academy of Sciences.

Xu, R. X., M. H. Lambert, et al. (2004). "A structural basis for constitutive activity in the human CAR/RXRa heterodimer." Molecular Cell 16: 919 - 928.

Yamamoto, Y., T. Kawamoto, et al. (2003). "The role of the nuclear receptor CAR as a coordinate regulator of hepatic gene expression in defense against chemical toxicity." Archives of Biochemistry and Biophysics 409(1): 207-211.

Yoshinari, K., K. Kaoru, et al. (2003). "Identification of the nuclear receptor CAR:HSP90 complex in mouse liver and recruitment of protein phosphatase 2A in response to phenobarbital." FEBS letters 548(1): 17-20.

Zelko, I., T. Sueyoshi, et al. (2001). "The peptide near the C terminus regulates receptor CAR nuclear translocation induced by xenochemicals in mouse liver." Mol Cell Biol 21: 2838 - 2846.

Ziegler, D. M. (1994). "Detoxication: oxidation and reduction in The Liver: Biology and Pathobiology." Raven Press, New York, NY: 415–427.

Curriculum vitae

PERSÖNLICHE DATEN

LUAM GHEBREGHIORGHIS

Geburtsdatum / -ort:	21.11.1979 in Kasala / Sudan
Familienstand:	ledig
Staatsangehörigkeit:	deutsch
Adresse:	Werastraße 139
	70190 Stuttgart

PRAKTISCHE ERFAHRUNG

04/2010 – 10/2010   **HiWi-Tätigfkeit am Institut für Technische Biochemie** in Zusammenarbeit mit dem Institut für Materialwissenschaft, Universität Stuttgart

Seit 02/2007   **Promotionsstudium am Institut für Technische Biochemie,** Universität Stuttgart

07/2006 bis 08/2006
03/2005 bis 05/2005   **HiWi-Tätigfkeit am ZMBP Tübingen** (Zentrum für Molekularbiologie der Pflanzen), Universität Tübingen

11/2002 bis 02/2003
11/2001 bis 02/2002   **HiWi-Tätigfkeit am Lehrstuhl für Spezielle Zoologie,** Universität Tübingen

AKADEMISCHE AUSBILDUNG

10/2000 - 07/2006   **Studium der Biologie** (Diplom) an der Eberhard Karls Universität Tübingen mit den Schwerpunkten Mikrobiologie (Hauptfach), Immunologie und Biochemie (Nebenfächer)

06/2005 – 06/2006   **Diplomarbeit** im Bereich Zellbiologie und Entwicklungsgenetik am ZMBP (Zentrum für Molekularbiologie der Pflanzen), Tübingen: *„Cytokinese bei Arabidopsis: Charakterisierung der Proteine RUNKEL und KNOLLE"*

SCHULBILDUNG

1990 – 1999   Otto-Hahn-Gymnasium, Ludwigsburg